

Quantifying the mechanical resistance of coppice trees against rockfall

Dissertation

Zur Erlangung der Würde des Doktors der Naturwissenschaften
des Fachbereichs Biologie, der Fakultät für Mathematik, Informatik
und Naturwissenschaften, der Universität Hamburg

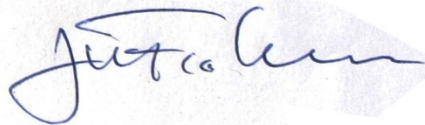
vorgelegt von

Oliver Jancke

Hamburg 2012

Genehmigt vom Fachbereich Biologie
der Fakultät für Mathematik, Informatik und Naturwissenschaften
an der Universität Hamburg
auf Antrag von Professor Dr. M. KÖHL
Weiterer Gutachter der Dissertation:
Priv.-Doz. Dr. habil. L. DORREN
Tag der Disputation: 22. November 2012

Hamburg, den 09. November 2010



Professor Dr. J. Fromm
Vorsitzender des Promotionsausschusses
Biologie

Acknowledgements

I would like to express my gratitude to my supervisors Frédéric Berger, Luuk Dorren and Michael Köhl for their commitment to help obtain funding for this thesis. Moreover, I am grateful for their continuous trust, support and expertise during more than four years. I will also never forget the everlasting good humor in the field or on other trips in the Alpine region.

In addition, I would like to thank Franck Bourrier for numerous scientific discussions, support and advice.

Apart from the rather cozy scientific office work this thesis is a result of sometimes hard manual labor. First and foremost I am grateful to Pascal Tardif and Eric Mermin who both never hesitated to go cut some trees on steep, slippery, somewhat impenetrable forest slopes and then forward the stems downhill by hand while it was snowing or to pull around these 60 kg granite balls on similar terrain. For such kind of 'fitness training', other work and the ever good ambience at Cemagref (now Irstea) I would in particular like to thank Jonas Huguenin and Jonas Ebeling, Frédéric Ousset, Gilles Favier, Nicolas Clouet, Dominik Cremer-Schulte, Ignacio Olmedo-Manich, Nils Durand, Christophe Corona, Emmanuel Defosse, Guillaume Consoli, Adrien Queyrel, Antoine Tabourdeau, David Toe, Christian Eymond-Gris, Christophe Bigot, Jean-Matthieu Monnet, Jerome Lopez, Bertrand Davin, Stéphane Lambert, Bruno Baq, Sandrine Tacon, Anna Radtke, Nathan Daumergue, Mathilde Gallouet, François Dhordain, Nicole Sardat, Valérie Antorino and Jean-Baptiste Moulin.

Furthermore I acknowledge Sébastien Laguet of the French National Forest Service (ONF) for providing an ideal forest test site in an 'all-round carefree package'. I would also like to thank Gérard Remiller

and Christian Bazin of the ONF for the permission to cut as many specimens as necessary for the pendulum impact tests in their coppice and fir forests.

Of course I will not forget the help of François Véron, Séverine Dujardin, Elodie Cavailé, Catherine Lukie and Geneviève Nouvellon in the jungle of the French administration.

Special thanks go to Marc Fuhr for his continuous support and the really good atmosphere during all these years in our office.

I send out a big THANK YOU to my former fellow students Chrille, Jan and Uli as well as my brother Felix for technical advice, corrections, endless discussions including unimportant details and constant mental support!

Finally, I am very grateful to my French and my German Family for continuous help and support, and above all to my dearest Anne, Rosalie and Edgar!

This Dissertation was funded by the German Academic Exchange Service (DAAD) with the PhD Scholarship D/07/47952 and by the INTERREG IV Alpine Space project MANFRED 9-2-3-D.



Table of Contents

Acknowledgements	I
Table of Contents	III
Abbreviations	VI
List of Figures	VII
List of Tables	XI
Summary	XII
Résumé	XVI
Zusammenfassung	XXI
1. General introduction	1
1.1 Motivation and objective	1
1.2 Overall framework	4
1.3 Dissertation outline	6
2. Additional background	8
2.1 The rockfall phenomenon	8
2.2 Social and economical implications of rockfall	9
2.3 General aspects of rockfall protection forests	12
2.4 Quantifying the protective role of forests	17
2.5 Features of broadleaf coppice relevant for rockfall	20
3. Assessing the mechanical resistance of coppice stems with full-scale pendulum impact tests	25
3.1 Introduction	25
3.2 Material and methods	26
3.3 Results	32

3.3.1	Test material	32
3.3.2	Pendulum tests	34
3.4	Discussion	44
3.5	Conclusion	51
4.	Full-scale impact tests in coppice forests. New insights on the rockfall protective function.	54
4.1	Introduction	54
4.2	Material and methods	57
4.2.1	Study site	57
4.2.2	Experimental setup	57
4.3	Results	59
4.4	Discussion	65
4.5	Conclusion	70
5.	Influence of tree species on the mechanical resistance against rockfall of small diameter trees	72
5.1	Introduction	72
5.2	Material and methods	77
5.2.1	Test material	77
5.2.2	Dynamic pendulum impact tests	77
5.2.3	Static 3-point bending tests	79
5.3	Results	80
5.3.1	Specimen properties	80
5.3.2	Dynamic pendulum impact tests	83
5.3.3	Static 3-point bending tests	90
5.4	Discussion	93
5.5	Conclusion	97
6.	Overall synthesis	99

7. References	103
8. Annex	116
8.1 High-speed camera image sequences of selected impacts conducted with the pendulum test device (chapters 3 and 5)	116
8.1.1 Impacts against beech specimens	117
8.1.2 Impacts against chestnut specimens	129
8.1.3 Impacts against fir specimens	133
8.2 High-speed camera image sequences of selected impact tests against beech coppice trees conducted with the forest test device (chapter 4)	136

Abbreviations

DBH [m]: Diameter of a tree measured at 1.3 m above ground

ΔE_{kin} [kJ]: Difference between the kinetic energy of an impactor before and after impacting a tree. This value is used (next to Δp) to quantify the potential of a tree to reduce the kinetic energy of an impacting rock. It is also referred to as mechanical resistance of a tree.

Δp [kg m s^{-1}]: Difference between the momentum of an impactor before and after impacting a tree. This value is used (next to ΔE_{kin}) to quantify the potential of a tree to reduce the momentum of an impacting rock. It is also referred to as mechanical resistance of a tree.

RMSPE: Root mean square percentage error

SD: Standard deviation

List of Figures

Figure 1.1:	Coppice clumps of (a) Hazel (<i>Corylus avellana</i> L.) (b) whitebeam (<i>Sorbus aria</i> L.) and (c) beech (<i>Fagus sylvatica</i> L.).	3
Figure 2.1:	Loss amount development of the cantonal building insurance of Zürich (GVZ).	12
Figure 2.2:	The rockfall hazard mitigating effect of forests.	13
Figure 2.3:	Exponential relationships between the tree diameter at breast height and the potential of a tree of reducing the kinetic energy of an impacting rock.	20
Figure 3.1:	Open-air impact pendulum device.	27
Figure 3.2:	Initial specimen configuration seen from the impact direction and illustration of the zone considered for central impacts around the central tree axis (CTA).	28
Figure 3.3:	Relationships between specimen mass and DBH for the first test series on 3 m segments and second test series on entire stems.	33
Figure 3.4:	Top view on the section of a specimen with ring shakes.	36
Figure 3.5:	Demonstration of the flexural deformation of an entire coppice tree during and after bob impact.	37

Figure 3.6:	The relationships between (a) Δp and DBH, (b) Δp and specimen mass for the first and second test series.	38
Figure 3.7:	The relationships between (a) ΔE_{kin} and DBH, (b) ΔE_{kin} and specimen mass for the first and second test series.	40
Figure 3.8:	$\Delta p / \Delta E_{kin}$ ratio for constant incident bob velocities.	41
Figure 3.9:	Δp and ΔE_{kin} as a function of the DBH (1 st test series).	42
Figure 3.10:	The decrease of the bob velocity during impact in 5 ms steps for four selected tests (cp. Table 3.2).	43
Figure 3.11:	Comparison of 3 models expressing the ΔE_{kin} -DBH relationship for 3 different species.	50
Figure 4.1:	Forest impact test device.	59
Figure 4.2:	Comparison of the forest tests of this study with the pendulum results of chapter 3 by referring to (a) Δp and (b) ΔE_{kin} plotted against the DBH.	64
Figure 4.3:	Comparison of four ΔE_{kin} -DBH relationships.	68
Figure 5.1:	Comparison of the stem taper of the three species defined as average diameter reduction per meter specimen length.	81
Figure 5.2:	Comparison of the stem mass-DBH relationships of all specimens of the three species.	82

Figure 5.3:	Occurrence of the main breakage types during impact.	84
Figure 5.4:	Section of a broken fir specimen.	86
Figure 5.5:	(a) Time to failure and (b) total impact duration of all specimens.	87
Figure 5.6:	Comparison of the relationships between ΔE_{kin} and DBH of the three species.	88
Figure 5.7:	Comparison of the relationships between ΔE_{kin} and specimen diameter at impact height of the three species.	89
Figure 5.8:	The mechanical resistance of all specimens expressed in kJ m^{-2} based on the respective specimen section surface at impact height.	90
Figure 5.9:	Comparison of the modulus of elasticity of all specimens.	91
Figure 5.10:	Comparison of the modulus of rupture of all specimens.	92
Figure 5.11:	Total bending energy of the static tests indicated by $E_{tot-ind}$.	93
Figure 8.1:	Image sequence of beech specimen S1 (chapter 3, Figure 3.10, Table 3.2).	117
Figure 8.2:	Image sequence of beech specimen S2 (chapter 3, Figure 3.10, Table 3.2).	118
Figure 8.3:	Image sequence of beech specimen S3 (chapter 3, Figure 3.10, Table 3.2).	119
Figure 8.4:	Image sequence of beech specimen S4 (chapter 3, Figure 3.10, Table 3.2).	120

Figure 8.5:	Image sequence of beech specimen 73.	121
Figure 8.6:	Image sequence of beech specimen 75.	122
Figure 8.7:	Image sequence of beech specimen 166.	123
Figure 8.8:	Image sequence of beech specimen E8 (entire stem).	124
Figure 8.9:	Image sequence of beech specimen E9 (entire stem; corresponds to the specimen depicted in Figure 3.5).	126
Figure 8.10:	Image sequence of chestnut specimen 822.	129
Figure 8.11:	Image sequence of chestnut specimen 832.	130
Figure 8.12:	Image sequence of chestnut specimen 836.	131
Figure 8.13:	Image sequence of fir specimen 514.	133
Figure 8.14:	Image sequence of fir specimen 532.	134
Figure 8.15:	Image sequence of fir specimen 537.	135
Figure 8.16:	Image sequence of two impactor-tree interactions in a coppice clump.	137
Figure 8.17:	Image sequence of four impactor-tree interactions in a coppice clump.	139

List of Tables

Table 3.1:	Details on the five test series.	31
Table 3.2:	Detailed properties of four representative 3 m long specimens (cp. Figure 3.10).	44
Table 4.1:	Details on the impact processes of all 13 test trees.	62
Table 4.2:	Rotational energy E_{rot} before and after impact.	65
Table 4.3:	Comparison of the impactor velocity and mass of the pendulum tests (chapter 3) and the forest tests of the present study.	67
Table 5.1:	Selected mechanical key properties of beech (<i>Fagus sylvatica</i> L.) chestnut (<i>Castanea sativa</i> Mill.) and fir (<i>Abies alba</i> Mill.).	76
Table 5.2:	The main properties of all specimens from the dynamic and the static tests.	83

Summary

In mountainous areas such as the Alps, forests protect human lives and infrastructure from natural hazards such as rockfall and avalanches. Rockfall protection forests are known as cost efficient mitigation structures that substantially reduce the hazard. In recent years they have been increasingly considered in rockfall hazard assessments and for land use planning.

For a reliable assessment of the rockfall protective function of forests the use of numerical simulation models relying on detailed site specific input data is the most appropriate approach. The input data include information on the potential of trees to reduce the kinetic energy of impacting rocks. This key parameter, also known as the mechanical resistance of a tree, has been assessed for the predominant conifers of the Alps (Norway spruce and silver fir) and mature European beech trees in previous studies based on full-scale impact tests in forests.

In contrast, the mechanical resistance against rockfall of small diameter broadleaf coppice trees is hitherto unknown. Coppice forests cover many lower altitude slopes of the Alps and they are often situated upslope of transportation routes and settlements where they fulfill a protective function. In addition to discrete rock-tree interactions the rockfall protective function of coppice forests is enhanced by numerous tree aggregations (coppice clumps) where impacting rocks get trapped and subsequently prevented from continuing their trajectory.

The objective of this dissertation is to quantify the mechanical resistance of small diameter broadleaf trees against rockfall. The aim is to supply reliable data for rockfall simulation models and to acquire additional understanding of the rock-tree interactions that are

substantially different from mature large diameter trees. The findings are also meant to provide a basis for better estimating the particular rockfall protective effect of coppice clumps.

The mechanical resistance of small diameter broadleaf trees (diameter at breast height (DBH) < 0.1 m) was assessed with full-scale dynamic impact tests. Two different test devices were used. The first was an open-air pendulum impact device where the root anchorage of the trees was replaced by a rigid restraint. This test arrangement allowed for carrying out numerous impact tests with relatively small effort. In this way, a large spectrum of different impact processes and the mechanical resistance of the trees as a function of their diameter could be assessed. The second test device was used in a coppice forest to impact trees that were part of coppice clumps. The main objective was to assess the representativeness of the pendulum results and to identify the key factors to be analyzed for naturally anchored trees.

All forest tests were done on beech (*Fagus sylvatica* L.). The pendulum tests included beech and for comparison also chestnut (*Castanea sativa* Mill.) and fir (*Abies alba* Mill.). The acquired data are suitable for being used as simulation model input data and they are more reliable than data of previous studies, because the impact process specific to small diameter trees (DBH < 0.1 m) was accounted for. It was found that the mechanical resistance increases exponentially with increasing tree diameter. For small diameter broadleaf trees the mechanical resistance is not determined by impact height at least for all impact heights between 0.2 and 1 m above ground. Impact tests showed that the impact angle influences the potential of trees to reduce the kinetic energy of impacting rocks. The natural root anchorage and the transition zone from the roots to the stems of coppice trees proved to sustain the stresses induced by the impacts. Hence, because these tree parts do not

constitute predetermined breaking points, the tests indicate that coppice trees in their natural environment are at least as resistant to dynamic impacts as those tested with the pendulum device.

Moreover, the results show that the impact process against small diameter trees (DBH < 0.1 m) is substantially different from larger diameter trees (DBH > 0.3 m). The high flexibility of the stems leads to relatively long lasting impact durations and only negligible damage at the point of impact on the stem. As a result, the mechanical resistance of the stems is partly determined by the impactor velocity and mass. This means that the mechanical resistance of a tree to dynamic impacts cannot be regarded as a constant material property. Consequently, the comparability of the acquired data as well as its application for the quantification of the rockfall protective function of forests is limited. This fact is certainly not restricted to small diameter stems. Therefore, it has to be evaluated in future studies whether it is necessary to consider impactor mass and velocity separately or if the implicated uncertainties of combining both impactor properties by referring to its momentum or kinetic energy are tolerable in rockfall hazard assessments.

Another major finding on small diameter trees is that most likely the mechanical resistance against rockfall impacts of the majority of broadleaf coppice species is not substantially different. Hence, future assessments of the rockfall protective function of coppice stands and other forests composed of small diameter broadleaf trees could be made without accounting for the spatial species distribution and the often manifold species composition. This could considerably facilitate forest inventories for acquiring simulation model input data and also simplify the rockfall simulations.

In addition to an emphasis on the implications of impactor velocity and mass, future studies should focus on the hazard mitigating effect of coppice clumps. Field observations and the findings of this dissertation indicate that this issue substantially contributes to the overall rockfall protective function of coppice forests. Further details on the effect of clumps could certainly also enhance and substantiate silvicultural interventions aiming to improve the long term protective function.

Finally, this work constitutes a decisive step towards a more objective quantification of the rockfall protective function of coppice stands. In addition to detailed data and understanding of the impact processes and breakage behaviors of the trees the dissertation highlights key issues on which future research should focus to increase the reliability of rockfall hazard assessments.

Résumé

En zone de montagne l'aléa chutes de pierres est un de ceux menaçant le plus de vies humaines et d'infrastructures. Les forêts situées entre les zones de départ de cet aléa et les enjeux en contre bas ont un rôle de protection. En effet, les arbres constituent des obstacles naturels pour les projectiles rocheux en mouvement. La quantification de ce rôle protecteur est nécessaire pour une évaluation réaliste du risque résiduel à l'aval des zones forestières et au niveau des enjeux menacés. Dans le contexte de l'aménagement du territoire, la prise en compte de cette fonction de protection des forêts permet à la fois d'optimiser l'occupation des sols et de minimiser, le cas échéant, les investissements nécessaires à la réalisation d'ouvrages de génie civil pare-pierres tels que des filets ou des merlons.

L'évaluation du rôle protecteur des forêts se fait généralement à l'aide de modèles de simulations trajectographiques de projectiles rocheux, modèles qui nécessitent pour chacun des sites d'études des relevés de terrain spécifiques. Pour réaliser une estimation précise, un des éléments clé dans les calculs est la caractérisation de la capacité des arbres à freiner et diminuer les hauteurs de rebonds des projectiles. Dans le contexte des chutes de pierres, cette propriété est souvent synthétisée sous le vocable : résistance mécanique d'un arbre. A ce jour, les principales données disponibles concernent principalement les conifères. Pourtant, dans des zones de montagne telles que les Alpes, les zones avals (< 1200 m d'altitude) des versants sont souvent couvertes par des taillis de feuillus. Ces peuplements se situent bien souvent à proximité et à l'amont de voies de communication et d'habitations, ce qui leur confère un rôle de protection. Les peuplements de type « taillis » se caractérisent par des arbres de faible diamètre qui croissent bien souvent en faisceaux qu'on appelle des cépées. Ces cépées sont issues la reproduction végétative sur des souches de feuillus, ces souches étant géné-

ralement obtenues par la réalisation d'une coupe rase du peuplement précédent. Compte tenu de ce mode de pratique sylvicole, la répartition spatiale des arbres au sens d'un taillis est donc de type agrégée.

Avant ce travail de thèse, la quantification du rôle protecteur des taillis était limitée par manque de données sur la résistance mécanique des arbres de feuillus de faible diamètre. En outre, les cépées fonctionnent souvent en tant que « petits filets de rétention » qui empêchent des pierres en mouvement de continuer leur trajectoire. Cependant, la contribution supplémentaire de cet effet particulier des cépées au rôle protecteur d'un peuplement n'avait jamais été évaluée à ce jour. En conséquence, les objectifs de cette thèse ont été de quantifier la résistance mécanique des feuillus de faible diamètre contre les chutes de pierres et d'accroître la connaissance et donc la compréhension des interactions pierres/arbres lors d'un impact dynamique. Les résultats obtenus peuvent entre autre être utilisés pour construire une base de données, dont l'analyse peut permettre une meilleure quantification et qualification de l'effet protecteur des cépées dans le futur.

Dans le cadre de ce travail de recherche, la résistance mécanique des feuillus de faible diamètre (diamètre à hauteur de poitrine (DHP) $< 0,1$ m) a été évaluée à l'aide de tests grandeur réelle d'impacts dynamiques. Deux dispositifs différents ont été conceptualisés et utilisés. Le premier était composé d'un pendule d'impact à l'air libre venant impacter une tige positionnée dans un dispositif où l'ancrage naturel des racines des arbres a été remplacé par un encastrement parfait. Ce dispositif expérimental a permis d'effectuer assez facilement un grand nombre de tests. Avec ce premier site expérimental il a été possible d'étudier différents processus d'impacts et d'évaluer la résistance mécanique des arbres en fonction de leur diamètre. Le deuxième dispositif a été conçu afin d'impacter, en forêt, des arbres

de cépées. L'objectif de ce deuxième dispositif a été d'évaluer la représentativité des résultats du dispositif pendule et d'identifier les facteurs déterminants des arbres naturellement enracinés.

Tous les tests en forêt ont été réalisés sur des tiges de hêtre (*Fagus sylvatica* L.). Les tests avec pendule ont, quant à eux, été menés sur des tiges de hêtre et pour des buts comparatifs aussi sur des tiges de châtaignier (*Castanea sativa* Mill.) et de sapin (*Abies alba* Mill.). Il a été montré que la résistance mécanique augmente de façon exponentielle avec un diamètre croissant. Pour des hauteurs d'impact entre 0.2 et 1 m la résistance mécanique n'est pas influencée par la hauteur d'impact. Les tests d'impact ont démontré que l'angle d'impact influence le potentiel d'un arbre à diminuer l'énergie cinétique d'un impactant. L'ancrage naturel des arbres par leurs racines et la zone de transition entre le tronc et le système racinaire ne constitue pas une zone de fragilité particulière. De ce fait on peut conclure que la résistance des arbres dans leur environnement naturel est au moins aussi élevée que celle des arbres testés avec le dispositif pendulaire.

Les résultats mettent en évidence que le processus d'impact sur des arbres de faible diamètre (DHP < 0.1 m) est substantiellement différent des arbres de diamètres plus larges (DHP > 0.3 m). La haute flexibilité des tiges induit une durée d'impact relativement longue et un endommagement de la tige au point d'impact d'une ampleur négligeable. De ce fait, la résistance mécanique des tiges est partiellement déterminée par la vitesse et la masse de l'impactant. En d'autres termes, la résistance mécanique d'un arbre à des impacts dynamiques ne peut pas être qualifiée comme étant une propriété constante du matériel. Par conséquent, l'utilisation de nos données expérimentales pour la quantification du rôle protecteur des taillis est à réaliser avec prudence. Cet état de fait ne concerne vraisemblablement pas que les arbres de faible diamètre. C'est pourquoi, il

faut dans l'avenir développer un nouvel axe de recherche pour déterminer s'il est nécessaire de considérer séparément la vitesse et la masse de l'impactant ou au contraire ne tenir compte que de la quantité de mouvement ou de l'énergie cinétique pour la prise en compte de l'action de la végétation forestière dans l'analyse du risque généré par les chutes de pierres.

Un autre résultat de cette thèse est que, pour des arbres d'essences feuillus de faible diamètre, la résistance mécanique lors d'un impact dynamique n'est pas fondamentalement différente d'une essence à l'autre. En conséquence, l'évaluation du rôle protecteur des taillis feuillus de faible diamètre peut être réalisé sans tenir compte ni de la répartition spatiale des tiges, ni de la composition en essences. Cette conclusion induit une simplification considérable des relevés forestiers pour l'acquisition des données d'entrées des modèles de simulations et des algorithmes de calculs.

Pour les recherches futures, si une inflexion des travaux sur la compréhension de la part respective de la vitesse et de la masse de l'impactant sur la résistance mécanique d'un arbre est nécessaire, il est tout aussi nécessaire de mener des travaux sur les motifs d'agrégations spatiales des arbres et plus particulièrement sur l'effet piège des cépées. Les observations de terrain et les résultats obtenus lors de cette thèse, confirment que la part des « structures » cépées dans la fonction de protection des peuplements de taillis est d'une ampleur non négligeable. Des travaux complémentaires sur l'effet mécanique des cépées permettraient aussi de mieux définir et cibler les interventions sylvicoles nécessaires à la pérennisation et l'optimisation de la fonction de protection des taillis et des autres peuplements forestiers.

Finalement, cet ouvrage constitue un pas en avant vers une quantification plus objective du rôle protecteur contre les chutes des

pierres des taillis alpins. En plus des données et d'une compréhension détaillée du processus d'impact et du comportement mécanique des tiges, l'étude met en avant les principaux axes de recherche nécessaires afin d'augmenter la fiabilité des expertises d'aléa des chutes de pierres dans le futur.

Zusammenfassung

In vielen Gebirgsregionen ist Steinschlag eine weitverbreitete Naturgefahr, die eine Bedrohung für die Bevölkerung und die technische Infrastruktur darstellt. Waldbestände, die sich zwischen Steinschlagquellen und gefährdeten Bereichen befinden, erfüllen eine Schutzfunktion, da die Bäume als natürliche Hindernisse den Niedergang von Steinen verhindern bzw. reduzieren. Durch die Quantifizierung dieser Schutzfunktion wird eine Berücksichtigung der Waldwirkung in Gefahrenanalysen ermöglicht. Es wird dadurch die Grundlage für eine optimierte Raumplanung geschaffen. Darüber hinaus können die Kosten für ingenieurbauliche Schutzmaßnahmen wie Steinschlagnetze und -dämme minimiert werden.

Die Schutzfunktion von Wäldern wird allgemein mit Hilfe von Steinschlag-Simulationsmodellen bestimmt, die auf ortsspezifischen Eingangsdaten basieren. Der Schlüsselfaktor für die Erstellung von verlässlichen Prognosen ist die Ermittlung des Potentials von Bäumen zur Reduzierung der kinetischen Energie eines niedergehenden Steines. In Bezug auf Steinschlag wird diese Eigenschaft häufig vereinfacht Baumstabilität genannt. Bislang vorhandene Daten zur Baumstabilität beziehen sich fast ausschließlich auf ausgewachsene Nadelbäume. In vielen Gebirgsregionen, einschließlich der Alpen, wachsen auf niederen Hanglagen (< 1200 m ü. NN) allerdings häufig Niederwälder. Sie befinden sich oft oberhalb von Verkehrswegen und Siedlungsräumen, wo sie eine Schutzfunktion gegenüber Steinschlag erfüllen. Niederwälder entstehen nach dem Kahlschlag eines Laubwaldes durch Ausschläge aus den verbliebenen Stämmen. Diese sogenannten Stockausschläge entwickeln sich nach einigen Wachstumsperioden zu einem Wald, der sich aus vielen Clustern von vornehmlich dünnstämmigen Bäumen (Stangenholz) zusammensetzt.

Die Möglichkeiten zur Quantifizierung der Schutzfunktion von Niederwäldern gegenüber Steinschlag sind derzeit begrenzt, da keine verlässlichen Daten zur Stabilität des Stangenholzes vorhanden sind. Darüber hinaus fungieren die einzelnen Stockausschläge häufig wie kleine Rückhaltezäune, die anprallende Steine auffangen bzw. deren Weiterrollen verhindern. Es bleibt allerdings unklar, in welchem Ausmaß dieser spezifische Effekt von Stockausschlägen die gesamte Schutzfunktion von Niederwäldern gegenüber Steinschlag erhöht. Vor diesem Hintergrund ist das Ziel der Dissertation, die Stabilität von Stangenholz gegenüber Steinschlag zu quantifizieren. Durch detaillierte Einblicke in die mechanischen Prozesse von Steinschlag gegen Stangenholz werden verlässliche Eingangsdaten für Steinschlag-Simulationsmodelle bereitgestellt. Die Erkenntnisse schaffen unter anderem eine Grundlage zur besseren Einschätzung des spezifischen Schutzeffektes von Stockausschlägen.

Im Rahmen der vorliegenden Arbeit wurde die Baumstabilität von kleinem Niederwald-Stangenholz (Brusthöhendurchmesser (BHD) < 0.1 m) durch dynamische Anpralltests bestimmt. Es kamen zwei unterschiedliche Versuchsaufbauten zum Einsatz. Bei der ersten Anlage handelt es sich um ein Freiluft Pendelschlagwerk, bei dem die Wurzelverankerung der Bäume durch eine feste, einseitige Einspannung ersetzt wurde. Durch diesen Versuchsaufbau konnte mit einem vergleichsweise geringen Aufwand eine Vielzahl von Anprallversuchen durchgeführt werden. Es konnten dadurch vielfältige Bruchverhalten analysiert und die Baumstabilität in Abhängigkeit des Baumdurchmessers bestimmt werden. Mittels des zweiten Versuchsaufbaus wurde der dynamische Anprall gegen einzelne, aus Stockausschlägen hervorgegangene Bäume in situ untersucht. Das Ziel bestand darin, die Repräsentativität der Pendelversuche beurteilen zu können und eventuelle Besonderheiten der natürlich verankerten Bäume zu analysieren.

Alle Versuche im Niederwald wurden an Buchen (*Fagus sylvatica* L.) durchgeführt. Mit dem Pendelschlagwerk wurden neben Buchen zu Vergleichszwecken auch Stämme von Edelkastanien (*Castanea sativa* Mill.) und Stämme von Tannen (*Abies alba* Mill.) getestet. Die Ergebnisse können als Eingangsdaten für Steinschlag-Simulationsmodelle verwendet werden. Sie sind zudem zuverlässiger als solche von vergangenen Untersuchungen, da das besondere Bruchverhalten von flexiblen Stangenhölzern berücksichtigt werden konnte. Es konnte ein exponentieller Anstieg der Baumstabilität mit dem Stammdurchmesser aufgezeigt werden. Die Anprallhöhe des Stoßkörpers bzw. Steines hat keinen Einfluss auf die Baumstabilität der Laubbäume für Anprallhöhen zwischen 0.2 und 1 m. Die Anprallversuche im Niederwald zeigen, dass der Anprallwinkel für das Potenzial der Bäume die kinetische Energie der Steine zu reduzieren ausschlaggebend ist. Es konnte auch festgestellt werden, dass die Wurzelverankerung und der Übergang zum Stamm keine mechanischen Schwachstellen darstellen. Folglich sind die im Wald getesteten Bäume mindestens so belastbar wie die Proben des Pendelschlagwerks.

Weiterhin zeigen die Ergebnisse, dass das Bruchverhalten von Stangenholz (BHD < 0.1 m) gegenüber dem von Baumholz (BHD > 0.3 m) sehr verschieden ist. Die hohe Flexibilität des Stangenholzes führt zu relativ langanhaltenden Anpralldauern und zu einer vergleichsweise vernachlässigbaren Beschädigung des Stammes an der Anprallstelle. Im Ergebnis zeigt sich, dass die Baumstabilität durch Geschwindigkeit und Masse des Stoßkörpers beeinflusst wird und somit nicht als konstante Materialeigenschaft betrachtet werden kann. Die Vergleichbarkeit und Nutzung der erhobenen Daten zur Quantifizierung der Steinschlag-Schutzfunktion von Wäldern ist folglich eingeschränkt. Eine Übertragbarkeit der für Stangenholz ermittelten Erkenntnisse auf die in der Praxis bereits verwendeten Daten zu ausgewachsenen Nadelbäumen ist nicht auszuschließen

und sollte durch weitere Versuche verifiziert werden. Im Mittelpunkt dieser Untersuchungen sollte die Frage stehen, inwiefern es nötig ist bei Steinschlag-Gefahrenanalysen die Geschwindigkeit und die Masse des Stoßkörpers getrennt zu betrachten. Diese Beurteilung sollte sich an den Unsicherheiten die aus einer Kombination beider Stoßkörpereigenschaften als mechanischen Impuls oder kinetische Energie resultieren orientieren.

Im Rahmen der mit Stangenhölzern durchgeführten Untersuchungen ließen sich keine signifikanten Unterschiede bei der Baumstabilität verschiedener Niederwald-Laubbaumarten feststellen. Zukünftige Bestimmungen der Steinschlag-Schutzfunktion von aus Stangenhölzern bestehenden Wäldern können folglich ohne Berücksichtigung der räumlichen Artenverteilung und der häufig vielfältigen Artenzusammensetzung durchgeführt werden. Vor diesem Hintergrund kann neben einer Erleichterung der für Steinschlag-Simulationsmodelle erforderlichen Waldinventuren auch eine Vereinfachung der Simulationen erreicht werden.

Neben einem Schwerpunkt auf den Implikationen von Stoßkörpergeschwindigkeit und -masse, sollten weiterführende Untersuchungen auch die spezifische Schutzfunktion von Stockausschlägen berücksichtigen. Feldbeobachtungen und die Erkenntnisse dieser Arbeit deuten darauf hin, dass der Effekt substantiell zu der Schutzfunktion von Niederwäldern beisteuert. Weitere Einblicke in diesen Aspekt würden sicherlich auch waldbauliche Maßnahmen zur Langzeit-Optimierung der Schutzfunktion von Niederwäldern verbessern und untermauern.

Schließlich stellt diese Dissertation einen entscheidenden Schritt in Richtung objektiverer Beurteilung der Steinschlag-Schutzfunktion von Niederwäldern dar. Zusätzlich zu detaillierten Daten und Erkenntnissen zum Anprallprozess und zum Bruchverhalten der

Stämme werden Schlüsselemente die im Fokus zukünftiger Untersuchungen zu Verbesserung der Steinschlag-Gefahrenanalyse stehen sollten hervorgehoben.

1. General introduction

1.1 Motivation and objective

In many mountainous regions rockfall is a common natural hazard threatening human lives and infrastructure (Evans and Hungr, 1993, Volkwein et al., 2011). Rock masses constituting rock faces in which failures potentially occur form source areas for rockfall of a wide range of magnitudes and frequencies. A typical low magnitude event is fragmental rockfall in which one or several individual rocks are involved (Evans and Hungr, 1993). A high magnitude event is rock mass fall, which refers to failure and downslope movement of large rock masses (Nemcök et al., 1972). Forests situated between source areas producing fragmental rockfall and potential elements at risk might have a protective function, because the trees can act as natural barriers for falling rocks (Jahn, 1988, Dorren and Berger, 2005, Stoffel et al., 2005, Dorren et al., 2007). Being able to quantify this protective effect allows accounting for the mitigating effect of forests in rockfall hazard assessments (Dorren et al., 2007, Jancke et al., 2009, Clouet et al., 2012). In recent years this has been increasingly done in the Alps, because it allows for optimizing investments in technical (civil engineering) protective measures, such as rockfall nets and dams, as well as in biological measures, such as forests.

The protective function of forests is generally assessed with the help of rockfall simulation models relying on site specific data (Dorren et al., 2007). For accurate predictions, the potential of the trees to reduce the kinetic energy of rocks during tree impacts is a decisive element (Dorren and Berger, 2005, Jonsson, 2007, Lundström et al., 2008). In the context of rockfall, this property is often referred to as the mechanical resistance of a tree. The hitherto available data on the mechanical resistance of trees is restricted to mature conifers

(Norway spruce and silver fir) and European beech that constitute the majority of the alpine protection forests (Couvreur, 1982, Dorren and Berger, 2005, Jonsson, 2007, Kalberer et al., 2007, Lundström et al., 2008, CIPRA, 2012). However, in temperate mountainous regions including the Alps, many low altitude slopes (< 1200 m a.s.l.) are covered with broadleaf coppice stands (Jancke et al., 2009). They are often situated upslope of transportation routes and settlements where they fulfill a protective function. Coppice forests are characterized by mainly small diameter trees that grow in clumps of multi-stemmed trees (Figure 1.1a, b and c). These clumps develop from the stools of broadleaf trees after clearcuts and cause a clustered spatial stem distribution (Mayer, 1992, Jancke et al., 2009).

Today, the quantification of the rockfall protective function of coppice stands is limited by a lack of data on the mechanical resistance of small diameter broadleaf trees (Dorren et al., 2007, Jancke et al., 2009). Moreover, coppice clumps often function as small rockfall retention fences, because falling rocks get trapped by the stems and are subsequently hindered to continue their trajectory (Figure 1.1c). However, the additional contribution of this particular effect of clumps to the protective function of coppice stands has never been evaluated (Dorren et al., 2007, Jancke et al., 2009). Additional background on rockfall processes and protection forests is provided in detail in Chapter 2.



Figure 1.1: Coppice clumps of (a) Hazel (*Corylus avellana* L.) (b) whitebeam (*Sorbus aria* L.) and (c) beech (*Fagus sylvatica* L.).

The objective of this dissertation is to quantify the mechanical resistance of small diameter broadleaf trees against rockfall. The aim is to supply reliable data for rockfall simulation models and to acquire additional understanding of the rock-tree interactions. The findings are meant to provide a basis for more objective future considerations of coppice stands and other forests composed of small

diameter broadleaf trees in rockfall hazard assessments. A more reliable quantification of this ecosystem service could improve its general recognition and allow for the implementation of optimal long term rockfall mitigation measures including forest management strategies. This could help reducing the costs of damages due to rockfall as well as for expensive civil engineering mitigation measures.

1.2 Overall framework

This dissertation aims to demonstrate that the rockfall protective function of coppice stands relies on a multitude of parameters specific to this forest type. The present approach with a focus on the mechanical resistance of the trees constitutes a decisive element towards an objective quantification of the protective function. However, an optimized application of the findings in rockfall hazard assessments would require considering several further research issues. In this context, the suggested overall framework below helps to integrate the dissertation (issue 2) into a broader perspective.

An overall approach for gaining knowledge on the protective function of various kinds of coppice forests against rockfall should address five key issues:

1. Developing of a rockfall specific typology of coppice stands

Here, the most prevalent coppice types should be classified with regard to species composition, spatial structure, stand history, growth dynamics, diameter distribution and stand density. The aim should be to consider the multitude of coppice appearances and to account for the main rockfall specific implications. The typology could be integrated into forest management guidelines and be used as decision support for practitioners and decision makers.

2. *Quantification of the mechanical resistance of **individual** coppice trees that are part of coppice clumps to rockfall impacts (main topic of this dissertation)*

This assessment should be based on full-scale impact tests. These tests should be representative for rockfall in coppice forests in terms of tree species, frequent tree diameters and impactor velocity and mass. The approach should regard the influence of the main rock properties (velocity, mass and shape) and the main tree properties (diameter, mass, species specific mechanical wood strength, and ground anchorage) on the mechanical resistance and the breakage behavior of coppice trees during rockfall impacts. Based on the findings, subsequent numerical modeling of the impact processes could be a valuable tool to extend the data to other than the tested impact configurations.

3. *Quantification of the effects of **entire coppice clumps** to rockfall impacts*

Here, the focus should be on the three main rockfall specific effects of coppice clumps (cp. chapter 2: additional background):

- Tree-tree interactions
- Serial rock-tree interactions
- Rock 'catching' and retention effect

In addition to half- or full-scale tests, a numerical modeling approach might facilitate this intricate task.

4. *Integration of the acquired data into a rockfall simulation model*

This model should account for the mitigating effects of both individual coppice trees that are part of coppice clumps and entire coppice clumps (i.e. issues 2 and 3).

5. Model validation

The model validation should be based on field data of past events and be in accordance with the quantitative data and the qualitative observations of all full-scale impact experiments.

Some of the aspects of issue 1 are addressed in Jancke et al., 2009. The approach helped to figure out on which aspects to focus in future studies. However, the study showed that more field data on an alpine scale are necessary to come up with a rockfall specific typology of coppice stands. Moreover, such a typology would be even more valuable if based on the quantitative data of issues 2 and 3. With a focus on the mechanical processes of rock-tree interactions during rockfall impacts against small diameter trees (issue 2), this dissertation aims to provide a basis for quantifying the rockfall protective function of coppice forests.

1.3 Dissertation outline

Chapter 2 provides additional background on rockfall and protection forests. It includes socio-economic implications and developments and emphasizes the rockfall specific particularities of coppice stands.

The main section of the Dissertation is divided into three studies constituting chapters 3, 4 and 5. Each study has been conducted independently and focuses on different elements of the rock-tree interactions of small diameter stems (diameter at breast height (DBH) < 0.1 m) during rockfall impacts.

The first study (chapter 3) focused on the mechanical resistance of small diameter fresh beech (*Fagus sylvatica* L.) stem segments. Dynamic full-scale impact tests with a specific open-air pendulum de-

vice permitted both to assess quantitative data and to make detailed qualitative observations of the impact processes. Moreover, the device allowed for carrying out numerous impact tests with relatively small effort. In this way, a large spectrum of different impact processes and the variability of the quantitative data could be assessed. The main objective was to establish a mathematical relationship between stem diameter and the mechanical resistance in order to provide species specific input data for rockfall simulation models.

The second study (chapter 4) aimed at comparing the data of the pendulum results with full-scale impact tests against beech coppice trees in a forest. The main objective was to assess the representativeness of the pendulum results and to identify the factors to be considered for naturally anchored trees. Because these field experiments were very laborious, the number of tests was limited. However, as a complement to the results of the preceding pendulum tests this study considerably strengthened the reliability of the data.

The third study (chapter 5) focused on the influence of tree species on the mechanical resistance against dynamic impacts. The study was based on dynamic and static mechanical tests on fresh stem segments of three tree species with very different anatomical wood structure and dry wood properties (beech (*Fagus sylvatica* L.), chestnut (*Castanea sativa* Mill.) and fir (*Abies alba* Mill.)). The main objective was to assess to what degree the data of the first two studies on beech were appropriate for conclusions to be drawn on the mechanical resistance of other species common in alpine forests.

The dissertation concludes with a synthesis of the main findings and their implications.

2. Additional background

2.1 The rockfall phenomenon

Rockfall is a natural process. In mountainous regions any surface of bare rock including various types of cliff faces degrades with time. This degradation is a long term process and its progression depends on various factors that can be categorized in internal parameters and external factors (e.g. Volkwein et al., 2011). The internal parameters refer to immanent aspects such as relief, geology, fracturing and other rock mechanical properties. The external factors can influence the internal parameters and include gravitational effects, hydrological factors, weathering, freeze and thaw processes, human activities, tectonics and many more (Jaboyedoff and Derron, 2005, Dorren et al., 2007, Volkwein et al., 2011). Rockfall is a part of the degradation process and defined as the removal of small and large rock fragments, or even large rock masses, that accelerate due to gravity. Subsequent rockfall trajectories of individual rocks on a talus slope below a cliff face are characterized by rolling and bouncing depending on the slope inclination and other parameters (e.g. Dorren, 2003). The term rockfall covers magnitudes reaching from fragmental rockfall to large rock mass falls of several million cubic meters and involves a plethora of different occurrences. The focus of this dissertation is limited to fragmental rockfall with volumes up to several cubic meters, because for volumes of more than five cubic meters the protective effect of forests against rockfall reduces rapidly (cp. Berger et al., 2002). Throughout the dissertation rock size will be indicated in metric units where necessary and the term rock will be used for all sizes without referring to gravel, cobbles, stones or boulders.

In mountainous regions such as the Alps, the natural process of rockfall threatens human lives, settlements and road and railway infrastructure. In contrast to other natural hazards (e.g. snow avalanches) rockfall is a widespread phenomenon and not restricted to a particular season or altitude. Nevertheless, rockfall frequency is increased during freeze and thaw cycles (springtime) and heavy rainfalls (Krautblatter and Moser, 2009). Although various methods have been developed in the past, both rockfall frequency and magnitude remain difficult to predict (Corominas et al., 2005, Stoffel et al., 2005, Dorren et al., 2007, Krautblatter and Moser, 2009, Volkwein et al., 2011). Generally, if reliable data on the source area are not available, the assessment often relies on recorded data on past events (Jaboyedoff and Derron, 2005) or dendrogeomorphology (Stoffel et al., 2005, Stoffel et al., 2010).

2.2 Social and economical implications of rockfall

In densely populated mountainous areas the increasing impact of rockfall on society is not determined by a change in rockfall frequency, but by human activities in rockfall hazard zones. In the Alps, an overall increase of the rockfall risk over the last 100 years is related to the emerging prosperity of the region (Bätzing, 2002). The human activities refer to the use and extension of the technical infrastructure (e.g. housing, roads and railways) and include the local population as well as externals (including tourists and all sorts of transients). Moreover, lifestyle and leisure activities of the local population and tourists play a role. The causes of the risk increase can be divided into an increase of the probability of rockfall accidents and an increase of the expected loss in the case of an accident.

The economic growth led to an increase of the probability of rockfall accidents due to the inevitable expansion of transport infrastructure

and housing (urban sprawl) to rockfall hazard zones (Bätzing, 2002). The three factors most accounting for the exposition to rockfall hazards are residents, tourists and freight transport. The total alpine population did not substantially increase since the 1950's and adds up to approximately 14 million residents today who principally live in the larger cities and main valleys (Bätzing, 2002, Alpine Convention, 2010). However, due to increased mobility the frequentation of endangered areas increased due to work, lifestyle and leisure activities (Perlik, 2011). In addition about 120 million tourists spread into the Alps every year (Alpine Convention, 2010). They frequently access remote areas such as narrow valleys where vast active rockfall slopes or cliff faces are situated just upslope of the main transportation routes. Here hazard mitigation measures have only limited effect and rockfall events regularly attain technical infrastructure. Finally, 190 million tons of freight transported across the Alps every year also condition the probability of rockfall accidents (Alpine Convention, 2010).

However, the rockfall related individual death probability (DP) on a country scale is with 10^{-8} per year very low (Hungr, 2011; for comparison the annual DP of being struck by a lightning is about 10^{-6} (Schneider, 1996)). In the case of France with about 65 million inhabitants this corresponds to one to two casualties due to rockfall per year (Hungr, 2011). Nevertheless, locally (e.g. for a daily car commuter) the death probability can exceed 10^{-5} . In Switzerland for instance, this threshold is now used to identify areas of high risk and constitutes a key element for the prioritization of countermeasures (FEDRO, 2010).

Hence, because the number of fatalities is relatively low, the main societal impacts of rockfall are of financial nature. The expected loss in the case of an accident can be divided into direct and indirect expenses. Additional costs result from hazard prevention including

rockfall hazard assessments and the installation of bio and civil engineering mitigation measures. With regard to infrastructure, a substantial part of the costs result from reparation of rockfall damage (direct expenses). However, the closing of major transportation routes can exceed the expenses of the actual damage by far resulting in considerable costs for the economy and population (indirect expenses; FEDRO, 2010). A well documented example is the closure of the 'Gotthard highway' A2 near Gurtellen in Switzerland (Kanton Uri, 2012). This highway had been closed during one month after a major rockfall in 2006 that claimed two casualties. In this case the economical losses even affected regions far beyond the Alps, because the highway constitutes one of the main transportation routes between Germany and Italy.

Rockfall related prevention costs refer in particular to the installation and maintenance of expensive civil engineering rockfall mitigation measures (including fences, dams and galleries). In many cases such measures are taken with hindsight after rockfall events, when the dislocation of the elements at risk is more costly than the mitigation measures. This is symptomatic for most natural hazards and demonstrates in some cases a lack of space, but in most cases a lack of awareness. In this context Figure 2.1 illustrates exemplarily the increase of the insurance loss amount expressed in percent of the total annual loss amount of the Swiss cantonal building insurance of Zürich (GVZ) since the 1970's. Whereas the loss amount for fire incidents decreased due to improvements in prevention and fire-fighting, the loss amount of all natural hazards combined shows an increase and is predicted to further increase in the future. This development is due to an underestimation of the hazard situation during planning and construction rather than to an increase of natural hazard events (Aller, 2012).

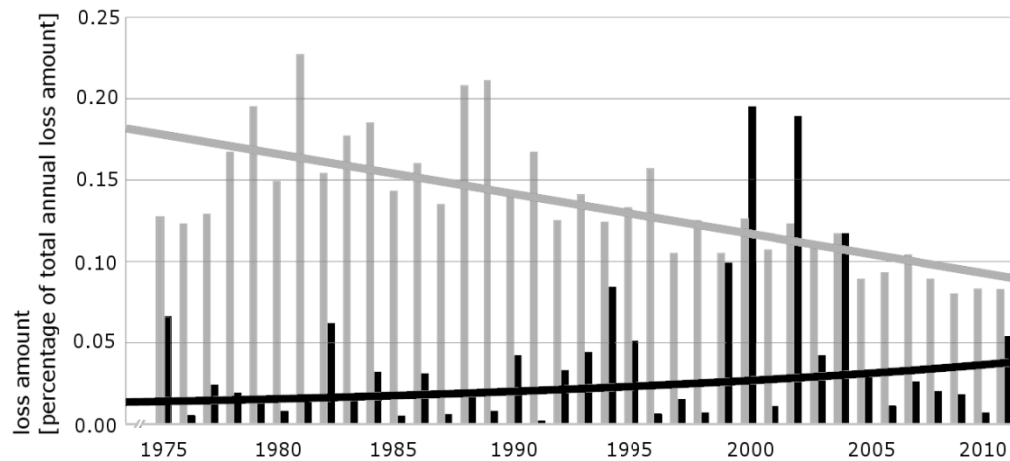


Figure 2.1: Loss amount development of the cantonal building insurance of Zürich (GVZ). Black bars: Increase of loss amount of all natural hazards combined. Grey bars: decrease of losses due to fire incidents (GVZ, 2011).

2.3 General aspects of rockfall protection forests

In the Alps, the protective role of forests against rockfall has been recognized for centuries (Motta and Haudemand, 2000). Rockfall protective forests are situated in the transition zone between the rockfall source area (e.g. cliff face) and the elements at risk (Figure 2.2). On their downslope trajectories the rocks encounter trees as natural obstacles. These tree impacts lead to a reduction in kinetic rock energies and bouncing heights (Dorren et al., 2007). In many hazard situations minimal silvicultural interventions can assure a sufficient long term protection by the forest alone. In other cases forests constitute a key protective element in addition to civil engineering measures (Motta and Haudemand, 2000, Dorren et al., 2007). For rock volumes of more than five cubic meters the protective effect of forests against rockfall is considered to become less effective (Berger et al., 2002).

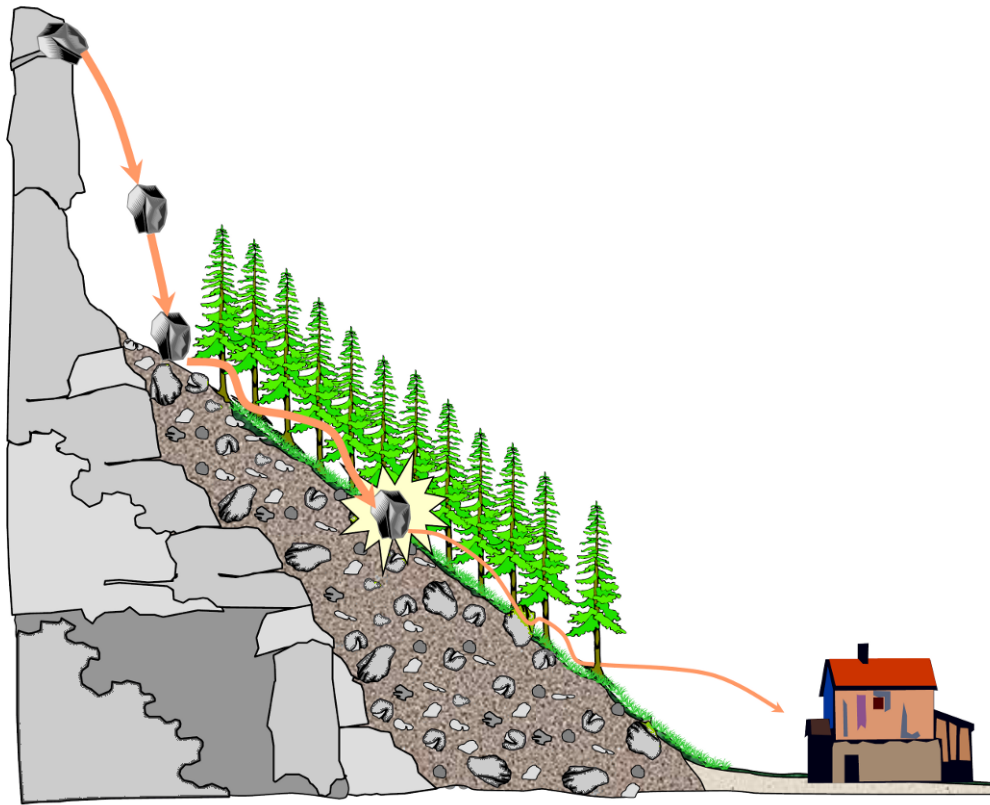


Figure 2.2: The rockfall hazard mitigating effect of forests. The trees act as natural obstacles in the rockfall transition zone between source areas and elements at risk (illustration: Frédéric Berger).

The protective role of a forest is conditioned by a plethora of factors. The most determining include the rock energy, forest properties such as the tree diameter distribution and stand density, the mechanical resistance of the trees, and the length of the forest in downslope direction. As a rule of thumb, for rocks of small volumes ($< 0.1 \text{ m}^3$) the stand density is the most determining parameter. That is, the higher the stand density, the higher the protective role, because in this case the mechanical resistance of the trees is less important than the impact probability (Jahn, 1998, Frehner et al., 2005, Dorren et al., 2007, Woltjer et al., 2008, Jancke et al., 2009). For large rocks of 1 m^3 and more, stand density remains important, but tree diameters have to be larger to be able to reduce the kinetic

energy of the rocks (Frehner et al., 2005, Dorren et al., 2007, Woltjer et al., 2008, Jancke et al., 2009). The total length of the forested part of a slope is extremely important as well, but hardly influenceable.

These general facts have two decisive consequences in theory. First, for a given hazard situation (i.e. rock sizes and energies) there is a potential stand development stage that offers optimal protection. Second, the state of optimal protection will not persist in time due to the forest growth dynamics. This dilemma has been addressed by various authors (e.g. Motta and Haudemand, 2000, Dorren et al., 2004, Frehner et al., 2005, Brang et al., 2006, O'Hara, 2006). The overall agreement is that it is best to maintain a forest in a suboptimal phase achieved with minimal silvicultural interventions to aim for a rather constant 'optimal long term' protective function. On the one hand this requires both precise knowledge on the rockfall hazard situation and the actual protective function of the forest. On the other hand, detailed insights on the consequences of silvicultural measures undertaken in a given forest ecosystem are needed (Brauner et al., 2005, Woltjer et al., 2008, Rammer et al., 2010). In this context, the Swiss guidelines for minimal tending of protective forests (Frehner et al., 2005) constitute a first approach to help practitioners and decision makers to address the described intricate task of maintaining the forest in an optimal long term state for rockfall protection. These guidelines refer to minimal values for stand density, tree diameters and other key parameters for different forest types and constitute a key tool for protection forest management. However, it is true that even sophisticated scientific approaches involve substantial uncertainties, both with regard to forest growth dynamics and to rockfall frequency and magnitude. Therefore, the theoretical aim of an optimal long term protective function might only rarely be achieved in reality.

Over the last decades mountain forestry has become expensive and in many regions exploitation costs are barely covered by the gains for timber sales (Brändli, 1999, Courbaud et al., 2010). The major reasons are limited rationalization possibilities of the labor intensive work on steep terrain as well as unfavorable forest property structures (Avocat et al., 2011). In combination with a reduced demand for local fire and construction wood, this development led to both increasingly aged forests and an increase of the stock of wood in the forests (Brändli, 1999, Courbaud et al., 2010, Avocat et al., 2011). Consequently, forests with a rockfall protective function tend to be more and more in development stages beyond optimal protection. Therefore, in many areas, there is a trend from exploitation to primarily protection forestry. The challenges of a focus on protection management are firstly that the costs for necessary silvicultural interventions cannot be covered with timber sales anymore. Secondly, successful interventions depend on the effective cooperation between experts, practitioners and decision makers (Motta and Haudemand, 2000, Dorren et al., 2004). Funding often results in a compromise between local and regional governments or governmental institutions and to some extent timber sales. However, leaving the felled trees on the forest ground increases the surface roughness and hence the protective function of the forest (Bourrier et al., 2012). Therefore, timber extraction should always be deliberated.

Current developments in alpine forestry are increasingly affected by the emerging demand for fuel wood as a renewable energy. The overall impact of this forest use on carbon sequestration depends on numerous context specific factors and is currently object of a scientific controversy (Köhl et al., 2009, Nitsch, 2009, Courbaud et al., 2010, Avocat et al., 2011, Hudiburg et al., 2011). In the French Alps and other alpine regions, the main implications derive from local and regional combined heat and power plants that aim to recover the energy from small diameter industrial wood and slash from lumber

operations (Avocat et al., 2011). Consequently, the increasing demand for fuel wood has led to a reconsideration of the large timber reserves situated on slopes where harvesting is cost-intensive (Courbaud et al., 2010, Avocat et al., 2011). In addition, the above-average stock of wood and the advanced forest development states in these areas lead to an increased susceptibility for calamities. This increases uncertainties for both forest management and climate change adaptation strategies (Courbaud et al., 2010). Consequently, it is hitherto difficult to predict how alpine forestry will develop in the future. Beyond any doubt these increased and sometimes competing or contradictory demands for the vast forest ecosystem services of mountain forests on local, regional, national and international level constitute major future challenges for all implicated stakeholders (Millennium Ecosystem Assessment, 2005, Courbaud et al., 2010). In this context it is crucial to prioritize the protective role of forests and to seek for further recognition of this essential function.

Considerable research efforts on rockfall and protection forests have contributed to improve both in-depth knowledge on the processes and awareness of the protective role of the forests among practitioners, decision makers, and local population in general (Frehner et al., 2005, Dorren et al., 2007, Volkwein et al., 2011). The cooperation of the parties involved on local, regional and international level constitutes a cornerstone for the long term recognition and existence of rockfall protection forests. This helps to maintain the forests as an integral part of the mountain landscape including most of its ecosystem services. Today, the protective role of a forest can be quantified in terms of the potential of rockfall hazard mitigation and in monetary values. Both approaches permit to integrate the forests into hazard and risk analyses that help to take optimal long term mitigation measures (Volkwein et al., 2011). Because forests are a very cost efficient means of protection, the expenses for ex-

pensive civil engineering mitigation measures can be reduced (Jancke et al., 2009, Dorren et al., 2007). However, in reality the implementation of this idea depends on the objectivity of the used hazard assessment approach and on the priorities of those who carry out the expertise. A profit oriented company selling civil engineering protection measures might not consider the forest in the same way as an independent group of experts.

2.4 Quantifying the protective role of forests

Although today forests are increasingly considered in hazard and risk assessments, the methods applied to quantify the protective function decisively influence the reliability of the results. The scope of quantification methods reaches from the inventory of silent witnesses (i.e. rockfall deposit locations) on site and records of past events via empirical models, stochastic approaches, one- and two-dimensional simulation models to sophisticated three-dimensional physical process based models and discrete element approaches combined with GIS-data and LIDAR remote sensing technology (Dorren et al., 2003, Dorren et al., 2007, Bourrier et al., 2009). The output data quality is very sensitive to the quality of the input data and the expertise of the model operator. These two factors are often more decisive for the reliability of the output data than the used approach itself. Therefore, intensive site inspection is a prerequisite for successful hazard assessment. Furthermore, all available information (e.g. silent witnesses, historical records) combined with empirical models (e.g. energy line principle (Heim, 1932, Meißl, 1998)) has to be used for counterchecking the output data of a more sophisticated model.

If these conditions are fulfilled, three-dimensional physical process based models can lead to satisfying and detailed results, especially when based on high resolution digital elevation models (Dorren et

al., 2007, Volkwein et al., 2011). When the protective role of the forest is considered, the key model input data include the main parameters conditioning the loss of kinetic energy or momentum and trajectory changes of a given rock due to tree impacts. Ideally, this would include on the one hand rock specific parameters referring to the material, shape, mass, translational and rotational velocity, and impact angle, height and centrality of the impact. On the other hand tree parameters such as the position on the slope, tree species, diameter, height, inclination, vitality and root anchorage are decisive (Foetzki, 2004, Jonsson, 2007, Dorren, 2012). One of the most decisive of these parameters, the effective potential of a given tree to reduce the velocity of a given rock cannot be derived theoretically from the tree parameters above. This attribute, often referred to as the mechanical resistance of a tree, has to be assessed with laborious full-scale impacts against forest trees (Foetzki, 2004, Dorren and Berger, 2006, Jonsson, 2007, Lundström, 2008). Other approaches based on static half- and full-scale tests and dynamic small- or half-scale tests have shown to lead to considerable underestimations of the mechanical resistance of trees (Jonsson, 2007).

Because the mechanical resistance of trees is a key determining factor for a reliable quantification of the protective role of forests, several full-scale approaches have been realized in the past. They are documented in Couvreur, 1982, Mizuyama and Narita 1988, Dorren and Berger, 2005, Dorren et al., 2006, Jonsson, 2007, Dorren et al., 2007, Kalberer et al., 2007, Lundström, 2008. Most of these studies refer to two major experiments in France (near Vaujany) on silver fir (*Abies alba* Mill.) and in Switzerland (near Davos) on Norway spruce (*Picea abies* (L.) Karst.). In addition to a considerable gain of understanding of the processes governing dynamic rock-tree interactions, two studies published exponential relationships between the tree diameter at breast height (DBH, measured at 1.3 m above ground) and the potential of reducing the kinetic energy of an impacting rock

(Dorren and Berger, 2005, Jonsson, 2007; Figure 2.3). The associated equations are suitable as simulation model input data. However, both had to be based on several assumptions potentially involving considerable uncertainties that will not be discussed here in detail. The main restrictions were that each approach focused on only one coniferous species and few impact tests against rather large trees. As a result, the influence of the rock mass and velocity on the degree of mechanical resistance of the trees was not assessed. Nevertheless, both relationships are not fundamentally different while being based on different approaches and referring to two coniferous species with similar wood anatomical structure and habitus. This indicates that the relationships could also be valid for other alpine coniferous genera with minor structural differences (e.g. *Pinus sp.*, *Larix sp.*).

Finally, despite the given uncertainties the use of these data in modern physical process based models such as Rockyfor3D leads to very satisfying and detailed results. Of course there is still room for improvements especially with regard to predictions of rockfall frequencies, magnitudes, shapes, movements (especially rebounds) and also rock-tree interactions.

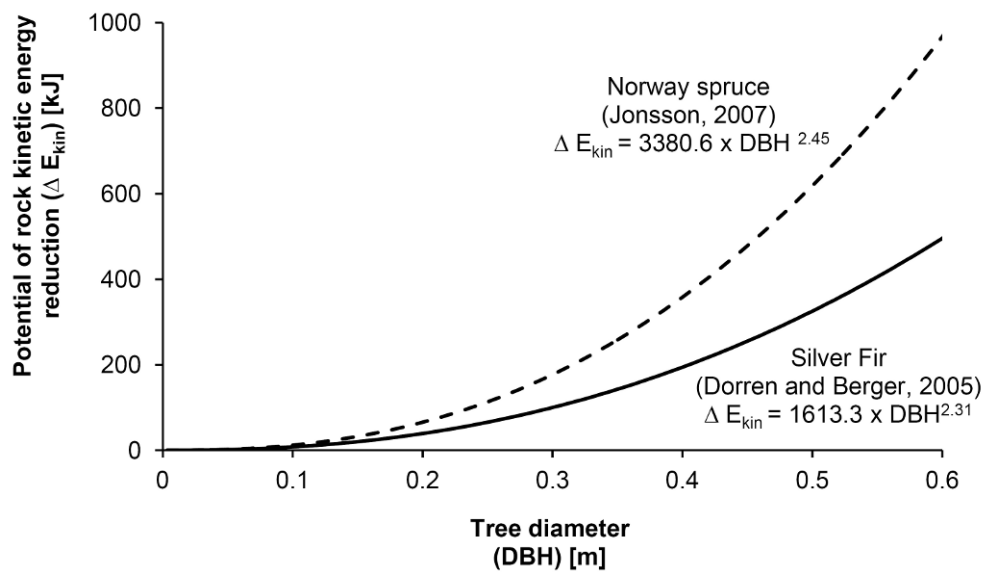


Figure 2.3: Exponential relationships between the tree diameter at breast height and the potential of a tree of reducing the kinetic energy of an impacting rock. Dorren and Berger (2005) are referring to Silver fir; Jonsson (2007) is referring to Norway spruce.

2.5 Features of broadleaf coppice relevant for rockfall

Most previous studies on the mechanical resistance of trees against rockfall focused on conifers that constitute mature high forests. As approximately 80% of the alpine forests are composed of conifers (primarily Norway spruce, CIPRA, 2008) the findings can be applied to a maximum of rockfall protection forests. However, at lower altitudes (< 1200 m a.s.l.) many alpine slopes are covered with deciduous coppice forests (Jancke et al., 2009). Often they are situated upslope of settlements and transport infrastructure where they fulfill a protective function against rockfall.

Coppice forests differ largely from high forests, because they regenerate vegetatively from tree stools (living stumps) following clearcuts. During the subsequent vegetation periods the new shoots develop to clusters of trees (i.e. multi-stemmed trees) called clumps (Figure 1.1). The length of the cutting cycles is very variable depending on management objectives and growth dynamics. Historically, coppicing was a widespread management practice, providing wood supply for various purposes for local populations over centuries. The main uses, fuel wood and charcoal production, were widespread throughout the Alps until the 20th century. With the subsequent substitution with coal and fossil fuel and increasing wealth in the second half of the 20th century coppicing declined (Mayer, 1992, Unterrichter, 1996, Agnoletti, 2002).

Today, coppice forests remain in many areas and even extend on former agricultural land. In general, they tend to be rather poorly managed. The main reasons are either difficult harvest conditions (e.g. on steep slopes just upside of transportation routes) or a heterogeneous forest ownership structure resulting in very small and thus inefficient management units. In these areas, occasional fuel wood supply for household purposes (clearcut surfaces well below 1 ha) entails generally the only interventions maintaining the coppice forests.

In analogy to other mountain forests increasing demand of combined heat and power plants for fuel wood has led to a reconsideration of coppicing as a very productive management practice. In the French Alps for instance current efforts to enable small privately owned coppice stands for larger scale management operations might substantially modify these woodlands in the near future (Avocat et al., 2011).

In areas where coppice forests fulfill a rockfall protective function (for instance against small rocks of football size) a lack of management often leads to a considerable decrease of stand density and hence a reduced potential for rockfall mitigation. When the rockfall threat becomes more evident because rocks exit at the downslope edge of the coppice stands, a common countermeasure recommended in national management guidelines (Frehner et al., 2005, Gauquelin et al., 2005) and executed throughout the Alps are small clearcuts (downslope length not extending 20 m). Although, this increases the rockfall hazard in the short term, only a few growth seasons later the coppice shoots generally constitute a dense thicket with increasing protective effect. On a slope scale, the regeneration of well distributed small patches (e.g. 40 x 20 m) with differed cutting cycles can be a good practice in order to maintain an optimal long rockfall protection state. However, the interventions should always comply with the effective regrowth of the patches before clearcutting a new series, because otherwise the rockfall hazard could be increased over a long time period (Jancke, 2007).

In the Alps, the most prevalent coppice species are beech (*Fagus sp.*), oak (*Quercus sp.*), chestnut (*Castanea sativa* Mill.), lime (*Tilia sp.*), maple (*Acer sp.*), ash (*Fraxinus sp.*), hazel (*Corylus avellana* L.), whitebeam and wild service tree (*Sorbus sp.*), hornbeam (*Carpinus betulus* L.), hop hornbeam (*Ostrya carpinifolia* Scop.) and increasingly black locust (*Robinia pseudoacacia* L.) (Jancke et al., 2009, Radtke et al., 2012). Field observations and a handful of studies confirm that coppice forests have the capacity to mitigate small-scale rockfall up to 1 m³ (Gsteiger, 1993, Gerber and Elsener, 1998, Schwitter, 1998, Frehner et al., 2005, Gauquelin et al., 2006, Jancke et al., 2009). However, no quantitative data on their mechanical properties are available and only few details on their mechanical response to rockfall are known (Jancke et al., 2009). In fact, the low wood quality led to the use for fuel wood and other mi-

nor products and thus to no interest of studying the mechanical wood properties in detail in the past. The low quality is due to the dense clump structure and also the slope inclination that cause various irregularities such as crooked or twisted growth and numerous branches (overgrown, dead or alive) implicating considerable growth stresses and the formation of tension wood (a particular wood tissue with over average tensile strength and impact toughness that trees use to influence the growth direction (Clarke, 1939, Pechmann 1953, Braun et al., 1982, Ferrand, 1983, Archer, 1986, Mattheck 1997, Fonti 2002)).

Another rockfall specific feature of coppice stands that has been poorly studied in the past is the fact that the dense spatial structure of a clump acts like a small retention fence where rocks get trapped between the stems (Dorren et al., 2007, Jancke et al., 2009, Figure 1.1b). The short distances between the stems of a clump condition the deceleration process of an impacting rock in three main ways. First, the dense clump structure increases the probability of localized serial rock-tree interactions where the rock continuously loses kinetic energy. Thus, in contrast to high forests the rock does not re-accelerate due to slope inclination between several tree contacts. Second, the short distances between the trees of a clump increase the probability of rock energy dissipation by tree-tree contacts (i.e. from stem to stem or crown to crown). This reduces the stresses an individual tree has to sustain and therefore indirectly amplifies its energy dissipative capacity. Third, the distances between the trees of a clump being generally smaller than the rock diameter, prevent the rock from continuing its trajectory due to slope inclination once it has lost almost its entire kinetic energy. Hence, for the quantification of the rockfall protective function of coppice stands the simple consideration of the number of stems is insufficient, because the clumps contribute to the overall protective function of the forest.

In addition to these features that remain difficult to assess, another major difference to high forests is the scope of rock volumes and tree sizes to be considered for rockfall protection. Whereas high forests comprise all potential tree diameters and rock volumes up to 5 m³ (Berger et al., 2002, Dorren et al., 2007), in coppice forests the tree diameter at breast height (DBH, measured 1.3 m above ground level) rarely exceeds 0.15 m, implicating only limited protection against large rocks (> 1 m³; Jancke et al., 2009). This means that for coppice forests the rock-tree interactions are limited to low energy rock impacts against highly flexible small diameter trees. In comparison to large diameter trees (DBH > 0.3 m) that constitute the main basis for the currently available data, the processes governing the impact for small diameter trees are different and conditioned by the increased flexibility. As a result, also the influence of each factor determining the mechanical resistance and response of the stem, including species specific material strength, mass, dimensions and anchorage of the tree, mass and velocity of the rock is different for small diameter trees. Hence, up- or downscaling of results of other studies focusing on different test specimen dimensions would be rather impractical. With regard to coppice forests this emphasizes the necessity of scale specific data acquisition for the reliable assessment of the mechanical resistance which is the aim of this dissertation.

3. Assessing the mechanical resistance of coppice stems with full-scale pendulum impact tests

3.1 Introduction

Broadleaf coppice forests have the capacity to mitigate the threat posed by rockfall in many mountainous regions (Gerber and Elsener, 1998, Frehner et al., 2005, Jancke et al., 2009). However, the limits of this protective function against rockfall are not identified, partly because no quantitative data on the mechanical resistance of the small diameter stems are available (Dorren et al., Jancke et al., 2009). Current rockfall simulation models that account for single rock impacts against trees for quantifying the protective function of forests rely on few data on the mechanical resistance of trees against dynamic impacts that refer mainly to mature conifers (Dorren et al., 2007, Woltjer et al., 2008, Dorren, 2012). Consequently they are not necessarily applicable to broadleaf coppice (Dorren et al., 2007, Jonsson, 2007, Lundström et al., 2008, Jancke et al., 2009).

Therefore, in this study full-scale experiments on fresh beech coppice stems were undertaken using a pendulum impact device. The main objective was to obtain quantitative data on the mechanical resistance of small diameter trees that are representative for impact magnitudes which occur frequently in reality. The dataset is meant to provide a more reliable basis for future estimations of the rockfall protective function of beech coppice stands and also of young beech forests constituted of small diameter trees. In addition to the acquisition of quantitative data the focus is on qualitative aspects of breakage behavior and wood properties specific to coppice stems.

3.2 Material and methods

In total, 73 impact tests were conducted on fresh beech (*Fagus sylvatica* L.) stems cut from a typical coppice stand near Grenoble in the French Alps (N 45° 35' 55.8"; E 05° 49' 45.1"; 820 m a.s.l.). To ensure the "fresh" status of the wood, all stems were tested at the latest one week after felling. Moreover the wood moisture content was verified by kiln drying of small stem sections before testing (n = 20; mean = 59.4%; standard deviation (SD) = 3.7%). Based on these data, total fiber saturation and a moisture content representative of living trees was assumed for all specimens.

To assess the mechanical properties of the stems an open air impact device that reflects to a certain degree the impact conditions of rockfall against single trees in a forest was developed (Figure 3.1). Root anchorage was substituted by a rigid restraint into which the test specimens were vertically clamped with their thicker end. The restraint consisted of a 0.3 m deep steel cylinder with the inner diameter adaptable to the stem diameter. The steel cylinder was embedded into a 1200 kg reinforced concrete slab casted into the ground. The other end of the specimens remained unrestrained. As impactor a spherical pendulum bob of reinforced concrete was used (mass = 84 kg). Pendulum radius and bob trajectory were defined by two static ropes attached at a height of approximately 10 m to two massive trees (DBH > 0.7 m) standing left and right from the concrete slab. The two ropes spanned an included angle of approximately 35° between each other. On the one hand this configuration guaranteed central impacts against the specimens. On the other hand the flexible ropes enabled ample bob trajectory deviations during impact similar to rockfall in forests. The impact direction was horizontal and the mean impact velocity of all tests was 11.3 ms⁻²

($SD = 0.4 \text{ ms}^{-2}$). Impact height was defined as the distance between the surface of the concrete slab (i.e. ground height) and the point of the first bob-specimen contact. The DBH (i.e. reference specimen diameter) was set at 1.3 m above the surface of the concrete slab (Figure 3.2).

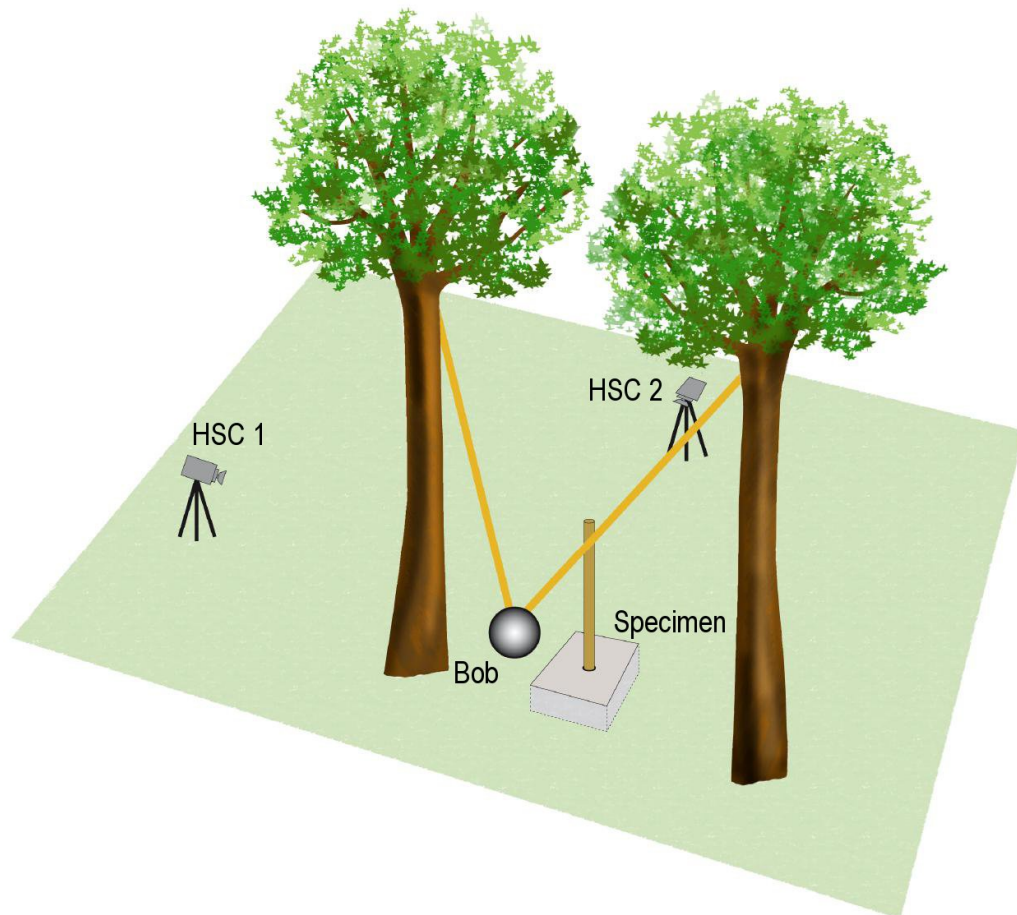


Figure 3.1: Open-air impact pendulum device. Before each test, a motor winch pulled the pendulum bob back towards the crown of a third tree. Then the bob was ready to be mechanically released at any time (illustration: Nicole Sardat).

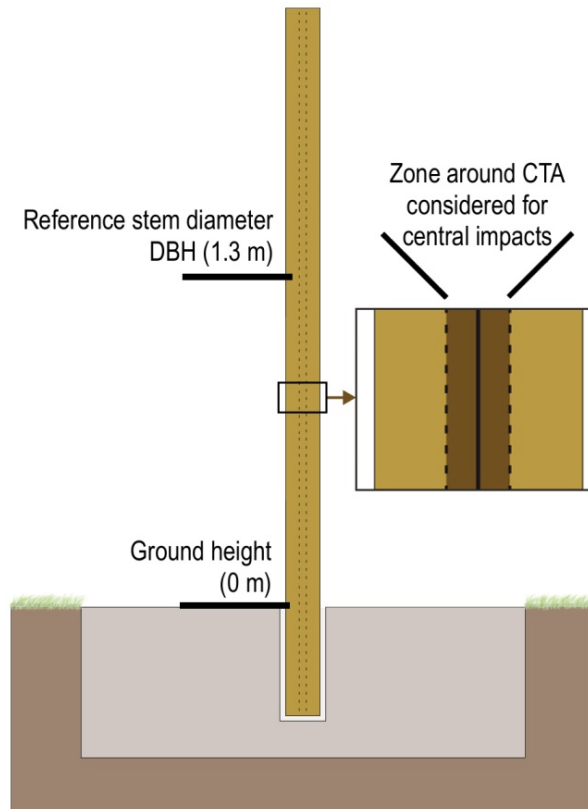


Figure 3.2: Initial specimen configuration seen from the impact direction and illustration of the zone considered for central impacts around the central tree axis (CTA) (illustration: Nicole Sardat).

Two test series were done using the pendulum device (cp. Table 3.1: 1st and 2nd test series). During the first one 59 stem segments each with a total length of 3 m and DBH varying between 0.03 m and 0.096 m were tested. For the second test series the entire above ground stem including tree crown of 14 coppice trees with a height of 5.5 to 9.5 m and DBH between 0.04 and 0.08 m was used. To assess the influence of impact height on the mechanical resistance two impact heights were applied: low (between 0.18 and 0.51 m above ground) and high (between 0.64 and 1.04 m above ground). The low impact height corresponds to typical rockfall jump heights of small rocks (volume < 0.1 m³) observed in several coppice stands in the French Alps. This height interval was of particular interest, because small diameter trees (DBH < 0.1 m) offer the best

protective function against this rock size (Jahn, 1988, Frehner et al., 2005, Jancke et al., 2009). High impact height was chosen, because it reflects the most frequently reported rockfall impact heights of various rock sizes (volume < 3 m³; Perret et al., 2004, Rickli et al., 2004, Stoffel, 2005, Bourrier et al., 2009).

For qualitative observations and quantitative analysis two digital high-speed cameras (HSC) were used. The first (IDT X-Stream XS3), was set up at a distance of 15 m perpendicular to the bob trajectory (HSC 1 in Figure 3.1). It recorded 200 images per second with one pixel corresponding to a surface of approximately 2.5 x 2.5 mm on stem and bob. The data were used to determine impact duration (i.e. time during which bob is in physical contact with the impacted specimen) and impact duration until the first visible crack occurrence on the specimen surface, hereinafter defined as time to failure. Although imprecise, this measure was used to indicate approximately when ultimate strength was reached. The experimental setup did not permit to quantify stem flexure in a consistent way, because of highly variable specimen shapes before and during impact. Moreover, in contrast to static or dynamic 3-point bending tests, the impact location only rarely coincided with the point of maximum deflection. The bob velocities before and after impact were derived from the bob displacement during 15 ms (corresponding to four successive images) just before and after physical bob-specimen contact. Based on these measures, the mechanical resistance of the stems was defined in two similar ways: First, as the difference of the bob momentum before and after impact following Equation 3.1:

$$\Delta p = v_1 \times m - v_2 \times m \quad (\text{Equation 3.1})$$

and second, as the difference of the kinetic energy of the bob before and after impact following Equation 3.2:

$$\Delta E_{kin} = \frac{1}{2} \times m \times (v_1^2 - v_2^2) \quad (\text{Equation 3.2})$$

m: mass of the bob (84 kg)

*v*₁: incident velocity

*v*₂: velocity after impact

The second HSC (Casio EX-FH25) was set up 15 m behind the test specimen, seen from the incident bob position, to determine the centrality of each impact (HSC 2 in Figure 3.1). This camera recorded 210 images per second with one pixel corresponding to a surface of approximately 10 x 10 mm on stem and bob at the moment of impact.

In this study, only central bob impacts against the specimens were considered. They were defined as impacts within a horizontal distance of 0.31 x 0.5 x DBH left and right from the vertical central tree axis (CTA) seen from the impact direction (Figure 3.2). This value accounts for the definition of central impacts of Dorren and Berger (2005) and constricts the deviation of the impulse transmission from the incident bob direction.

Table 3.1: Details on the five test series.

Test series	Test device	Test conditions	No. of specimens	Specimen dimensions	Remarks
1 st	Open air pendulum device	Low impact height: Mean = 0.348 m SD = 0.068 m	47	DBH: 0.03-0.096 m Length: 3 m	Fresh wood
		High impact height: Mean = 0.966 m SD = 0.052 m	12	DBH: 0.035-0.095 m Length: 3 m	Fresh wood
2 nd	Open air pendulum device	Low impact height: Mean = 0.367 m SD = 0.078 m	11	DBH: 0.044-0.08 m Length: 5.5-9.4 m	Fresh wood
		High impact height: Mean = 0.683 m SD = 0.04 m	3	DBH: 0.04-0.06 m Length: 7.0-9.2 m	Fresh wood
3 rd	Bandsaw quartering	Two longitudinal bandsaw cuts perpendicular to each other on half the length of the specimens	4	Mean diam.: 0.052-0.068 m Length: 1 m	Fresh wood
4 th	Light microscope	Microtome sections coloured with safranin and astra-blue	4	Rectangular: 1.0 x 0.8 mm	Taken from air-dried specimens
5 th	Laboratory pendulum device	German standard DIN 52189	36	Cuboid: 0.3 x 0.02 x 0.02 m	Air dried. Mean moisture content U \approx 11.5%

For further characterization of the test material the stem diameter was measured at four positions of each specimen: at the lower end, at ground height, at 1.3 m (DBH) and at 3 m (cp. Figure 3.2). The mass of each specimen was determined using a scale. The diameter

measurements permitted to conclude for the volume including bark (bark thickness ≈ 0.001 m) of the 3 m long stem segments of the first test series. These data were used to calculate fresh wood density and stem taper (i.e. average diameter reduction per meter specimen length). Oven-dry wood density was determined for 8 cuboid samples (volume ≈ 20 cm³) of randomly selected stems using the water displacement method.

In addition, supplementary investigations on selected specimens were conducted (cp. Table 3.1). Four 1 m long stems were longitudinally quartered on half their length using a bandsaw to verify the presence of unsymmetrical growth stresses (3rd test series). This qualitative method refers to the prong test frequently used in the wood processing industry for the detection of casehardened lumber (Archer, 1986, Fuller, 1995). The modified prong test used in this study indicates unsymmetrical growth stresses when the quarters distort to different degrees (i.e. the widths of the saw cut kerfs between the tips of the quarters are distinct). From two other specimens four microtome sections for light-microscopic analysis were taken. The sections were coloured with safranine and astra-blue to detect the presence of tension wood (Jourez et al., 2001; 4th test series). Finally 36 air dried samples (0.3 x 0.02 x 0.02 m) were tested with a laboratory impact device according to the German standard DIN 52 189 (5th test series). Here, the aim was to verify whether the impact toughness of the beech wood from the chosen coppice stand was consistent with literature data.

3.3 Results

3.3.1 Test material

Both fresh and oven-dry wood density of the specimens are consistent with literature data on beech wood (mean $\rho_{fresh} =$

1027 kg m⁻³; $SD_{fresh} = 108 \text{ kg m}^{-3}$; $n_{fresh} = 59$; mean $\rho_{dry} = 751 \text{ kg m}^{-3}$; $SD_{dry} = 24 \text{ kg m}^{-3}$; $n_{dry} = 8$; (cp. Vorreiter, 1949, Pechmann, 1953, Wagenführ, 1985, Sell, 1987). For both the 3 m long stem segments of the first test series and the entire stems of the second test series specimen mass highly correlates with DBH (Figure 3.3). For entire stems the mass increase is larger with respect to diameter increase, because here specimen mass also changes with individual specimen length. An average stem diameter decrease of 8.0 % per meter specimen length (SD = 2.6%) indicates rather cylindrical stem shapes for the first 3 m above ground height.

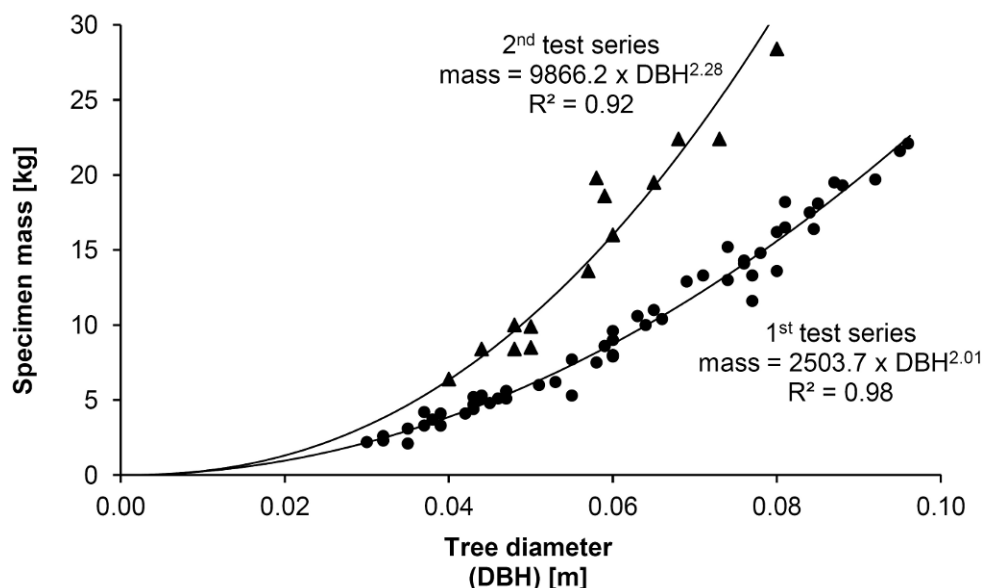


Figure 3.3: Relationships between specimen mass and DBH for the first test series on 3 m segments and second test series on entire stems.

The three supplementary test series for further characterization of the test material confirm wood properties expectable for coppice stems (e.g. Mattheck, 1997). The longitudinal quartering (3rd test series) indicates considerable and unsymmetrical growth stresses.

In all cases the four quarters immediately bent apart after cutting. The width of the saw cut kerfs at the tips of the quarters varied largely between the quarters. The microscopical analysis (4th test series) showed large amounts of tension wood in all 8 samples. This confirms the typical coppice wood properties and supports the findings of growth stresses from the 3rd test series. The results of the laboratory impact tests on 36 air dried samples (5th test series) reflect average impact toughness values for beech (mean = 92 kJ m⁻²; *ibid.*). However, the standard deviation of 52 kJ m⁻² and a range from 33 - 232 kJ m⁻² confirm a high variability of the mechanical properties of the specimens.

3.3.2 *Pendulum tests*

Various breakage behaviors of the test specimens, including breakage at impact height, breakage at ground height, longitudinal splitting, random detachment of small and large stem fragments, and considerable flexural deformations were observed. Apart from the flexural deformations that were often more pronounced for smaller diameters, the occurrence of one or several of these phenomena was not correlated with DBH, impact height, Δp or ΔE_{kin} . The pronounced flexural deformations before and after the first crack occurrence on the specimen surface led to long lasting impacts in some cases. However, as a consequence of the manifold breakage behaviors, the impact duration was highly variable (20 - 150 ms) and not correlated to Δp , ΔE_{kin} or other decisive parameters. Time to failure (15 - 95 ms) was not correlated to Δp , ΔE_{kin} , but it was on average shorter for low impact height (15 - 35 ms) than for high impact height (25 - 95 ms). Apart from local bark excoriation the bob-specimen contact surface did not show considerable signs of damage. High-speed camera image sequences of selected specimens are shown in Annex 8.1.

The Δp - and ΔE_{kin} -values of the two main impact heights were not significantly different for test series 1 and 2. Therefore, the following results are presented without referring to impact height. In all tests, all transverse fracture surfaces were long fibrous. Brash fractures with remaining short fibrous splinters shorter than 0.005 m were never observed (visual fracture surface characterization used by Kollmann, 1951).

In the first test series, on 3 m long stem segments, 86% of all specimens broke transversely at ground height and about half of these (47%) additionally at impact height. 71% of the specimens also showed longitudinal fractures. In 67% of these cases ring shakes were observed (i.e. fractures that follow the annual ring structure propagating in axial direction on the tension side). This resulted in smooth concave and convex fracture surfaces (cp. Figure 3.4). In the case of considerable flexural deformations before breakage (about 70% of all tests) the specimens assumed a curved shape due to the inertia of the top. This led either to breakage at impact height, or to breakage at ground height while the specimens regained their initial shape. Seven specimens (DBH: 0.075 - 0.09 m) were too strong, that is bob velocity was not sufficient to provoke total stem breakage. These stems were all considerably damaged, but none of them failed. The impacts led to stopping or negligible trajectory reversal of the bob. Although a reliable estimation of their maximum potential mechanical resistance was impossible, the seven stems were not excluded from the dataset. Four of them were impacted a second time. Two of them then broke totally, but in all four cases the Δp - and ΔE_{kin} -values were about as high as for the first impact.

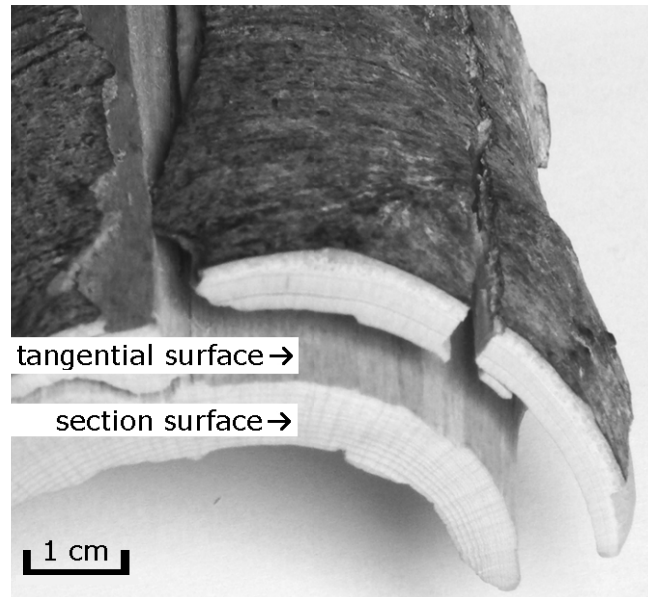


Figure 3.4: Top view on the section of a specimen with ring shakes. In some cases the fracture followed the annual ring structure in axial direction on a length of more than 1 m.

The second test series, on the entire above ground stems of coppice trees, showed similar results. All specimens broke transversely at ground height and 36% as well at impact height. 50% also fractured longitudinally, while two-thirds of these were ring shakes. In the case of considerable flexural deformations before breakage, the bob impact caused the propagation of a mechanical wave along the stem. This process led to a whiplash-like movement of the whole specimen that caused the breaking off of parts of the crown in 3 cases (Figure 3.5).



Figure 3.5: Demonstration of the flexural deformation of an entire coppice tree during and after bob impact (total tree height: 8.3 m; stem height (with diameter > 0.025 m): 6.5 m; DBH = 0.05 m). Each of the seven sketches depicting stem and bob shape is extracted from high-speed camera images.

Another implication of the high stem flexibility is the fact that during impact the bob sooner or later slipped around the specimen because it bent sideways or downwards (cp. Figure 3.5). This applies primarily to central impacts on highly flexible stems. In these cases the transmitted energy was always sufficient to break a given specimen, but the flexure of the stem and the consequent loss of contact with the bob reduced the theoretical maximum impact duration. On numerous non-central impacts excluded from this analysis, these kind of bob-specimen interactions were much more pronounced. Here, especially at high impact heights around 1 m, the specimens had a strong tendency to deform around the impacting bob. This resulted in minimal impact durations and almost undamaged specimens.

Figure 3.6a shows the relationship between bob momentum reduction Δp and DBH for the first and the second test series. Although the small number of tests of the second test series ($n = 14$) was insufficient to conclude for significant differences, linear regressions were used to indicate the Δp increase with DBH for test series 1 and 2. Especially for $DBH < 0.06$ m the entire stems show slightly

higher Δp -values compared to those of the 3 m long stem segments, whereas for DBH between 0.06 and 0.08 m the Δp -values are similar for test series 1 and 2. In Figure 3.6b linear regressions indicate different relationships between Δp and specimen mass for test series 1 and 2. The data show similar Δp -values for specimen masses between 5 and 10 kg, whereas for specimen masses of more than 15 kg the Δp -values of 3 m long stem segments are on average superior to those of entire stems.

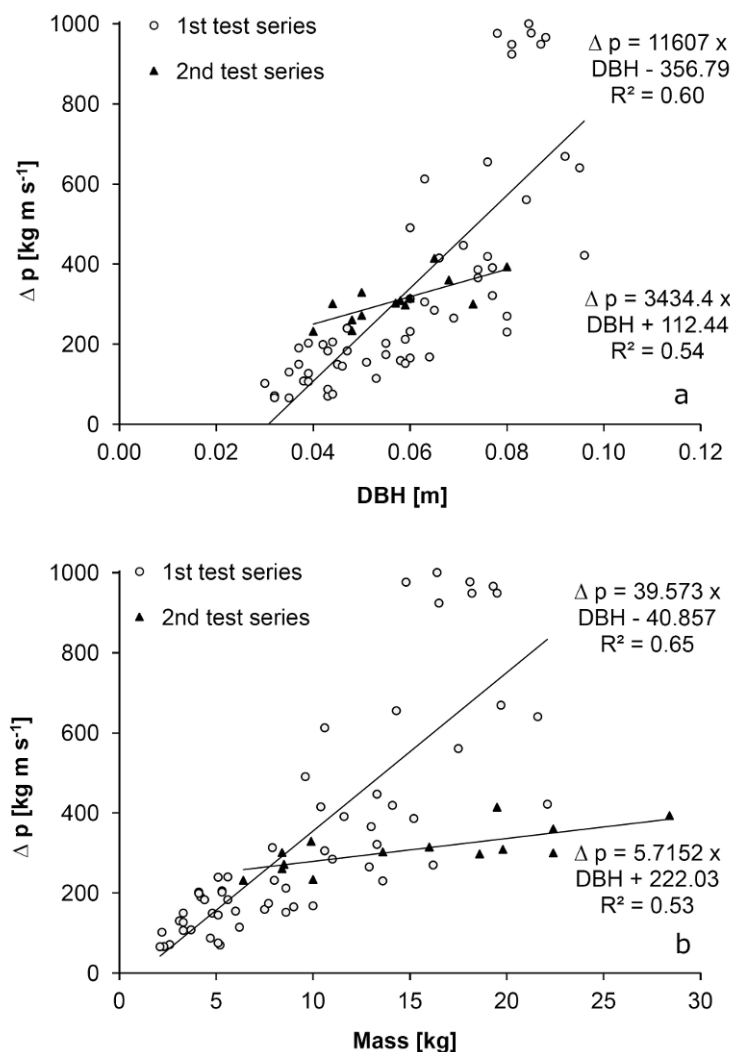


Figure 3.6: The relationships between (a) Δp and DBH, (b) Δp and specimen mass for the first and second test series.

The relationships between the reduction of the kinetic energy ΔE_{kin} and DBH as well as ΔE_{kin} and specimen mass are shown in Figures 3.7a and b. The data point distributions are similar to those of Figures 3.6a and b referring to Δp . Accordingly, the results indicate analogous differences and tendencies for test series 1 and 2. The only small differences between the data point distributions are linked to the fact that the bob mass was constant and the impact velocities were almost identical for all impacts. Note that for constant bob mass and constant impact velocity the $\Delta p / \Delta E_{kin}$ ratio changes in a mathematically defined way with decreasing velocity after impact (cp. Figure 3.8).

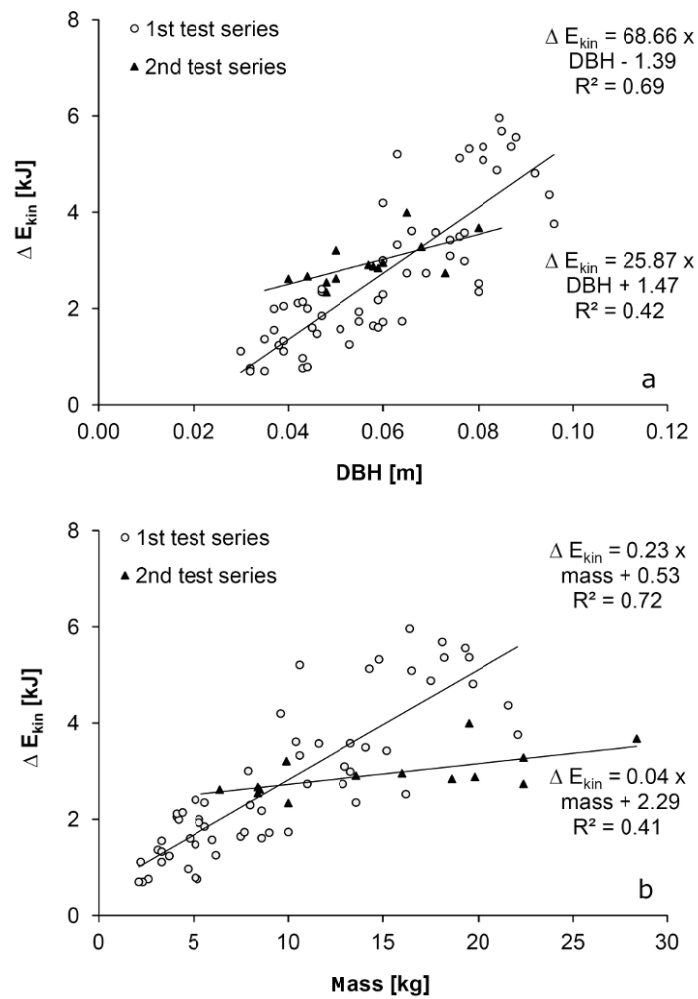


Figure 3.7: The relationships between (a) ΔE_{kin} and DBH, (b) ΔE_{kin} and specimen mass for the first and second test series.

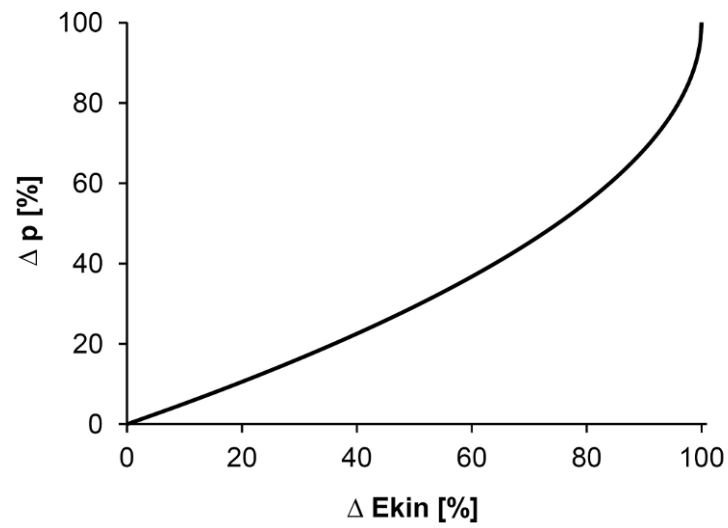


Figure 3.8: $\Delta p / \Delta E_{kin}$ ratio for constant incident bob velocities.

For direct comparison, Figure 3.9 shows the results of both Δp and ΔE_{kin} in function of the DBH for the first test series. The best-fit regression models show an exponential relationship for both parameters:

$$\Delta p = 83810 \times DBH^{2.02} \quad (\text{Equation 3.3})$$

$$\Delta E_{kin} = 210.49 \times DBH^{1.57} \quad (\text{Equation 3.4})$$

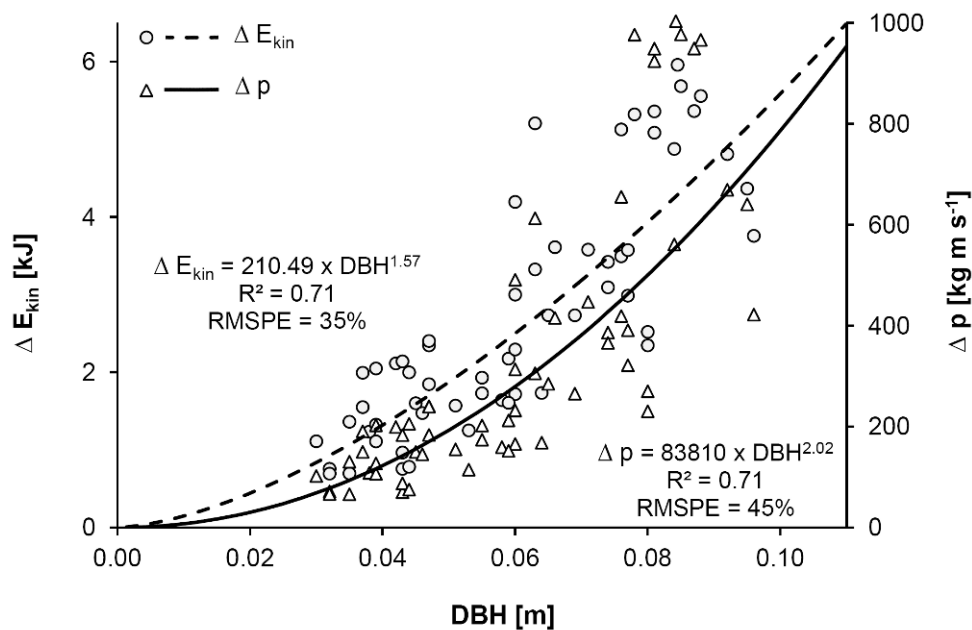


Figure 3.9: Δp and ΔE_{kin} as a function of the DBH (1st test series). Due to the $\Delta p / \Delta E_{kin}$ ratio depicted in Figure 3.8 the data point distributions and the runs of the curves are similar.

In the following, the focus will be on the bob deceleration during short- and long-lasting impacts against four selected stems. For each case two examples with small and two with large DBH were chosen (Figure 3.10 and Table 3.2). The bob deceleration derived from HSC images permits to set two points in time during impact. Point A represents the instant after which the first image with visible cracks in a specimen appears (i.e. the impact phase before A corresponds to time to failure). Point B indicates the last image where bob and specimen are in physical contact (i.e. the end of the impact duration). The deceleration curves in Figure 3.10 reflect that for a given DBH qualitatively different breakage processes can lead to similar Δp - and ΔE_{kin} -values. Among the smaller DBH, specimen S1 deforms considerably before point A and thereafter loses bob contact only when the specimen is almost completely torn to the ground. In contrast, the breakage process of specimen S2 is charac-

terized by minimal flexural deformation before point A and a relatively short phase after point A where the specimen breaks transversely at impact and at ground height. Among the larger DBH specimens the phase before point A is about twice as long for S3 compared to S4. However, the total impact duration of S3 is less than half as long, because once the first cracks occur the bob loses physical contact and the specimen breaks transversely at ground height. In contrast, for S4 the phase after point A is characterized by longitudinal crack propagation in two planes starting close to impact height and followed by transverse breakage at ground height. In addition to Figure 3.10 and Table 3.2 the image sequences of the four specimens are shown in Annex 8.1.

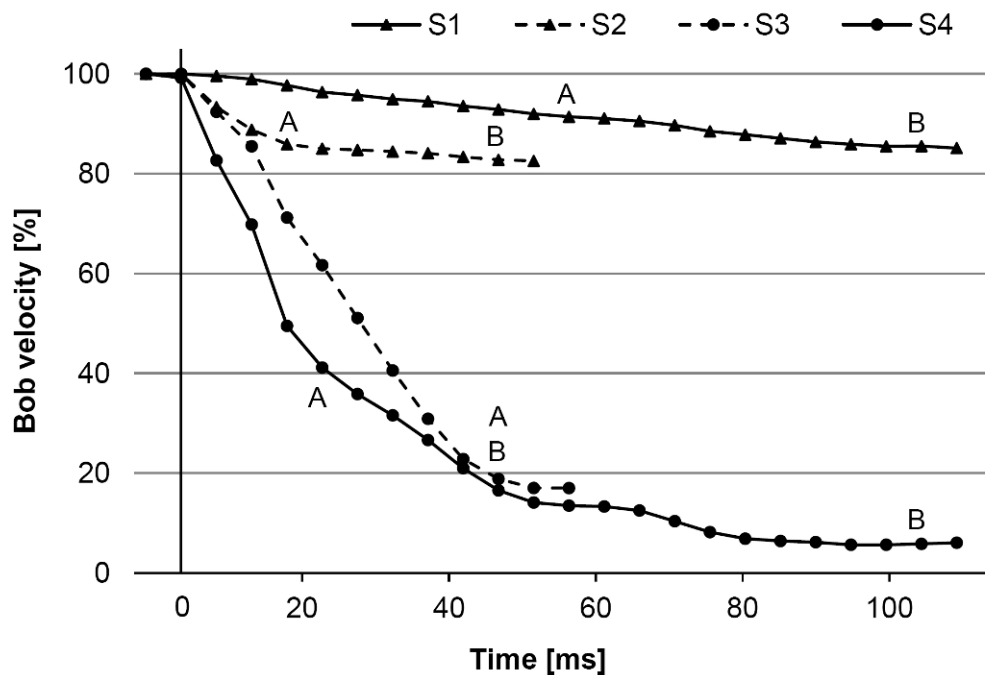


Figure 3.10: The decrease of the bob velocity during impact in 5 ms steps for four selected tests (cp. Table 3.2). A indicates the first image with visible cracks. B indicates the last image where bob and specimen are in physical contact.

Table 3.2: Detailed properties of four representative 3 m long specimens (cp. Figure 3.10).

Specimen no.	DBH [m]	Δp [kg ms ⁻²]	ΔE_{kin} [kJ]	Contact time [ms]	Time to failure [ms]	Impact height [m]	Crack characteristics in image A
S1	0.039	126.9	1.33	105	55	0.97	Transverse at ground height
S2	0.043	183.2	2.14	35	15	0.35	Transverse at impact and ground height
S3	0.095	640.5	4.36	45	45	0.95	Transverse at ground height
S4	0.092	669.2	4.81	105	25	0.46	Longitudinal close to compression side below impact

3.4 Discussion

The main objective of this study was to obtain quantitative data on the mechanical resistance of small diameter trees that are representative for impact magnitudes which occur frequently in reality. The wood properties of the specimens that were used in this study are expectable for coppice trees. Whereas wood density and moisture content are consistent with literature data, the three supplementary tests for further wood characterization indicate considerable unsymmetrical growth stresses and show highly variable toughness values. These variations are certainly due to the coppice specific growth conditions on slopes to which every tree adapts its shape and fiber tissue (e.g. tension wood) individually (cp. Mattheck, 1997). As a result, the variability of the mechanical wood properties within each tree is higher compared to lowland standards (trees that developed from seedlings in lowland high forests). The multiple breakage behaviors of the stems during the pendulum tests reflect these differences. They indicate that the continuous adaptive growth

in the forest leads to individual mechanical weak spots when the trees are loaded in a way (e.g. by rockfall impacts) that does not correspond to their mechanical adaptation strategy. However, the fact that breakage behavior was not correlated to any measured parameter indicates that the individual wood properties might influence the variability of the test results, but not predominantly determine the mechanical resistance.

In the following, the main parameters conditioning the mechanical resistance will be highlighted and discussed with respect to the implications for the rockfall protective function of forests constituted of small DBH trees. The relationships between the mechanical resistance (Δp or ΔE_{kin}) and the specimen mass are different for test series 1 and 2 (cp. Figures 3.6b and 3.7b). This is due to the fact that the mass-DBH ratio changes with the specimen length (cp. Figure 3.3). The mechanical resistance of the specimens of the second test series shows a lower increase with increasing stem mass, because the mass of the upper stem part obviously does not affect bob deceleration to the same degree as the mass in the lower part. This confirms the findings of Lundström et al. (2008) who found that the upper two thirds of a tree do not considerably contribute to the energy dissipation process.

In contrast to the relationships between the mechanical resistance and specimen mass, the data do not permit to conclude for significant differences between test series 1 and 2 when using the DBH instead of the specimen mass as independent variable (cp. Figures 3.6a and 3.7a). This shows that the DBH is a better predictor for the mechanical resistance of the stems. However, because the DBH influences both the mass of the lower stem part and the flexibility of the stem (i.e. flexural stiffness: product of the modulus of elasticity and second moment of area) it remains unclear to what degree mass and flexibility determine the mechanical resistance. Due to the

fact that the second moment of the area increases with DBH by the fourth power, whereas the mass of the lower stem part increases with DBH by the second power, the influence of the flexibility on the mechanical resistance might increase with increasing DBH. Consequently, also the processes governing the dynamic impact against a stem might considerably change for DBH beyond 0.1 m. Here, a higher proportion of transverse shear forces and more damage of the stem at the impact location as often observed on large DBH trees in rockfall zones would be expectable (Dorren, 2007).

However, for DBH below 0.1 m the high-speed camera recordings of this study show that the high flexibility of the stems allows for the acceleration of a considerable part of the specimen mass before the ultimate strength is attained (time to failure: 15 - 95 ms). Therefore, it is very likely that the specimen mass in proximity to the point of impact (i.e. lower stem part) has a major influence on the mechanical resistance. This is backed up by the stronger correlation between the mechanical resistance (Δp or ΔE_{kin}) and the mass of the lower part of a tree (1st test series) compared to the relationship between the mechanical resistance and the mass of the entire stem (2nd test series). Furthermore, the fact that four specimens showed similar Δp - or ΔE_{kin} -values when impacted for a second time also indicates that specimen mass in proximity to the point of impact is likely to play a more important role for the mechanical resistance than wood strength under the given impact conditions.

The decisive role of the specimen mass on the impact process suggests that the bob velocity and mass might also have a strong influence on the mechanical resistance. In this context, the perfectly elastic collision is a well-known example. Here, the velocity of an impactor after impacting a motionless object depends only on the masses of both objects and the incident velocity of the impactor. In this case, for instance, a twofold increase in incident velocity leads

to a twofold increase in Δp and a fourfold increase in ΔE_{kin} . Other examples where the impact velocity conditions the loss of kinetic energy during impact are rockfall rebounds on a hillslope (Labieuse and Heidenreich, 2009), impact tests against concrete beams (Banthia, 1987) and against small defect free drywood specimens (Krech, 1960). Of course, in these examples the effect of the impactor kinematics before impact on the kinetic energy loss during impact is only partly dependent on specimen mass. Especially fracture mechanics and strength properties are decisive parameters.

However, in this study on highly flexible specimens, the time to failure is relatively long and specimen mass acceleration is a major factor for the bob energy reduction during this first impact phase. Hence, although the impact conditions of the pendulum tests do not correspond to those of a perfectly elastic collision, it is very likely that for higher incident velocities the mechanical resistance of the stems will be substantially higher, too. However, this increase of mechanical resistance is certainly limited to an unknown degree, because increasing impact velocity also causes a higher peak force sustained by the specimens (Krech, 1960). Hence, there must be a threshold where the specimens break before the stem mass acceleration reaches its maximum effect on the impactor deceleration. Whether this threshold is situated within the scope of common rockfall velocities (up to 25 m s^{-1} ; Dorren and Berger, 2005) can only be estimated with adequate full-scale impact tests.

The examples above and the results of this study emphasize the necessity of considering the influence of the incident velocity and also the mass of the impactor in future studies. In analogy to the elastic collision it is moreover likely that impactor velocity and mass influence energy loss during impact to a different degree. Therefore, both should be treated separately and not combined as kinetic energy or momentum in future research.

Previous studies focusing on dynamic rockfall impacts against trees did not account for the influence of impact velocity and mass (Couvreur, 1982, Mizuyama and Narita, 1988, Dorren et al., 2005, Dorren and Berger, 2005, Dorren et al., 2006, Jonsson, 2007, Kalberer et al., 2007, Lundström et al., 2008). Jonsson (2007) accounted for negligible strain rate effects on wood strength in his numerical single tree model (NSTM), but the overall effect of impactor speed and mass on the total energy loss during impact was not considered. However, all previous studies focused on rather large DBH trees (DBH > 0.3 m) with reduced flexibility. Hence, the influence of impact velocity and mass might be different than for highly flexible small diameter trees.

Moreover, in all previous studies the tested tree dimensions and rock velocities and masses were, though representative for rockfall, different for each impact. Therefore, the exponential relationships between DBH and ΔE_{kin} published by Jonsson (2007) and Dorren and Berger (2005) reflect mean values representative for frequent rockfall scenarios. Hence, using these data for quantifying the rockfall protective function of entire forests might yield results corresponding to the real hazard situation in most cases, even if the influence of rock impact velocity and mass on the loss of kinetic energy during impact is not integrated into the model.

The exponential relationships between the mechanical resistance (Δp or ΔE_{kin}) and specimen DBH of this study (Figure 3.9) reflect average impact velocities and masses (Dorren et al., 2005). Therefore, both models would not overvalue the rockfall protective function of an entire forest if the influence of rock impact velocity and mass on the loss of kinetic energy was considerable. However, it is difficult to estimate to what degree the pendulum tests are representative for rockfall in forests. The impact device reflects to a cer-

tain degree rockfall impacts (impact height; unrestraint upper specimen end) and the results are reproducible. Its main advantage is to be able to generate a large dataset with relatively small effort. The main uncertainties are on the one hand due to the rigid restraint that could cause local peak stresses during impact, which are less pronounced in the case of the more flexible natural root anchorage. On the other hand, in coppice clumps the transition zone between stem and roots could constitute initials for failure. It is characterized by irregularities in the stem shape and wood tissue due to the immediate vicinity of other trees during growth and the remains of the stump of the previous cutting cycle. Consequently, impact tests against coppice trees in their natural condition in the forest are necessary to verify the role of root anchorage.

In Figure 3.11 the regression models of Jonsson (2007) and Dorren and Berger (2005) representing the relationships of ΔE_{kin} to DBH are shown in comparison to the results of the pendulum tests including the regression model and root mean square percentage error (RMSPE). Despite large differences of the respective experiments in terms of impact velocity and mass, tree species, DBH, height, root anchorage and impact height the results appear to be not fundamentally different for DBH smaller than 0.1 m. The high variability of the test results and the fact that both other models are extrapolations from tests against larger DBH trees are possible explanations. However, this fact emphasizes the importance of assessing the influence of each impact parameter for a broader understanding of the impact processes. Moreover, it reflects the necessity of considering the high variability of the mechanical resistance in expertise on the rockfall protective function of forests. Finally, the similarities indicate that the influence of tree species on the mechanical resistance might not be substantial for the diameter range. Although this would considerably facilitate rockfall hazard assessments this notion has to be confirmed in future studies.

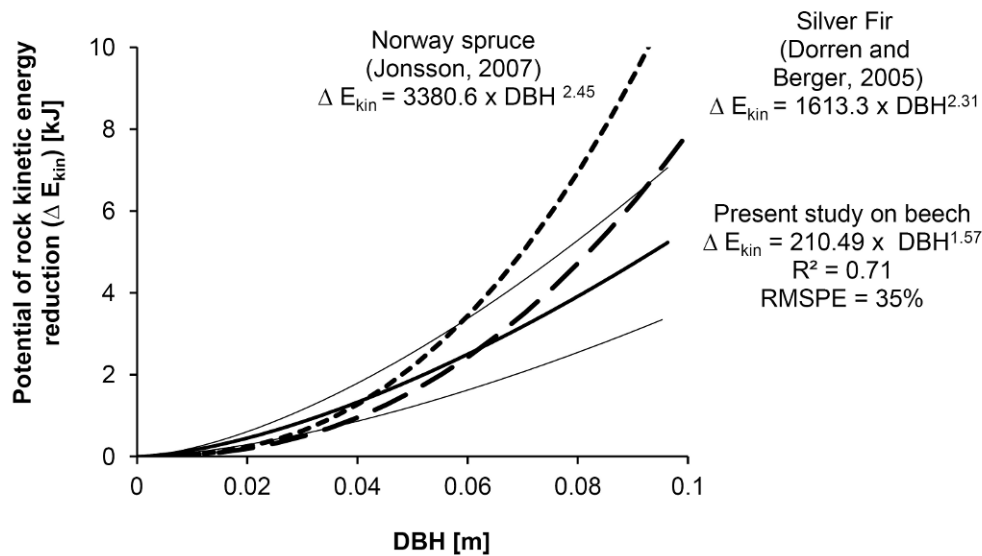


Figure 3.11: Comparison of 3 models expressing the ΔE_{kin} -DBH relationship for 3 different species. The thinner continuous lines above and below the model for beech indicate the root mean square percentage error (RMSPE) of 35%.

The fact that the high flexibility of the small DBH stems causes the impactor to glide off under certain impact conditions, suggests that the maximum possible reduction of ΔE_{kin} is not always attained. Furthermore, it indicates that non-central impacts against small DBH stems are likely to dissipate relatively less impact energy than large DBH trees, because they have the ability to give way to the impactor.

The ring shakes observed on the broken specimens are rather rarely documented for beech wood. However, for chestnut trees (*Castanea sativa* L.) frequently cultivated in coppice stands, this fracture type is frequent and poses problems to the forest and wood processing industry. Ring shakes in chestnut are due growth stresses conditioned by forest management practices. (Fonti, 2002). Hence, this points out that the ring shakes in the beech specimens are due to

the high growth stresses already indicated by test series 3, 4 and 5. Consequently, this confirms that growth stresses influence the variability of the mechanical resistance and explains why the breakage behaviors were so manifold and not related to DBH, impact height, Δp or ΔE_{kin} .

3.5 Conclusion

The dataset obtained in this study provides a basis for estimating the rockfall protective function of beech coppice stands and also of young beech forests constituted of small DBH trees. For the target DBH range the regression model is more reliable than data of previous studies, because the DBH specific impact process was considered. Due to the increased flexibility of small DBH trees ($DBH < 0.1$ m) compared to large DBH trees ($DBH > 0.3$ m) the processes governing the impact are distinct. The impact process is characterized by only negligible damage at the impact location, pronounced flexural deformation and acceleration of the stem before breakage. For small DBH trees the DBH is a key determining parameter, because it conditions the tree mass in proximity to the point of impact (i.e. inertia) and the flexibility of the stem. However, it is very likely that the relationship between the mechanical resistance and the DBH is dependent on the impact velocity and mass. The degree and the limits of this dependence should be assessed in future studies by treating velocity and mass separately and not combined (e.g. as momentum or kinetic energy).

This study showed that quantifying the mechanical resistance by using either Δp (impactor momentum loss) or ΔE_{kin} (impactor kinetic energy loss) does not make a considerable difference for the result interpretation, because impactor mass and velocity were nearly constant for all tests. However, for the result comparison of

similar impact test series against small DBH trees where different impact velocities and masses are applied, both quantification methods would pose a problem because they combine velocity and mass in a defined inflexible way. On the one hand the use of Δp presumes that the influence of velocity and mass on the mechanical resistance are identical (cp. Equation 3.1). On the other hand, the use of ΔE_{kin} presumes that the influence of velocity is much more important (to the second power) than mass (factor 0.5; cp. Equation 3.2). But, none of these speculations is justified because the mechanical resistance to dynamic impacts is not a constant material property.

Hence, the dilemma consists in the fact of defining the mechanical resistance by means of the change of momentum or energy of another object (i.e. the impactor). Because of this indirect method the result depends necessarily on the main impactor properties velocity and mass and other such as impactor shape in the case of rockfall. Consequently, comparisons of impact test data using Δp - or ΔE_{kin} -values should only be made when impactor velocity and mass and other decisive factors are identical for all tests. In other words, up- or downscaling the results of this study to conclude for the mechanical resistance of beech trees of other than the tested dimensions might not lead to reliable results.

Therefore, if rock velocity and mass were considered separately for the quantification of the rockfall protective function of forests, this might constitute a substantial gain of reliability. Because both rock properties could be considered by physical process based rockfall models, such as rockyfor-3D, (Dorren, 2012), further emphasis should be placed on these details in future studies.

Although the used full-scale pendulum impact device cannot account for the natural root anchorage of trees, it is a valuable tool to gen-

erate large datasets with relatively little time and effort. The assessment of the mechanical resistance including its variability and multiple qualitative observations have given seminal insights on the breakage process of small diameter beech trees.

4. Full-scale impact tests in coppice forests. New insights on the rockfall protective function.

4.1 Introduction

In the last decade, research on the protective role of forests against rockfall emphasized their potential for mitigating the rockfall hazard in mountainous regions (Dorren et al., 2007). The reliable quantification of this protective function is a prerequisite, both for hazard assessment and for cost efficient long term regional planning. It is commonly assessed using rockfall simulation models based on forest inventories (Dorren et al., 2007, Woltjer et al., 2008). Models that additionally consider rock-tree interactions in a consistent way incorporate data on the mechanical resistance of trees obtained from full-scale impact tests in forests. However, existing reliable data being mainly restricted to mature conifers (silver fir and Norway spruce) limit the assessment of the rockfall protective function with regard to other forest types (mixed stands, mature broadleaf forests and coppice).

For assessing the rockfall protective function of broadleaf coppice forests the necessity for adequate data is most evident. Coppice trees regenerate vegetatively after cutting and develop to clusters of low diameter, multi-stemmed trees called clumps. The root anchorage and mechanical properties differ greatly from those of mature conifers (Jancke et al., 2009). Consequently, the processes governing a rock impact against coppice trees are also very different (cp. chapter 3). The full-scale pendulum impact tests against small diameter beech coppice stems described in chapter 3 have shown that the mechanical resistance of trees depends to a large extent on the

tree dimensions. In fact, the mechanical response of small diameter trees (diameter at breast height (DBH) < 0.1 m) subjected to low scale rock impacts (< 6 kJ) is strongly influenced by the flexibility of the stem. Therefore, in contrast to large DBH trees (DBH > 0.3 m) the breakage process is characterized by negligible damage at the impact location and rather long times to failure (mean: 28 ms; range: 15 - 95 ms) and long total impact durations (mean: 62 ms; range: 25 - 120 ms). As a result, the stem mass acceleration plays a major role for reducing the kinetic impactor energy. Therefore, it is very likely that especially for small DBH trees the mechanical resistance increases with increasing impactor velocity and mass. Finally, these DBH dependent qualitative differences complicate the comparison with quantitative data focusing on other DBH ranges, tree species and impactor characteristics.

Apart from the different mechanical responses of large DBH trees compared to individual small DBH coppice trees, the dense spatial structure of coppice clumps also constitutes additional rockfall specific features that increase the protective role of coppice forests. The short distances between the stems of a clump induce the following three effects (cp. chapter 2):

- Increase of the probability of localized serial rock-tree interactions where the rock continuously loses kinetic energy. In contrast to high forests there is no rock acceleration between several tree contacts.

- Increase of the probability of rock energy dissipation by tree-tree contacts i.e. from stem to stem or crown to crown leading to an indirect amplification of the energy dissipative capacity of an individual tree.

- Increase of the probability of an impacting rock to be stopped, if the distances between the trees of a clump are shorter than the rock diameter. Hence, the trees act like a fence preventing the rock from continuing its trajectory due to slope inclination and gravity.

These features are very difficult to quantify and require further investigation. However, considerable amounts of small rocks stacked against the trees of coppice clumps in many coppice forests on active rockfall slopes indicate that the effects are substantial (Figure 1.1c).

In chapter 3, the main results are based on full-scale pendulum impact tests against coppice tree stems fixed into a rigid restraint embedded into a concrete slab. Therefore, the influence of the natural tree anchorage in the forest ground could not be considered. However, in coppice forests the transition zone between stem and root system is characterized by various irregularities including tension wood, pronounced grain deviations, bark inclusions and uncylindrical stem sections due to the immediate vicinity of other trees during growth or the remains of the stump of the previous cutting cycle (cp. chapter 2, Mattheck, 1997). Hence, it is unknown what implications these features and the root anchorage might have on the mechanical resistance of the trees exposed to rockfall. Therefore, in this study, full-scale impact tests were conducted in a coppice forest environment. Here, the focus of the experimental setup was on the mechanical response of individually impacted trees that were part of a coppice clump. As a matter of fact, this excluded studying the effect of entire clumps facing rock impacts as a whole in a consistent way. The main objectives of this study were to give qualitative insights on the breakage process of coppice trees and to assess quantitative data on their potential for reducing the kinetic energy of rockfall.

4.2 Material and methods

4.2.1 *Study site*

Dynamic impact tests were conducted in a mixed broadleaf coppice stand mainly constituted of beech (*Fagus sylvatica* L.), lime (*Tilia cordata* Mill.), maple (*Acer spp.*) and whitebeam (*Sorbus aria* L.). It is situated in the French Alps, near Chambéry, on the eastern slope of the Mont de l'Épine (N 45° 35' 55.8"; E 05° 49' 45.1"; 820 m a.s.l.). It had developed without any silvicultural interventions after a clear cut of the previous stand 26 years ago.

The mechanical resistance was tested of a total of 13 trees that were part of three beech coppice clumps. The diameters at breast height (DBH) varied between 0.054 and 0.106 m. The trees had fully developed foliage since all tests were done in September. In the centre of each clump, the remains of the stumps from the previous cutting cycle were still visible, but largely deteriorated by lignicolous fungi.

4.2.2 *Experimental setup*

The experiments consisted in impacting each of the 13 trees individually with a spherical granite ball (mass: 60 kg; diameter: 0.35 m). It was accelerated by gravity up to 16 m/s in a 40 m long tube system composed of elements of construction-site rubble chutes and drainage pipes (Figure 4.1a). The tube system was fixed on the slope above of the target trees using large pegs and tension belts. In this way, a short free flight through the air before impact could be controlled. The experiments focused on the individual mechanical response of a coppice tree to a dynamic impact. To exclude any physical contact between the tree stems during impact, several trees entangled with or standing behind the target trees were removed. In addition, the coppice clumps were freed from numerous small sprouts and branches with DBH below 0.04 m to improve the

visibility and access to the test specimens. Based on the assumption that the average and also the most frequent impact angle of rolling and bouncing rocks in reality would be close to the slope angle, all test trees were chosen to be impacted parallel to the slope with an impact angle of approximately 30° (Figure 4.1a). The impact heights varied between 0.3 and 0.7 m above ground.

The impact process was recorded with four digital high-speed cameras (HSC) placed in four different positions around the tested trees (Figure 4.2b). HSC 1 (IDT X-Stream XS3) was placed at a distance of 8 m perpendicular to the granite ball trajectory. It was used for angular and translational velocity measurements and recorded 200 images per second with one pixel corresponding to approximately 1 x 1 mm on the granite ball surface during impact. Due to unfavorable light conditions the angular velocity measurements were not exact in all cases. Although the angular velocity changes were very variable depending on the impact conditions, the average angular velocity decrease was relatively small. Therefore, the angular velocity was neglected for the evaluation of the mechanical resistance of the coppice trees.

Based on the translational velocity of the granite ball before and after impact the mechanical resistance of the stems was assessed in two similar ways in analogy to chapter 3: First, as the difference of the (translational) granite ball momentum before and after impact following Equation 3.1:

$$\Delta p = v_1 \times m - v_2 \times m \quad (\text{Equation 3.1})$$

and second, as the difference of the (translational) kinetic energy of the granite ball before and after impact following Equation 3.2:

$$\Delta E_{kin} = \frac{1}{2} \times m \times (v_1^2 - v_2^2) \quad (\text{Equation 3.2})$$

m : mass of the granite ball (60 kg)

v_1 : incident velocity

v_2 : velocity after impact

For detailed qualitative observations of the impact process another three high-speed cameras (Casio EX-FH25) were placed about 8 m upslope (HSC 2), 8 m sideward (HSC 3) and 8 m downslope (HSC 4) of the test trees. These HSC recorded 210 images per second with one pixel corresponding to approximately 8 x 8 mm on the surface of the test trees (Figure 4.1b).

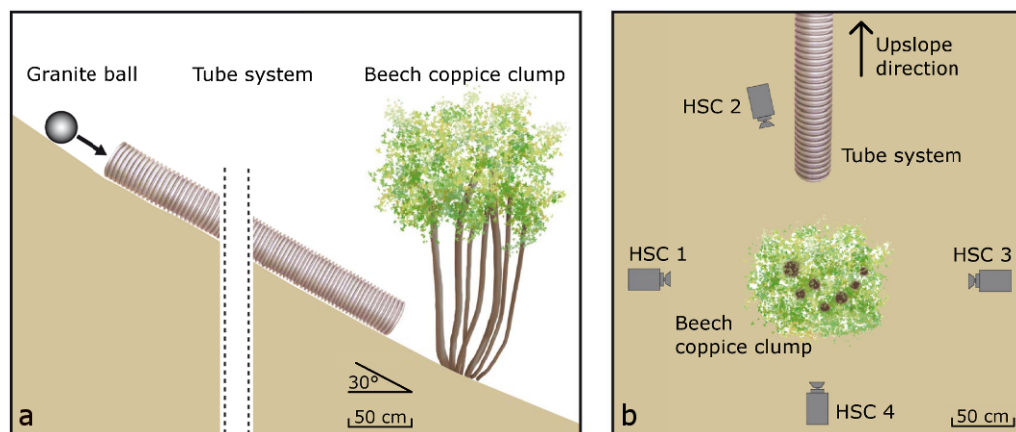


Figure 4.1: Forest impact test device. (a) Side view. (b) Top view (illustration: Nicole Sardat).

4.3 Results

This study focuses on central tree impacts that are defined as impacts within a horizontal distance of 0.31×0.5 DBH from the vertical central tree axis (CTA) seen from the impact direction (c.p. Figure 3.2 in chapter 3, Dorren and Berger, 2005). However, during the experiments it turned out to be difficult to impact the trees centrally every time, even though the distance between the lower end of the tube system and the specimens was only about 0.6 m. One reason for this was some remaining lateral inertia of the granite ball

although it had been confined by the tube system. Moreover, very flexible, slightly crooked or twisted trees tended to bend away sideways, virtually avoiding the kinetic energy transmission of a per definition central impact.

As a result, 29 granite ball impacts were necessary to provoke the total breakage of the 13 test trees. The scenarios for the 13 trees are subsumed in four different impact categories (Table 4.1). Only two trees showed total breakage after one central impact. Both broke only at ground height in the transition zone between stem and root system that displayed the weak spot. For seven trees one non-central and one central impact were necessary to provoke total breakage. Here, the individual mechanical response of the coppice trees was very variable. Non-central impacts generally led to small cracks and possibly invisible damage. Central impacts provoked breakage at impact or ground height, considerable flexural deformations or longitudinal splitting (i.e. shear failures) in two or three main planes. For two test trees two central impacts were necessary to provoke total breakage. They constituted the upper limit of the test device. Although the first impacts led to considerable damage, the reduction of the kinetic energy of the granite ball was not necessarily lower for the second impacts. Only two trees did not break at all, even after up to 7 rather central impacts. These trees, showing only small cracks, were beyond the limits of the test device. No correlations between the mechanical response of the specimens and Δp , ΔE_{kin} , DBH, impact height or impact duration were found.

The anchorage of the coppice trees proved to be tough in most cases. None of the 29 impacts caused uprooting of the coppice trees. As a consequence, a mechanical wave was transmitted to the ground (soaring of the upper ground layer). Despite this fact, considerable movements or oscillations of the other trees that were part of the same clump were not observed. Only four trees broke exclu-

sively at ground height (trees 1, 2, 4 and 6). In these cases the wood fractured in the transition zone between stem and roots. Despite the proximity of the remains of the stump of the previous cutting cycle that were colonized by lignicolous fungi, no signs of fungal decomposition were evident on any fracture surface of the tested trees.

The field experiments focused on the individual mechanical response of the test trees during impact. However, in 11 of 29 tests the granite ball subsequently rebounded against other trees of the same clump. These rebounds led to considerable reductions of the remaining kinetic energy and to horizontal deviations of the initial granite ball trajectory in all conceivable directions. Note that the quoted quantity of rebounds is not representative for rebound probabilities within beech coppice clumps, because in this study the number of stems per coppice clump was reduced by initial clearing and with each additional impact test.

Table 4.1: Details on the impact processes of all 13 test trees. For each tree only the maximum Δp - and ΔE_{kin} -values were considered.

Tree no.	DBH [cm]	Δp [kg m s ⁻¹]	ΔE_{kin} [kJ]	Δp [% of initial p]	ΔE_{kin} [% of initial E_{kin}]	Impact category
1	8.1	535.8	6.2	56	80	(1) one central impact
2	7.2	354.5	4.3	39	63	(1) one central impact
3	6.0	420.9	4.9	46	71	(2) one non-central and one central impact
4	5.9	350.6	4.4	38	61	(2) one non-central and one central impact
5	8.1	472.9	5.7	49	74	(2) one non-central and one central impact
6	5.7	400.8	4.5	46	71	(2) one non-central and one central impact
7	9.1	427.7	5.1	46	71	(2) one non-central and one central impact
8	5.4	341.1	4.2	37	61	(2) one non-central and one central impact
9	5.4	273.2	3.5	30	51	(2) one non-central and one central impact
10	9.1	846.7	6.0	100	100	(3) two central impacts
11	8.1	919.4	7.0	100	100	(3) two central impacts
12	10.6	958.3	7.7	100	100	(4) multiple central impacts – no breakage
13	9.6	880.9	6.5	100	100	(4) multiple central impacts – no breakage

The measurements of the loss of momentum Δp and kinetic energy ΔE_{kin} of the granite ball due to tree impacts were affected by two main factors interfering with each other. Both, the occasional eccentricity of the impacts and the fact that not all impacts led to complete failure caused Δp - and ΔE_{kin} -values that are below the maximum potential Δp - and ΔE_{kin} -values of 11 out of 13 coppice trees (trees 3 - 13 Table 4.1). Although the degree of this undervaluation

is not assessable, it is certainly most pronounced among the test trees of impact categories 3 and 4 (Table 4.1). For each of the 13 trees only the maximum Δp - and ΔE_{kin} -values were considered, because summing up the Δp - and ΔE_{kin} -values of consecutive impacts against a given test tree would not have been appropriate (multiple consideration of stem mass acceleration and elastic deformations).

All maximum Δp - and ΔE_{kin} -values of the 13 test trees are shown in Figures 4.2a and b plotted against the DBH. The data points also indicate the impact categories (i.e. the degree of undervaluation; Table 4.1). The data of the pendulum impact tests of chapter 3 (Figure 3.9, Equations 3.3 and 3.4) including the respective regression models are shown for comparison (dashed lines). The Δp -values of this study are on average 1.23 times higher than the regression model from the pendulum tests. The ΔE_{kin} -values are all superior to the regression model and on average 1.55 times higher. For better illustration, these differences are indicated with solid lines.

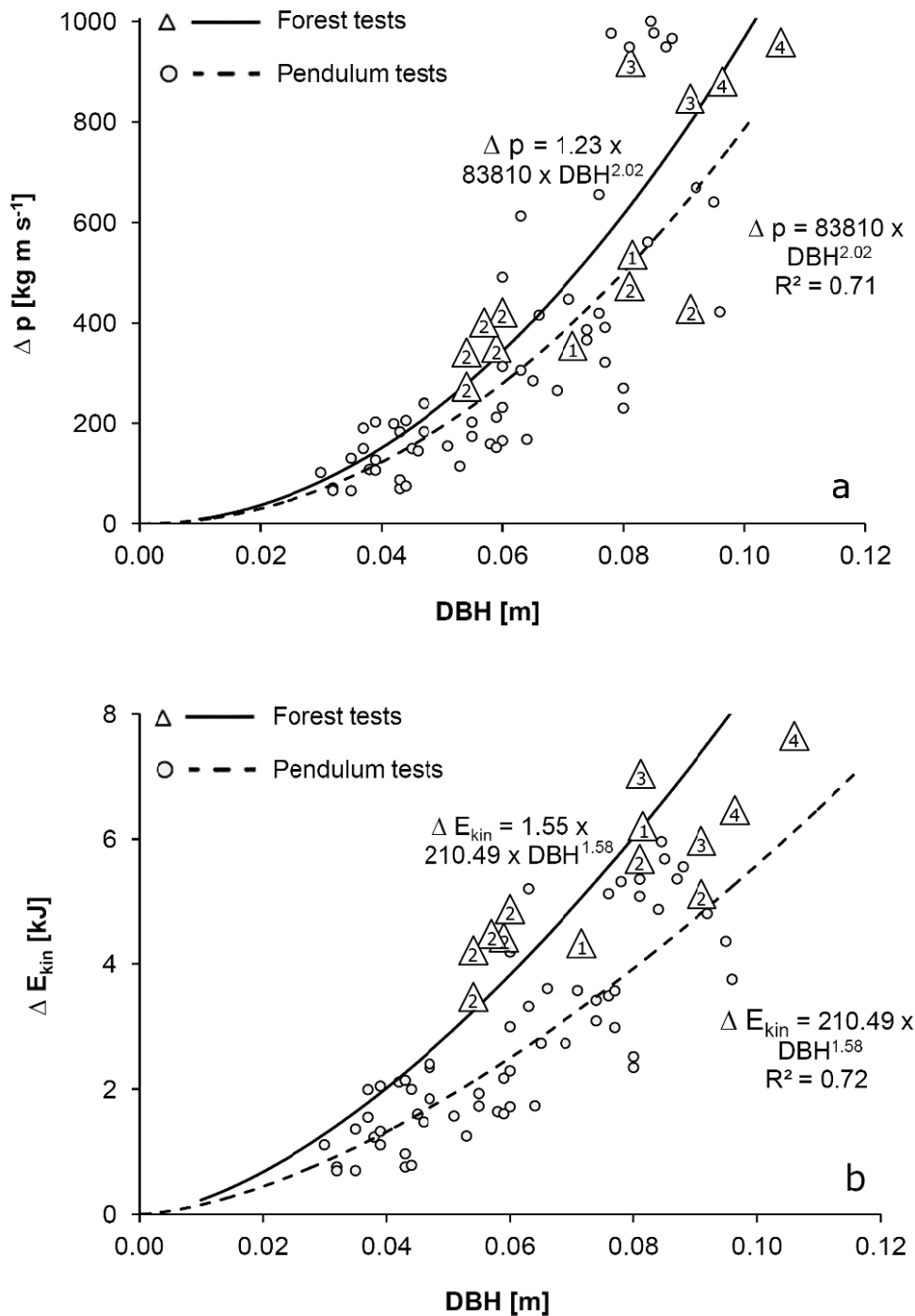


Figure 4.2: Comparison of the forest tests of this study with the pendulum results of chapter 3 by referring to (a) Δp and (b) ΔE_{kin} plotted against the DBH. The solid line represents the average difference between the forest test data points and the regression model of the respective pendulum test data. The numbers in the forest tests data points represent the four impact categories in Table 4.1.

The angular velocity measurements were inaccurate due to unfavorable light conditions in the forest. Nevertheless, the results with a focus on rotational energy (E_{rot}) are summarized in Table 4.2 and reflect overall tendencies. E_{rot} before impact represented on average about a quarter of the total impact energy and did not show large variations. In contrast, E_{rot} after impact was highly variable and depended on local impact conditions (i.e. friction and stem breakage behavior). For all tests, the proportion of E_{rot} dissipated during impact was small compared to the reduction of translational energy. As a result, the percentage of E_{rot} of the total energy was higher after impact.

Table 4.2: Rotational energy E_{rot} before and after impact.

	E_{rot} before impact [kJ]	E_{rot} before impact [in % of E_{total} before impact]	E_{rot} after impact [in % of E_{total} after impact]	E_{rot} after impact [% of E_{rot} before impact]
Mean	2.4	26.1	56.0	61.7
SD	0.3	4.7	26.8	21.4
Max	3.0	34.7	100.0	100.0
Min	1.8	17.1	33.7	37.9

4.4 Discussion

In this study, the breakage behaviors of the trees were akin to those of the pendulum impact tests against similar trees where the root system was replaced by a rigid restraint (cp. chapter 3). The overall implications of the root system on the mechanical resistance remain difficult to assess. However, with regard to the mechanical resistance of the transition zone between stem and roots, the four specimens broken only at ground height show either average Δp - and ΔE_{kin} -values (trees 1 and 2) or else refer to specimens impact-

ed for a second time (trees 4 and 6; Figures 4.2a and b). Thus, if even for those specimens with their weakest spot at ground height the transition zone between stem and roots does not lead to below average Δp - or ΔE_{kin} -values, this tree part should not be seen as an element with particular influence on the mechanical resistance of the entire tree.

Figures 4.2a and b illustrate in a demonstrative manner the limits of quantifying the mechanical resistance by means of the change of momentum or energy of another object (i.e. the impactor; cp. chapter 3). In Figure 4.2a the Δp -values correspond to those of the pendulum test series and show only negligible differences. Here, one possible data interpretation would be that the mechanical resistance assessed in the forest is similar to the mechanical resistance of stem segments where the root system is replaced by a rigid restraint. Hence, the root system would be of only minor influence and all future tests on small diameter trees could be done with a pendulum impact device. However, the ΔE_{kin} -values in Figure 3b are all superior to the regression model of the impact test series and furthermore they are substantially higher (1.55 times on average). Now, this could indicate that the mechanical resistance of coppice trees anchored via their root system is on average about 1.5 times higher than for coppice stems clamped into a rigid restraint. Another possible interpretation could be made with regard to the supposition made in chapter 3 that especially increased impactor velocity would lead to higher ΔE_{kin} -values. In this context it would be plausible that the apparent 1.5-fold ΔE_{kin} increase for coppice trees anchored in the forest ground is only due to the 1.34 times higher impact velocity of the field experiments (Table 4.3).

Table 4.3: Comparison of the impactor velocity and mass of the pendulum tests (chapter 3) and the forest tests of the present study.

	Mean impact velocity [m s ⁻¹]	Impactor mass [kg]	Mean impact energy [kJ]	Mean impact momentum [kg m s ⁻¹]
Pendulum	11.36	84	5.42	954
Coppice forest	15.23	60	6.95	914
Ratio	1.34	0.71	1.28	0.96

Evidently, the interpretations above are all contradictory. Only a larger dataset, on the basis of a set of different impact velocities and masses applied to similar specimens could elucidate the actual facts. However, the results of this study show that the mechanical resistance of individual coppice trees in their natural condition is not substantially different from those tested with the pendulum device. Obviously, the root anchorage constitutes neither a weak spot nor a decisive element that increases the mechanical resistance.

A major drawback of both regression models that express the relationship between mechanical resistance (Δp and ΔE_{kin}) and the stem diameter (DBH) is the fact that most trees among the larger DBH did not completely fail during impact (this accounts for both approaches pendulum and forest impact device). Consequently, especially the exponent of the best-fit power function should be higher in reality. As a result, any application of the data in rockfall simulation models would lead rather to an underestimation of the actual protective function of a forest.

In this context, the comparison of the ΔE_{kin} -DBH relationship with the data of Dorren and Berger (2005) and Jonsson (2007) also indicates that a higher exponent of the regression model would be more appropriate (Figure 4.3). Although the results of both other studies

emanate from very different test settings and refer only to ΔE_{kin} , the datasets are not fundamentally different. Therefore, despite the problematic inaccuracies of referring only to ΔE_{kin} for the mechanical resistance, the use of such ΔE_{kin} -DBH relationships could constitute a pragmatic compromise for the quantification of the rockfall protective function of forests with rockfall simulation models.

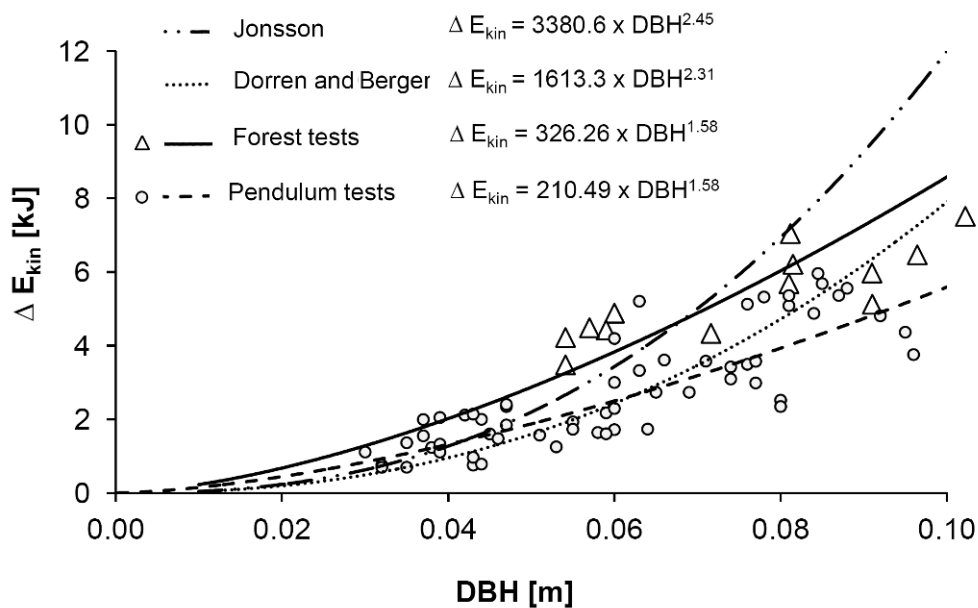


Figure 4.3: Comparison of four ΔE_{kin} -DBH relationships. The study of Jonsson (2007) refers to a model based on full-scale tests against mature Norway spruce trees. The regression model of Dorren and Berger (2005) is based on nine impacts against mature silver fir trees. The ΔE_{kin} -DBH relationship of the forest tests of the present study is based on the average difference between the 13 data points and the regression model of the pendulum results (cp. chapter 3).

The spherical shape of the granite ball permitted to neglect the influence of the angular velocity on the mechanical resistance. However, for rockfall impacts an angular rock shape would have several implications that could not be considered in this study. First, the ro-

tational momentum and energy transmission to the trees would be more pronounced. Consequently, the rock rotation would contribute more to tree breakage and thus be reduced to a larger degree after impact. Second, the variability of the momentum and energy transmission as well as of the direction of the trajectory after impact would be increased and thus even less predictable. Third, the rock edges could have a notching effect on the stem with considerable effects on breakage behavior and mechanical resistance. This issue was also addressed in the study of Jonsson 2007 where a wedge shaped steel trolley was used as impactor against large DBH (> 0.3 m) spruce trees. In this case the notching effect might have been even more pronounced because of the reduced flexibility of the target trees. Hence, for the highly flexible small diameter trees of this study the sphere shaped impactor could stand for a representative mean that allows for focusing on the dominant effects of translational momentum and energy transmission during impact.

Another factor influencing the ΔE_{kin} -values is the used impact angle of approximately 30° (cp. Figure 4.1). A detailed study by Jonsson (2007) on the influence of the impact angle specifies a maximum mechanical resistance of large DBH spruce trees for impact angles between 25° and 40° , for horizontal impact angles (0°) for instance the mechanical resistance is reduced to 70%. Besides, preliminary tests of the device using impact angles below 0° (rock moving upwards during impact) resulted in trajectory deviations in vertical direction limiting the quantification of the kinetic energy loss during impact. In these cases the coppice trees showed pronounced flexural deformations and acted as a jump rather than an obstacle. Hence, the flexibility of the stems and the root anchorage might condition the influence of the impact angle on the mechanical resistance. Consequently, the underlying dataset of this study is only representative for impact angles of approximately 30° .

4.5 Conclusion

The main objectives of this study were to give qualitative insights on the breakage process of coppice trees that are part of coppice clumps and to assess quantitative data on their mechanical resistance. The results show that natural root anchorage does not constitute a mechanically weak spot. Although the natural tree anchorage does not lead to a substantially different mechanical resistance of a tree than a rigid restraint it remains unclear in what way it contributes to the impact energy dissipation process.

Although, constant impact angles were used (about 30°) preliminary tests indicate, that the influence of the impact angle on the mechanical resistance of the trees might be non-negligible. Especially with regard to high flexibility of the stems this aspect should be considered in future studies.

Breakage behavior of small DBH trees is characterized by pronounced flexural deformations that would certainly lead to tree-tree contacts within a natural coppice clump that was not freed from trees before impact and thus influence the whole impact process. Moreover the study showed that the probability of rock rebounds against multiple trees of the same clump is potentially very high. The consequences of these rockfall specific features of clumps for the rockfall protective function of coppice forests should be investigated in future studies.

This study emphasized the limits of using the loss of momentum or kinetic energy of an impactor to assess and compare the mechanical resistance of trees. In future studies, impact velocity and mass should be treated separately to assess the influence of both factors on mechanical resistance. In depth knowledge on this aspect would

permit to better estimate the uncertainties when referring only to kinetic energy loss for practical reasons in rockfall hazard assessments.

The used test device proved to be very useful. Its major advantage of generating a free flight of the impactor before impact was a prerequisite, both for the quantitative and the qualitative results. However, the tube system should be reinforced at its lower end in order to increase the control of the granite ball trajectory and thus the centrality of the impacts. In future studies, impact energy should be increased in order to assess the influence of impact velocity and mass and to extend the measuring range to larger tree diameters.

5. Influence of tree species on the mechanical resistance against rockfall of small diameter trees

5.1 Introduction

Reliable quantification of the rockfall protective function of forests using rockfall simulation models remains a difficult task. In the past, several full-scale approaches have been realized to establish mathematical relationships between the tree diameter and the potential of individual trees to reduce the kinetic energy of an impacting rock (Couvreur, 1982, Mizuyama and Narita 1988, Dorren and Berger, 2005, Dorren et al., 2006, Jonsson, 2007, Dorren et al., 2007, Kalberer et al., 2007, Lundström, 2008).

Each study relied on a different experimental setup and variable tree and rock properties. Therefore, the data are difficult to compare and do not permit to assess the influence of the tree species on the impact process in a consistent way. However, from a practical point of view, data on the mechanical resistance of additional species could considerably improve the reliability of rockfall simulation models that so far may rely on mean values for coniferous or broadleaf trees without accounting for the enormous variability of wood strength properties within these two categories (cp. Vorreiter, 1949, Wagenführ, 1985, Sell, 1987, Dorren, 2007).

The two precedent studies of this dissertation (chapters 3 and 4) focused on the mechanical resistance of beech coppice trees (*Fagus sylvatica* L.) against rockfall. This study aims to assess the influence of the tree species on the mechanical resistance of small diameter

stems in order elucidate how to extend the data on beech to other species.

To extend existing data to different species, two approaches have been used in the past. One refers to the impact toughness ratio between different species based on small knot free green or dry wood specimens (Dorren and Berger, 2005, Jancke et al., 2009). The other method compares the integral of the total overturning moment of different species during static winching tests on forest trees (Stokes et al., 2005). Both approaches assign a higher mechanical resistance to broadleaf trees than to coniferous species. However, each of the used methods leads to considerable underestimations of the potential of trees to reduce the energy of impacting rocks, because the experiments do not reflect the processes governing the impact to the same degree as full-scale impacts in forests (Dorren et al., 2007, Jonsson 2007). Therefore, it is questionable if these indirect approaches are suitable to conclude for the mechanical resistance of other species by simply referring to the ratio of total breakage energy.

Moreover, extending existing data from full-scale impact tests to other tree species is based on the assumption that wood strength properties have the same influence on the energy necessary to break a specimen for both the two indirect approaches and rockfall impacts against forest trees. However, this is unlikely, especially because the influence of the factors conditioning the energy necessary to break a specimen (including impactor mass and velocity, specimen dimensions and mass) are numerous and moreover often interdependent (Kollman, 1951, Lundström et al., 2008).

This idea is furthermore supported by the findings of the pendulum tests in chapter 3. It was shown that for the small diameter stems (DBH < 0.1m) the impact process is substantially different from the

one of large diameter trees (DBH > 0.3 m) and characterized by considerable flexural deformations of the stems during impact and negligible destruction of the wood tissue at the point of impact. It was suggested that the potential of a tree to reduce the kinetic energy of an impactor depends predominantly on the mass of the stem which is accelerated during impact and the stem flexibility allowing for the mass acceleration. Hence, because the breakage process is fundamentally different from dry wood toughness tests and winching tests on forest trees, the two abovementioned approaches do not seem appropriate to conclude for the potential of other tree species to reduce the kinetic energy of an impactor. Consequently, the degree to which the species specific wood strength conditions the energy necessary to break a given tree is not constant and certainly changes with changing tree dimensions.

The hypothesis made in chapter 3 on the predominant influence of stem mass has a major implication on the species specific differences for reducing the kinetic energy of an impactor, because in living trees wood density conditioning the mass of an impacted stem does not vary to a large extent between most species (e.g. Table 5.1). This is due to the fact that most fresh wood cell lumina are filled with water and not with air as in dry wood. Hence, if the stem mass strongly determines the reduction the kinetic energy of an impactor during impact and stem mass is similar for most species, the species specific wood strength should play only a negligible role for the potential of any small DBH tree to reduce the kinetic energy of rockfall. Accordingly, the hypothesis of this study is that for small DBH tree stems the mechanical resistance against rockfall does not markedly depend on the species. Consequently dry wood properties or static test data should be inappropriate indicators of the mechanical resistance of other species.

To verify these hypotheses in a consistent way full-scale dynamic impact tests were conducted. The focus was on small DBH stem segments (DBH < 0.1 m) of beech (*Fagus sylvatica* L.), chestnut (*Castanea sativa* Mill.) and fir (*Abies alba* Mill.). These three species were chosen, because they fulfilled the two preconditions of being widespread in rockfall protection forests in the Alps and of consisting of wood with considerably different properties. In this way a maximum of species specific parameters potentially influencing the mechanical resistance to rockfall impacts were included. Table 5.1 summarizes selected wood properties of the three species based on literature data referring to multiple authors.

The main objectives of the experiments were to quantify the mechanical resistance of the species against dynamic impacts, to verify the hypotheses above and to provide new data that can be used for quantifying the rockfall protective function of forests. Here, the data on beech and chestnut are especially relevant with regard to the protective function of broadleaf coppice forests. The dynamic tests were supplemented with data from static 3-point bending tests on the same species to provide information on the modulus of rupture and the modulus of elasticity of the tested species. The aim was to assess whether mean values were distinct between the species and if there were analogies to the results of the impact tests.

Table 5.1: Selected mechanical key properties of beech (*Fagus sylvatica* L.) chestnut (*Castanea sativa* Mill.) and fir (*Abies alba* Mill.).

	Unit	Beech	Chestnut	Fir	Ratio
Wood density (air dried) ¹	[kg m ⁻³]	630	555	425	1.48 : 1.30 : 1
Wood density (green) ³	[kg m ⁻³]	1070	1060	850	1.26 : 1.25 : 1
Impact toughness (air dried) ¹	[kJ m ⁻²]	100	57	50	2.00 : 1.14 : 1
Modulus of rupture (air dried) ¹	[N mm ⁻²]	108	71	68	1.59 : 1.04 : 1
Tensile strength (air dried) ¹	[N mm ⁻²]	118	129	87	1.36 : 1.48 : 1
Modulus of elasticity (air dried) ¹	[N mm ⁻²]	14350	8500	12250	1.17 : 0.69 : 1
Main cell type ²	n.a.	Fibers + vessels	Fibers + vessels	Tracheids	n.a.
Fiber / tracheid length ^{2,3}	mm	0.72	1.22	3.70	0.19 : 0.33 : 1
Wood ray height ^{2,3}	mm	1.0	0.5	0.2	5.00 : 2.50 : 1
Annual ring structure ²	n.a.	semi-ring-porous to diffuse-porous	ring-porous	decreasing cell lumina from early to late wood	n.a.

¹Sell, 1987: mean values of several studies; ²Richter and Dallwitz, 2000; ³Wagenführ, 1996

5.2 Material and methods

5.2.1 Test material

The test material was cut from three different sites in the French Alps. Both broadleaf species stem from coppice forests (beech: N 45° 35' 55.8"; E 05° 49' 45.1"; 820 m a.s.l.; chestnut: N 45° 17' 14.1"; E 05° 17' 14.1"; 660 m a.s.l.). The fir specimens stem from a heterogeneous stand mainly composed of fir, spruce (*Picea abies* (L.) Karst.) and some broadleaf species (N 45° 12' 13.3"; E 06° 02' 57.7"; 1220 m a.s.l.). The fir trees had supported very different competition situations resulting in variations of average DBH increments between the trees of roughly 1.5 to 8 mm year⁻¹. Table 5.2 gives an overview of the number of tested specimens and their main properties. All specimens were tested in "fresh" status (i.e. the wood moisture content was beyond fiber saturation) and including bark. The pendulum impact tests against the beech stem segments have already been described in detail in chapter 3.

5.2.2 Dynamic pendulum impact tests

The pendulum impact device is identical with the one described in chapter 3. In the centre at ground height the specimens were vertically clamped into a rigid restraint with their thicker end. The restraint consisted of a 0.3 m deep steel cylinder with the inner diameter adaptable to the stem diameter. The steel cylinder was embedded into a 1200 kg reinforced concrete slab casted into the ground. The other end of the specimens remained unrestrained. The impactor was a spherical pendulum bob of reinforced concrete (mass = 84 kg). The bob trajectory was defined by two static ropes attached at a height of approximately 10 m to two massive trees (DBH > 0.7 m) standing left and right from the concrete slab. The two ropes spanned an included angle of approximately 35° between each other (Figure 3.1).

This configuration enabled central impacts against the specimens without impeding bob trajectory deviations during impact. Impact direction was horizontal and the mean impact velocity of all tests was 11.3 m s^{-2} ($\text{SD} = 0.4 \text{ m s}^{-2}$). Impact height was defined as the distance between the surface of the concrete slab (i.e. ground height) and the point of the first bob-specimen contact. Because in chapter 3 no significant differences of ΔE_{kin} between mean impact heights of 0.348 and 0.966 m against beech specimens were observed, only one impact height level (mean height = 0.368 m) was applied to chestnut and fir in this study. The DBH (i.e. reference specimen diameter) was set at 1.3 m above the surface of the concrete slab (Figure 3.2).

Prior to the tests, remaining branches were removed from the specimens. Then, a stem section was cut to determine wood moisture content by oven drying and dry wood density by using the water displacement method (Table 5.2). All specimens were trimmed to a length of 3 m (except from 19 small diameter fir specimens with a total length between 1.6 m and 3.0 m due to their pronounced stem taper). Specimen diameters including bark were measured at the lower end, at ground height, at 1.3 m (DBH) and at the upper end (cp. Figure 3.2). Stem taper was expressed in percent and defined as average diameter reduction per meter specimen length. Mass measurements of each specimen combined with the diameter measurements constituted the basis for determining fresh wood density and specimen volume.

Data acquisition during the pendulum tests was based on two high-speed camera (HSC) recordings. HSC 1 (IDT X-Stream XS3) filmed the impact process perpendicular to the bob trajectory (Figure 3.1). It recorded 200 images per second with one pixel corresponding to approximately $2.5 \times 2.5 \text{ mm}$ on specimen and bob. In addition to detailed qualitative observations, the image sequences permitted to

determine bob velocity before and after impact. From the bob velocity measurements the kinetic energy was calculated. The mechanical resistance of the specimens was defined as the loss of kinetic bob energy following Equation 3.2:

$$\Delta E_{kin} = \frac{1}{2} \times m \times (v_1^2 - v_2^2) \quad (\text{Equation 3.2})$$

m: mass of the bob (84 kg)

*v*₁: incident velocity

*v*₂: velocity after impact

The second high-speed camera (Casio EX-FH25; HSC 2 in Figure 3.1) was mainly used to determine the centrality of the impact and recorded 210 images per second with one pixel corresponding to 10 x 10 mm on specimen and bob. Excentric impacts were excluded from the dataset and were defined as impacts beyond a horizontal distance of 0.31 x 0.5 x DBH left and right from the vertical central tree axis (CTA) seen from the impact direction (cp. Dorren and Berger, 2005; Figure 3.2). The focus on central impacts aimed at assessing the maximum potential for reducing the kinetic bob energy of each specimen.

5.2.3 Static 3-point bending tests

For the static 3-point bending tests a standard testing machine was used. The total span for all specimens was 1 m. During testing the force was continuously measured and applied at mid-span with a constant deflection rate (0.08 mm s⁻¹). The supports were V-shaped in order to maintain the specimens in position. Specimen preparation included branch removal, diameter measurements at all three force application points and determination of wood moisture content by oven drying.

For all specimens the modulus of rupture (MOR) was calculated following Equation 5.1:

$$MOR = \frac{8 \times F_{max} \times L}{\pi \times D^3} \quad (\text{Equation 5.1})$$

Where F_{max} is the maximum force measured during testing, L the total span and D the specimen diameter at mid-span.

The modulus of elasticity (E_{mod}) was calculated following Equation 5.2:

$$E_{mod} = \frac{F_{el}}{f_{el}} \times \frac{L^3}{48 I_z} \quad (\text{Equation 5.2})$$

Where F_{el} is the maximum force that does not entail plastic strains of the stem (end of the linear phase of the relationship between the applied force and the stem deflection at mid-span measured for each test), f_{el} is the stem deflection corresponding to the measured force F_{el} , and $I_z = \frac{\pi \times D^4}{64}$ is the bending moment of inertia.

5.3 Results

5.3.1 Specimen properties

Table 5.2 summarizes the main characteristics of the specimens of the dynamic and static test series. The variability of these data was high and generally most important for fir and least important for beech. Stem taper was on average slightly more pronounced for chestnut than for beech. The fir specimens were on average considerably more tapered than both other species. In addition, stem taper decrease with increasing DBH was most pronounced for fir (Figure 5.1). The overall difference in stem taper decreases with in-

creasing DBH and might become negligible beyond 0.1 m DBH. Beech had the highest dry wood density and consequently also the lowest wood moisture content. In accordance with its semi-ring-porous to diffuse-porous annual ring structure the variability of dry wood density and moisture content was the least pronounced among the three species. Fresh wood density was similar for all three species. As a result, also the relationships between specimen DBH and mass were very similar (Figure 5.2).

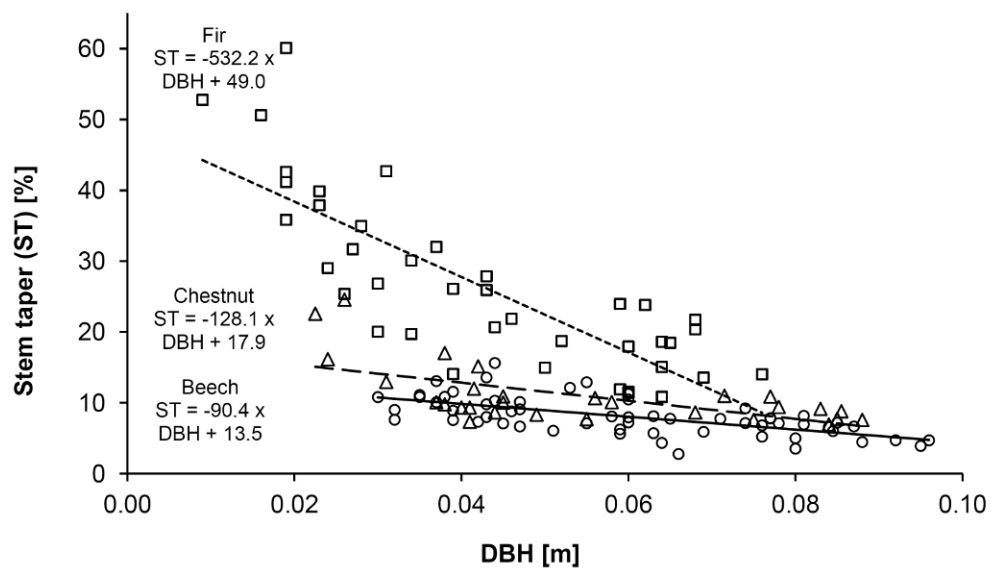


Figure 5.1: Comparison of the stem taper of the three species defined as average diameter reduction per meter specimen length.

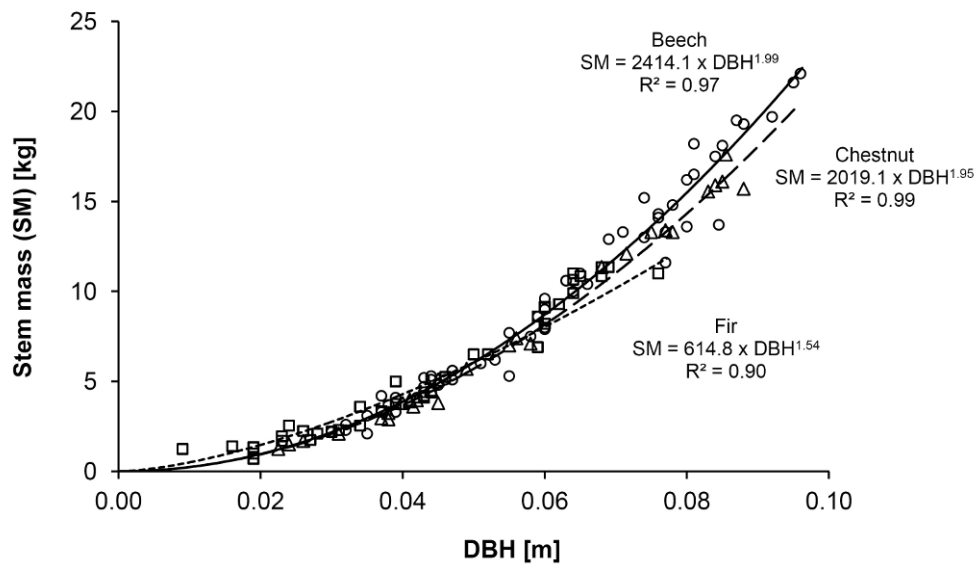


Figure 5.2: Comparison of the stem mass-DBH relationships of all specimens of the three species.

Table 5.2: The main properties of all specimens from the dynamic and the static tests.

Species			Dynamic pendulum impact tests			Static 3-point bending tests		
			Beech	Chestnut	Fir	Beech	Chestnut	Fir
No. of stems	n		59	31	40	36	27	28
DBH or mid-span diameter	min	[m]	0.030	0.023	0.009	0.030	0.035	0.033
	max	[m]	0.096	0.088	0.076	0.110	0.110	0.104
Length		[m]	3	3	1.6-3	1.5	1.5	1.5
Stem taper		[% m ⁻¹]	8.0	11.0	26.4	8.4	9.4	11.4
		SD	2.6	4.3	12.2	5.1	4.7	5.8
		n	59	31	40	36	27	28
Wood moisture content		%	59.4	81.9	100.3	57.4	98.5	101.2
	fresh	SD	3.7	11.1	27.5	4.3	10.8	24.3
		n	20	26	40	36	27	28
Wood density	fresh	[kg m ⁻³]	1017	932	1060	n.a.	n.a.	n.a.
		SD	77	65	162	n.a.	n.a.	n.a.
		n	59	31	40	n.a.	n.a.	n.a.
Wood density	oven dry	[kg m ⁻³]	751	632	593	n.a.	n.a.	n.a.
		SD	24	114	140	n.a.	n.a.	n.a.
		n	8	5	11	n.a.	n.a.	n.a.

5.3.2 Dynamic pendulum impact tests

The qualitative and quantitative results of the pendulum impact tests against the 59 beech stems have been shown in detail in chapter 3. Breakage behaviors of the chestnut and fir specimens were as variable as those of beech. Figure 5.3 distinguishes five major elements of the breakage processes of the three species that can occur simultaneously during impact. Apart from seven beech and four chestnut specimens that did not totally break during impact, be-

cause the kinetic bob energy was insufficient, all specimens broke at ground height. The proportion of stems that also broke at impact height is substantially higher for fir than for both broadleaf species. In addition, in contrast to the broadleaf species, fir specimens with DBH larger than 0.059 m (14 in the set of specimens) systematically broke at impact height, whereas about half of the more flexible, smaller DBH specimens did not. The larger DBH fir specimens did not considerably deform before breakage and time to failure (defined as impact duration until the first visible crack occurrence on the specimen surface) and total impact duration were shorter than for the two broadleaf species. A large number of beech and chestnut specimens showed longitudinal fractures of several decimeters, frequently in the form of ring shakes. Longitudinal failures of several decimeters were absent for fir. The visible damage at the bob-specimen contact surface was limited to local bark excoriation for all specimens. Image sequences of typical breakage behaviors of the three species are shown in Annex 8.1.

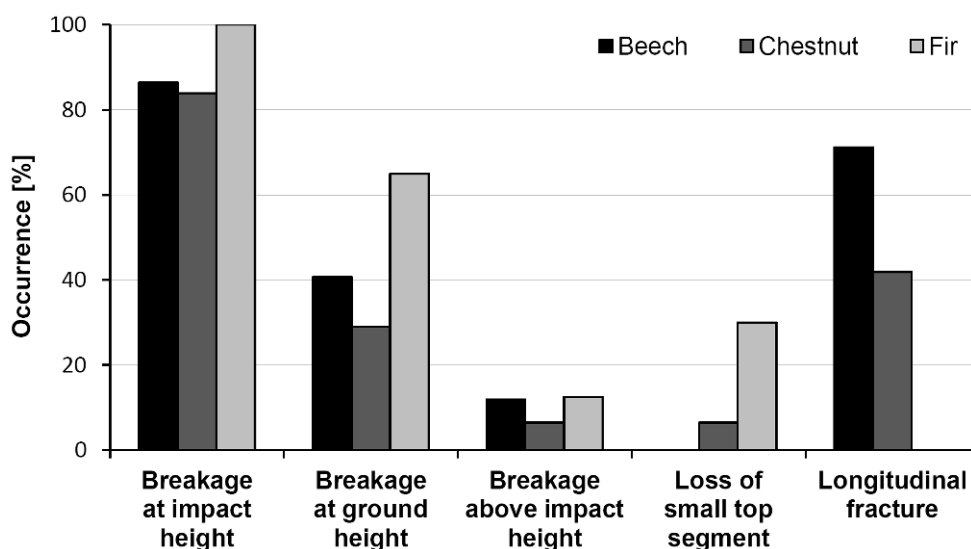


Figure 5.3: Occurrence of the main breakage types during impact.

The propagation of a mechanical wave along the specimens during impact provoked the loss of a small segment of the upper end with a maximum length of 0.3 m of two chestnut and a quarter of the fir specimens. In all these cases the upper end diameter was below 0.025 m. Therefore, the fir specimens were certainly most prone to this aspect, because due to the more pronounced stem taper more than 60% of the specimens had smaller upper end diameters whereas the beech specimens never fell below the limit of 0.025 m. This observation resembles the loss of the tree tops during full-scale impact experiments against entire trees (cp. 2nd test series chapter 3, Dorren et al., 2005, Jonsson, 2007).

Fracture surfaces of the fir specimens were substantially different from those of the two broadleaf species. Longitudinal ringshakes extending several decimeters in axial direction were absent for fir (cp. also chapter 3). However, on the transverse fracture surfaces the dissociation of the annual rings was often visible (Figure 5.4). The transversal fracture surfaces of fir could be qualified as brash (cp. Kollmann 1951) in most cases whereas those for beech and chestnut all transverse fracture surfaces were long fibrous.

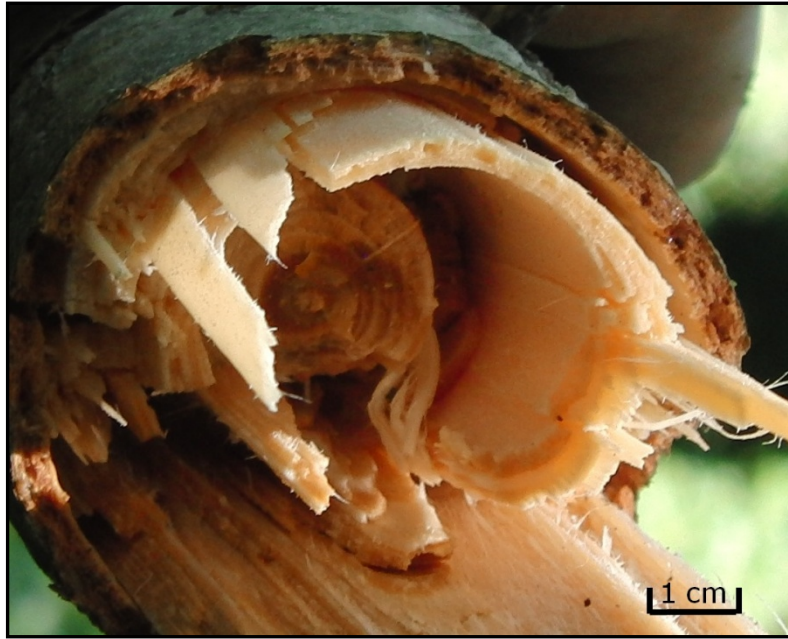


Figure 5.4: Section of a broken fir specimen. Some annual rings are dissociated. The concave and convex fracture surfaces of these ring shakes are located in the transition from late- to earlywood.

Impact duration was on average shortest for fir and longest for chestnut. However, it was highly variable for all species and not correlated to DBH or ΔE_{kin} . Time to failure was neither correlated to DBH or ΔE_{kin} . The average and maximum times to failure for beech are higher than for both other species, because beech was the only species impacted 12 times between 0.64 and 1.04 m above ground (Figure 5.5). At this impact height times to failure were sometimes longer due to less pronounced shear stresses in the specimens close to ground height.

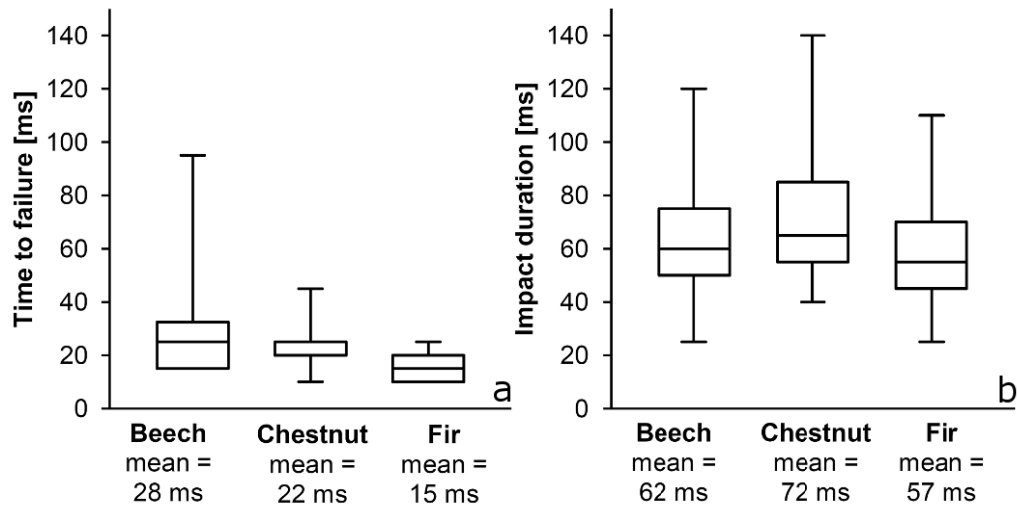


Figure 5.5: (a) Time to failure and (b) total impact duration of all specimens.

The relationships between the reduction of the kinetic energy ΔE_{kin} and DBH for all three species are shown in Figure 5.6. The variability expressed as root mean square percentage error (RMSPE) was high for all species and most pronounced for fir and least for chestnut ($RMSPE_{fir} = 42\%$; $RMSPE_{beech} = 35\%$; $RMSPE_{chestnut} = 28\%$). Apart from the high variability, the results are influenced by the fact that seven beech and four chestnut specimens among the larger DBH did not totally break during impact, because the kinetic bob energy was insufficient. Therefore, especially the ΔE_{kin} -values of the larger DBH should be seen as rather indicative. The reduction of the diameter range with the objective to exclude these 11 specimens would not have changed the overall interpretation. However, because these values still indicate the exponential character of the relationships they were integrated into the dataset.

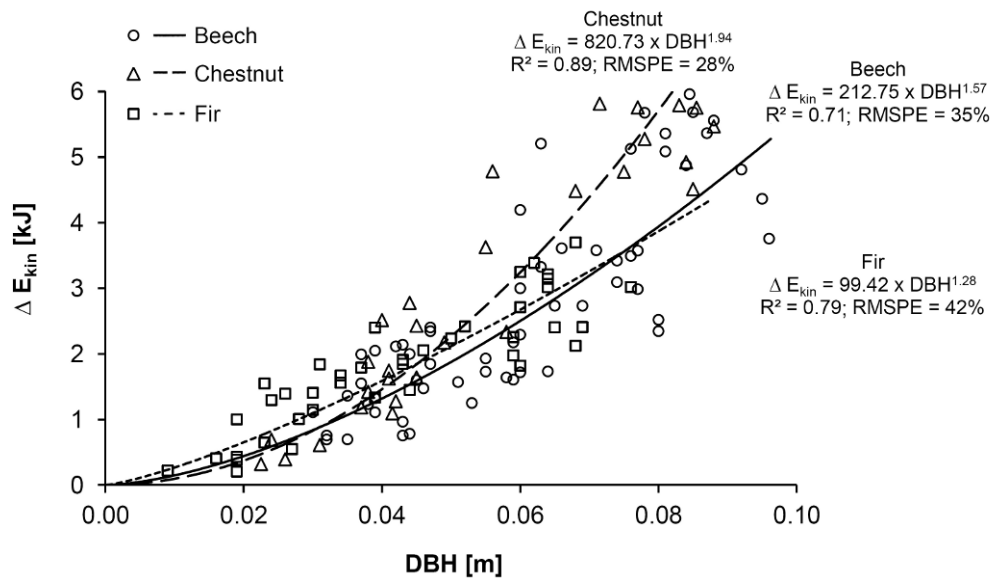


Figure 5.6: Comparison of the relationships between ΔE_{kin} and DBH of the three species.

The use of the diameter at impact height instead of the DBH does not considerably change the interpretation of the relationship to ΔE_{kin} (Figure 5.7). Nevertheless, in this way the apparent differences between species are even less pronounced.

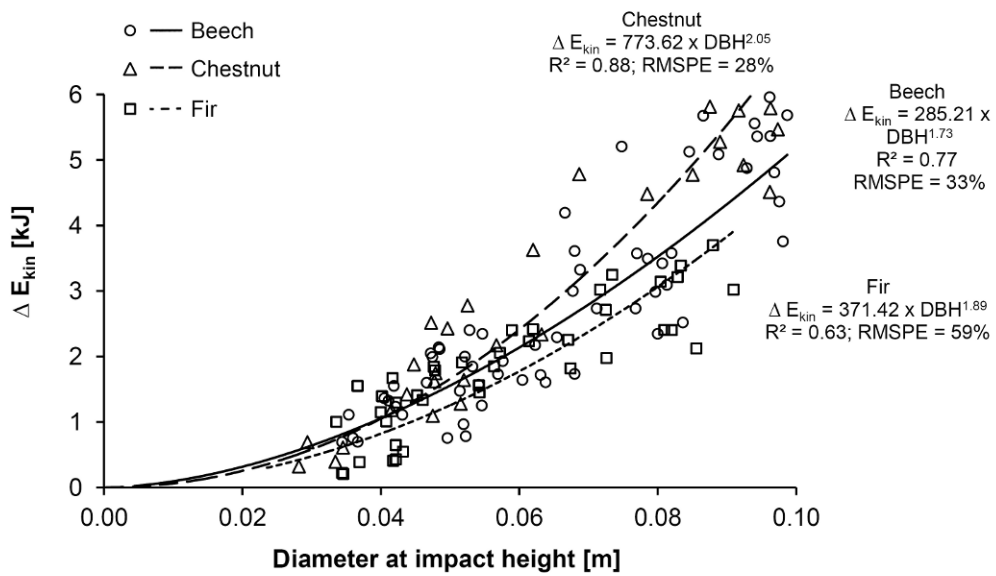


Figure 5.7: Comparison of the relationships between ΔE_{kin} and specimen diameter at impact height of the three species.

In analogy to the impact toughness tests on small defect free dry wood samples (cp. Table 5.1) species specific energy reduction during impact expressed in kJ per m^2 is shown in Figure 5.8. The surface was calculated based on the specimen diameter at impact height. All mean values were multiples of the respective literature data in Table 5.1. The individual values of each species were not correlated to specimen diameter and the mean values were not fundamentally different between species.

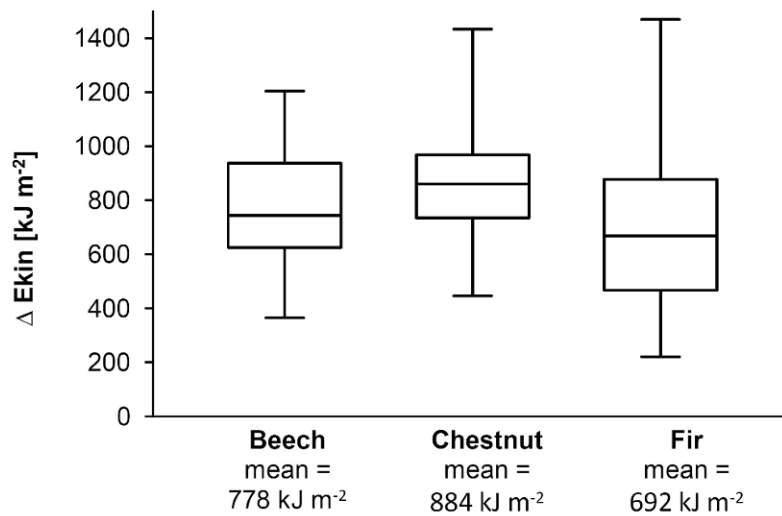


Figure 5.8: The mechanical resistance of all specimens expressed in kJ m⁻² based on the respective specimen section surface at impact height. For comparison, the impact toughness values in Table 5.1 for beech, chestnut and fir are 100, 57 and 50 kJ m⁻² respectively.

5.3.3 Static 3-point bending tests

For all three species the mean values of the modulus of elasticity were considerably lower compared to literature data referring to dry wood in Table 5.1 (Figure 5.9). Moreover, the results were very similar between the species with maximum differences of the mean values below 5%. However, as indicated in Figure 5.9 variability was very high and most pronounced for fir.

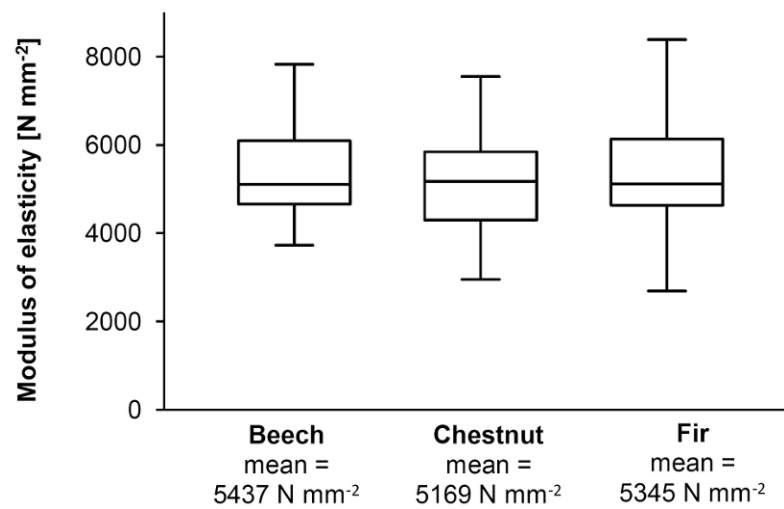


Figure 5.9: Comparison of the modulus of elasticity of all specimens.

The modulus of rupture (MOR) was also well below the dry wood values for all three species (cp. Table 5.1; Figure 5.10). Despite the pronounced variability the general gradient from beech via chestnut down to fir was clearly visible. There was no correlation between modulus of elasticity and MOR. Moreover, both modulus of elasticity and MOR were not correlated to specimen diameter for any of the three species.

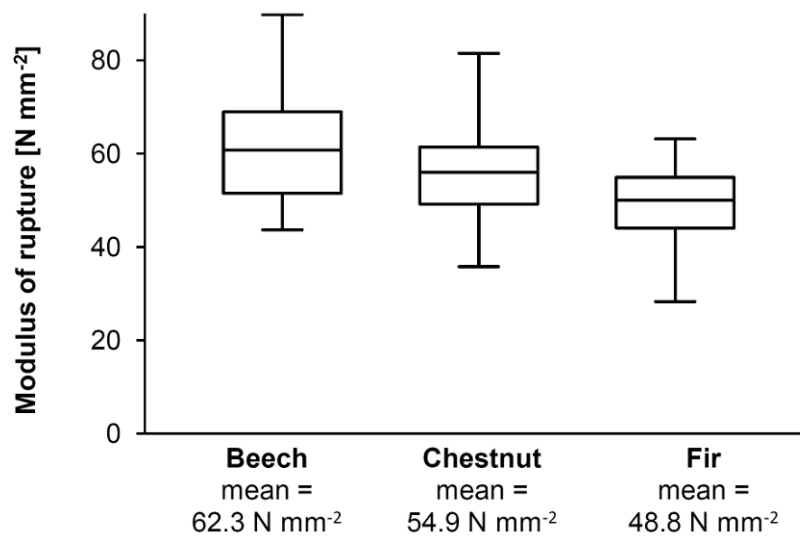


Figure 5.10: Comparison of the modulus of rupture of all specimens.

Estimations of the total energy required to cause stem failure, calculated as the work of the force applied at mid-span, by integrating the force-mid-span deflection curves did not lead to reliable results. Consequently, the product of F_{\max} and the deflection at F_{\max} referred to as $E_{\text{tot-ind}}$ was used as indicator for the total bending energy. This measure certainly overvalued the total bending energy in all cases to an unknown degree. Figure 5.11 shows the relationship between the diameter at mid-span and $E_{\text{tot-ind}}$ for all three species. In all cases and for the entire diameter range to 0.1 m $E_{\text{tot-ind}}$ did not exceed 35% of the corresponding total energy ΔE_{kin} of the dynamic pendulum tests represented by the regression models shown in Figures 5.6 and 5.7.

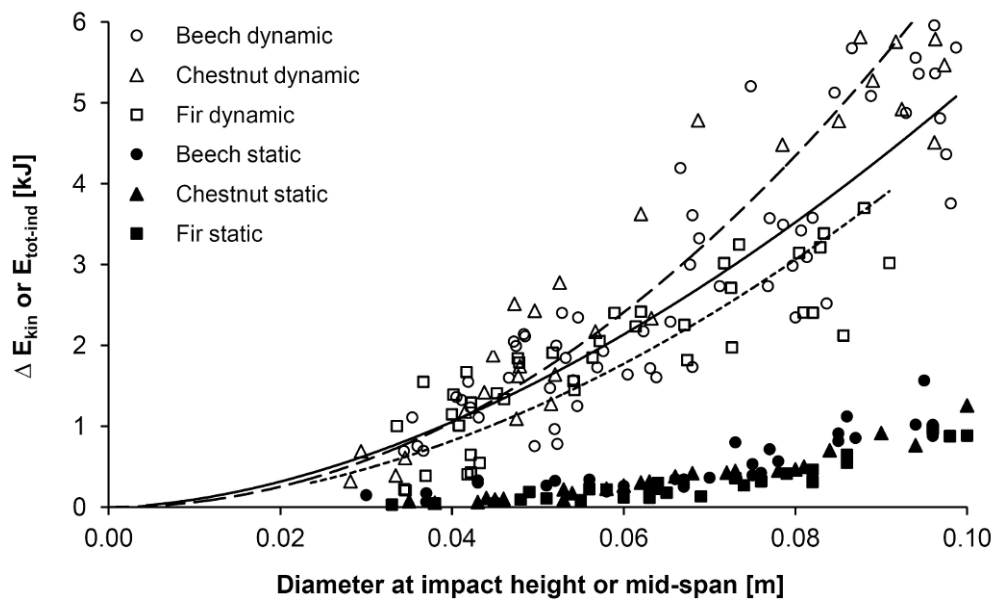


Figure 5.11: Total bending energy of the static tests indicated by $E_{tot-ind}$. The ΔE_{kin} -values of the dynamic pendulum tests (cp. Figure 5.7 are shown for comparison.

5.4 Discussion

The hypothesis of this study was that the potential of the specimens to reduce the kinetic energy of the impactor during impact (referred to as the mechanical resistance) of small DBH tree stems to dynamic impacts is not fundamentally different for different species. The reasoning behind this hypothesis was the presumption made in chapter 3 that mechanical resistance is predominantly determined by the specimen mass for small DBH stems. As fresh wood mass is similar for most species the mechanical resistance should therefore not be fundamentally different.

Measurements of fresh wood density and relationships between stem mass and stem diameter in this study confirm similar mean values for all three species. Moreover, the results of the dynamic impact tests indicate only minor differences of mechanical resistance between the species. The variability of the data was too high to de-

termine distinct species specific relationships between ΔE_{kin} and specimen DBH. Therefore, this study confirms the initial hypothesis that species specific differences have only negligible influence. However, this fact refers only to small diameter specimens under the applied test conditions, and the similarities of the relationships between ΔE_{kin} and DBH do not prove the predominant role of specimen mass in the breakage process.

One precondition for a predominant and similar role of specimen mass in the breakage process of different species would be that the flexural stiffness (related to modulus of elasticity and stem diameter in particular) that allows for the mass acceleration is also similar for all species. In this context the static 3-point bending tests on a total of 91 specimens of different diameters indicate equivalent mean values for the modulus of elasticity of the three species. This finding supports the precondition and hence the idea of the specimen mass as crucial element governing the impact process. However, all data assessed in this study show a high variability involving substantial uncertainties. Therefore, a detailed understanding of the impact process can only be achieved by supplementary tests with varying impact conditions supported by numerical modeling of the impact process in future studies.

The different relationships between stem taper and DBH have some relevant implications for the comparison of the mechanical resistance of the three species. For instance, by referring to the DBH to express the mechanical resistance of a species, the mechanical resistance of the fir specimens seems to be overestimated, because due to the pronounced stem taper the diameter at impact height is relatively larger than the one of both broadleaf species. But then, by referring to the diameter at impact height to express the mechanical resistance of a species, the mechanical resistance of the two broadleaf species seems to be overestimated because in this case their

stem mass is much higher than that of the more tapered fir specimens. This dilemma is of course specific to the applied impact height in this study (mean height = 0.368 m). Hence, for fir the mechanical resistance is certainly correlated to impact height and for higher impact heights this species is surely less resistant than both other species. Moreover, the fact that the ΔE_{kin} -values of the less tapered larger DBH specimens of fir are on average lower than those of beech and chestnut, indicates that for this species the species specific wood strength partly conditions the mechanical resistance.

Another aspect relativizing the conclusion of minor influence of the tree species on the mechanical resistance of small diameter trees is the fact that impact velocity was relatively low ($\approx 11.6 \text{ m s}^{-1}$). Although this value is representative, rockfall velocities can easily attain 25 m s^{-1} on forested slopes (Dorren and Berger, 2005). In this context, the relatively small flexural deformations and the early failure of the fir specimens could indicate that the mechanical strength of fir might not be sufficient to sustain considerably faster impacts in the same way as both broadleaf species. Hence, possibly the species specific influence on the mechanical resistance of small diameter trees might increase with increasing impactor velocity. This hypothesis is in accordance with the suggestion made in chapter 3 that the influence of stem mass is certainly limited by an increase of the peak force sustained by the specimens impacted with increasing impact velocities. It is argued that there must be a threshold where specimens break before the stem mass acceleration reaches its maximum effect on the impactor deceleration. Hence, with an increasing peak force, also the influence of species specific wood strength on the mechanical resistance should increase. Consequently, it seems to be most adequate to restrict the initial hypothesis of this study to the broadleaf species until further insights are available.

Due to limited species specific data on the mechanical resistance of trees against rockfall impacts, several precedent studies used indirect approaches to conclude for the mechanical resistance of tree species that had never been tested in full scale impact tests (Stokes et al., 2005, Jancke et al., 2009, Dorren and Berger, 2005). These approaches have in common to rely on the ratio of the values of other mechanical properties between the species. This study proves that such methods do not lead to reliable results for small diameter trees (DBH < 0.1 m). The negligible and not statistically firm differences assign the highest mechanical resistance to chestnut, followed by beech and finally fir. In contrast, literature data on impact toughness and the static 3-point bending tests of this study display a more distinct general gradient of mechanical strength between the three species from beech via chestnut down to fir (cp. Table 5.1 and Figure 5.10). This gradient can also be identified for dry wood density values. Dry wood density conditions most mechanical wood properties (Kollmann, 1951, Bodig and Jayne, 1982; Table 5.1), but obviously, during full-scale dynamic impacts other wood anatomical properties are more determining. Apart from specimen mass, annual ring structure and wood ray properties could be decisive elements (cp. Mattheck, 1997). The incomparableness of dynamic and static energy dissipation processes was furthermore highlighted by the approximately 3-fold difference between ΔE_{kin} and $E_{tot-ind}$ (used as indicator for the total bending energy of the static tests). Such differences have already been observed for larger diameter trees (cp. Dorren et al., 2007, Jonsson, 2007).

With regard to the impact conditions of the dynamic test series (spherical impactor, rather low velocity and mass, flexible specimens) should be considered that the pendulum bob caused only negligible damage at the point of impact on the specimens. For other impactor shapes or larger stem diameters, the damage at the point of impact could constitute a decisive element of the impact

and energy dissipation process. In this case, the species specific dry wood density would condition the degree of damage to a large extent and hence increase the influence of tree species on the mechanical resistance.

5.5 Conclusion

As a complement to detailed data on beech (*Fagus sylvatica* L.), this study provides new facts on the mechanical resistance of small diameter trees of chestnut (*Castanea sativa* Mill.) and fir (*Abies alba* Mill.) against rockfall. It could be shown that the influence of tree species on the mechanical resistance of small diameter trees (DBH < 0.1 m) against rockfall impacts is minimal under the applied test conditions. However, the results refer to only one, relatively low impact velocity and impactor shape. Therefore, it should be investigated in future studies to what degree the species specific influence on the mechanical resistance changes with increasing impact velocity and different impactor shapes.

The results indicate that at least for the two broadleaf species mechanical resistance should be similar for most hazard situations. Probably this accounts also for nearly all species constituting coppice stands in the Alps (the main genera are: *Quercus.*, *Tilia*, *Acer*, *Fraxinus*, *Castanea*, *Robinia*, *Corylus*, *Sorbus* (Jancke et al., 2009, Radtke et al., 2012)). Hence, assessing the rockfall protective function of coppice stands and other forests composed of small diameter broadleaf trees without accounting for the spatial species distribution and the often manifold species composition by applying the regression model for beech (the most substantiated of the three) might lead to realistic results. This could considerably facilitate forest inventories for acquiring simulation model input data and also simplify the rockfall simulations.

The specimen mass and the flexural stiffness of the specimens seem to predominantly determine the mechanical resistance. However, this assumption could not be proven and has to be verified in future studies. Furthermore, especially the high variability of the results and the plethora of possible impact conditions of rockfall against trees limit the validity of such general conclusions. The effect of stems with DBH of less than 0.025 m on the impactor kinematics is only negligible for the used impactor velocity and mass.

Finally, the study confirmed that other mechanical tests than full-scale impact tests do not lead to reliable results for concluding for the mechanical resistance of different species to rockfall impacts. The main reason is that other mechanical tests cannot account for the complex interactions of multiple factors influencing the dynamic impact process of rockfall against trees.

6. Overall synthesis

The objective of this dissertation was to assess the potential of small diameter trees representative for coppice forests to reduce the velocity (i.e. momentum and kinetic energy) of an impacting rock. The purpose was to provide quantitative data for assessing the rockfall protective function of coppice stands with rockfall simulation models. The data presented in three studies (chapters 3, 4 and 5) are suitable for being used as simulation model input data and they are more reliable than data of previous studies, because the impact process specific to small diameter trees (DBH < 0.1 m) was considered.

It was found that the mechanical resistance increases exponentially with increasing tree diameter. For small diameter broadleaf trees the mechanical resistance is not determined by impact height at least for all impact heights between 0.2 and 1 m. In coppice forests the impact angle might substantially influence the potential of the trees to reduce the velocities of impacting rocks. Natural root anchorage and the transition zone from roots to the stems of the coppice trees proved to sustain the stresses induced by the impacts. Hence, because these tree parts do not constitute predetermined breaking points, the tests indicate that coppice trees in their natural environment are at least as resistant to dynamic impacts as those tested with the pendulum device.

Moreover, the third study shows that most likely for small diameter broadleaf trees the mechanical resistance against rockfall of the majority of coppice species is not substantially different. Hence, future assessments of the rockfall protective function of coppice stands and other forests composed of small diameter broadleaf trees could be made without accounting for the spatial species distribution and the often manifold species composition. This could considerably facilitate

forest inventories for acquiring simulation model input data and also simplify the rockfall simulations.

Nevertheless, the three studies also put forward insights on the rock-tree interactions that relativize the general conclusions above to a certain degree. The studies showed that the mechanical resistance of a tree with a given diameter is not a constant material property. It changes as a function of both impactor properties mass and velocity. Unfortunately, it remains unclear to what degree both factors determine the mechanical resistance. Because of these facts, the comparability of results of different test series based on different impactor properties is very limited. Moreover, whether the mechanical resistance is expressed in momentum loss (Δp) or kinetic energy loss (ΔE_{kin}) of the impactor in such comparisons leads to diverging conclusions. Therefore, it is difficult to estimate to what degree the results of the three studies are representative for other impactor masses and velocities frequently occurring on active rockfall slopes.

This dilemma does not only curtail the conclusions of this study, but also narrows the reliability of the data of previous studies that are actually used for integrating the rockfall protective function of forests into rockfall hazard assessments. Therefore, future studies should focus on the influence of impactor mass and velocity separately and include a large tree diameter range. If full-scale tests are estimated to be too laborious, a numerical modeling approach could be a good compromise. From the modeling results, the uncertainties of expressing the mechanical resistance as ΔE_{kin} could be estimated. Moreover, it could be assessed whether it is more appropriate to express the mechanical resistance with Δp or ΔE_{kin} or else if it would be necessary to treat impactor mass and velocity separately. The latter might substantially increase the reliability of physical process based models which could easily be adapted to such an approach.

Apart from the uncertainties described above the data might substantially underestimate the rockfall protective function of coppice forests, because the rockfall hazard mitigating effects of coppice clumps have not been accounted for. Although their consideration was not intended in this dissertation some findings contribute to a better understanding. First, the observed pronounced flexural deformations of the stems should lead to a high probability of tree-tree contacts within dense coppice clumps during impact. Second, the impact tests conducted in a coppice forest indicate that the probability of serial rock-tree interactions within a coppice clump might also be very high. Both findings emphasizing the positive hazard mitigating effect of coppice clumps indicate that this issue is worthwhile to be quantified in future studies to more realistically estimate the protective function. Moreover, further details on the effect of clumps could certainly enhance and substantiate silvicultural interventions aiming to improve the rockfall protective function of coppice stands.

Finally, this work constitutes a decisive step towards a more objective quantification of the rockfall protective function of coppice stands. In addition to detailed data and understanding of the impact process and breakage behaviors of the trees the dissertation highlights key issues on which future research should focus to increase the reliability of rockfall hazard assessments.

7. References

Agnoletti M. 2002. Ecological balance and socio-economic development: the attempt to establish a productive forest ecosystem in southern Europe. IUFRO News of Forest History 2002: 9-17.

Aller D. 2012. Secure and insure – key factors to the Swiss integrated natural hazards risk management. Keynote lecture at the Interpraevent 2012.

Alpine Convention. 2010. International treaty for the promotion, development and protection of the Alps - Objectives and activities. Permanent Secretariat of the Alpine Convention: Innsbruck

Archer RR. 1987. Growth stresses and strains in trees. Springer Verlag: Heidelberg

Avocat H, Tabourdeau A, Chauvin C, De Sede Marceau M-H. 2011. Energy and wood in the French Alps: strategies for an uncertain resource. Revue de géographie alpine 99-4. DOI : 10.4000/rga.1616

Banthia N. 1987. Impact Resistance of Concrete. PhD Thesis University of British Columbia: Vancouver

Bätzing W. 2002. Die aktuellen Veränderungen von Umwelt, Wirtschaft, Gesellschaft und Bevölkerung in den Alpen. Bundesministerium für Umwelt, Naturschutz und Reaktorsicherheit: Berlin

Beimgraben T. 2002. Auftreten von Wachstumsspannungen im Stammholz der Buche (*Fagus sylvatica* L.) und Möglichkeiten zu deren Verminderung. PhD Thesis Albert-Ludwigs-Universität: Freiburg im Breisgau

Berger F, Quéstel C, Dorren LKA. 2002. Forest: a natural protection mean against rockfall, but with which efficiency? The objectives and methodology of the ROCKFOR project. *Interpraevent* 2002 **2**: 815-826.

Bodig J, Jayne B. 1982. *Mechanics of Wood and Wood composites*. Van Nostrand Reinhold Company: New York

Bourrier F, Dorren L, Nicot F, Berger F, Darve F. 2009. Toward objective rockfall trajectory simulation using a stochastic impact model. *Geomorphology* **110**: 3-4. doi:10.1016/j.geomorph.2009.03.017

Bourrier F, Dorren L, Berger F. 2012. Full scale field tests on rockfall impacting trees felled across the slope. *Interpraevent* 2012. Extended abstracts 56-57.

Brändli U-B. 1999. Zustand der Schutzwälder. Ergebnisse aus dem zweiten LFI. *Wald und Holz* **80 (5)**: 11-14.

Brang P, Schönenberger W, Frehner M, Schwitter R, Thormann J-J, Wasser B. 2006. Management of protection forests in the European Alps: an overview. *Forest Snow and Landscape Research* **1**: 23-44.

Braun HJ, Oberdorfer E, Siebert D. 1982. *Lehrbuch der Forstbotanik*. Fischer Verlag: Stuttgart, New York

Brauner M, Weinmeister W, Agner P, Vospernick S, Hoesle B. 2005. Forest management decision support for evaluating forest protection effects against rockfall. *Forest Ecology and Management* **207**: 75-85. 10.1016/j.foreco.2004.10.018

Bunce CM, Cruden DM, Morgenstern NR. 1997. Assessment of the hazard from rockfall on a highway. *Canadian Geotechnical Journal* **34**: 344-356.

CIPRA: International Commission for the Protection of the Alps.
http://www.cipra.org/fr/climalp/construction-renovation/sur-le-chemin-du-bois/la-foret-dans-lespace-alpin/la-foret-dans-lespace-alpin/?set_language=fr. 07.10.2008. Accessed 10.05.2012.

Clarke SH. 1939. Stresses and strains in growing timber. *Forestry* **13**: 68-79.

Clouet N, Berger F, Liévois J. 2012. Rockfall modelling and risk zoning. *Interpraevent 2012*. Extended abstracts 82-83.

Corominas J, Copons R, Moya J, Vilaplana JM, Altimir J, Amigó J. 2005. Quantitative assessment of the residual risk in a rockfall protected area. *Landslides* **2**: 343-357. DOI: 10.1007/s10346-005-0022-z

Courbaud B, Kunstler G, Morin X, Cordonnier T. 2010. What is the future of the ecosystem services of the Alpine forest against a backdrop of climate change? *Revue de géographie alpine* 98-4. DOI: 10.4000/rga.1317

Couvreur S. 1982. Les forêts de protection contre les risques naturels. MSc Thesis. École Nationale du Génie Rural des Eaux et Forêts: Nancy

DIN 52 189 (T1). 1981. Prüfung von Holz: Schlagbiegeversuch, Bestimmung der Bruchschlagarbeit. Deutsches Institut für Normung: Berlin

Dorren LKA, 2003. A review of rockfall mechanics and modeling approaches. *Progress in Physical Geography* **27 (1)**: 69-87.

Dorren LKA. 2012. Rockyfor3D (v5.0) revealed - Transparent description of the complete 3D rockfall model. ecorisQ paper: www.ecorisq.org. Accessed 20.05.2012.

Dorren LKA, Berger F, Imeson AC, Maier B, Rey F. 2004. Integrity, stability and management of protection forests in the European Alps. *Forest Ecology and Management* **195**:165-176.

Dorren LKA, Berger F. 2005. Stem breakage of trees and energy dissipation during rockfall impacts. *Tree Physiology* **26 (1)**: 63-71. doi: 10.1093/treephys/26.1.63

Dorren LKA, Berger F, le Hir C, Mermin E, Tardif P. 2005. Mechanisms, effects and management implications of rockfall in forests. *Forest Ecology and Management* **215**: 183-195. doi:10.1016/j.foreco.2005.05.012

Dorren LKA, Berger F, Putters US. 2006. Real-size experiments and 3-D simulation of rockfall on forested and non-forested slopes. *Natural Hazards and Earth Systems Sciences* **6**:145-153. doi:10.5194/nhess-6-145-2006

Dorren LKA, Berger F, Jonsson M, Krautblatter M, Moelk M, Stoffel M, Wehrli A. 2007. State of the art in rockfall–forest interactions. *Schweizerische Zeitschrift für Forstwesen* **158 6**: 128–141. DOI: 10.3188/szf.2007.0128

Evans S, Hungr O. 1993. The assessment of rockfall hazard at the base of talus slopes. *Canadian Geotechnical Journal* **30**: 620-636.

- FEDRO. 2009. Risk concept for natural hazards on national roads. Swiss Federal Roads Office: Bern
http://www.astra.admin.ch/dienstleistungen/00129/00183/01156/index.html?lang=en&download=NHZLpZeg7t,lnp6I0NTU042I2Z6ln1ad1IZn4Z2qZpnO2Yuq2Z6gpJCDeXt6gmym162epYbg2c_JjKbNoKSn6A--. Accessed 04.05.12.
- FEDRO. 2010. Roads & Traffic - Facts & Figures 2010. Swiss Federal Roads Office: Bern
http://www.astra.admin.ch/dokumentation/00119/04028/index.html?lang=en&download=NHZLpZeg7t,lnp6I0NTU042I2Z6ln1ad1IZn4Z2qZpnO2Yuq2Z6gpJCDe4J,hGym162epYbg2c_JjKbNoKSn6A--. Accessed 04.05.12.
- Ferrand JC. 1983. Growth stresses and silviculture of eucalyptus. *Australian Forest Research* **13 (1)**: 75-82.
- Foetzki A, Jonsson M, Kalberer M, Simon H, Mayer A, Lundström T, Stöckli V, Ammann WJ. 2004. Die mechanische Stabilität von Bäumen: das Projekt Baumstabilität des FB Naturgefahren. *Forum für Wissen* 35-24.
- Fonti P. 2002. Investigations into ring shake of chestnut. PhD Thesis. Eidgenössische Technische Hochschule Zürich No. 14732: Zurich
- Frehner M, Wasser B, Schwitter R. 2005. Nachhaltigkeit und Erfolgskontrolle im Schutzwald. Wegleitung für Pflegemassnahmen in Wäldern mit Schutzfunktion. Bundesamt für Umwelt, Wald und Landschaft: Bern
- Fuller J. 1995. Conditioning stress development and factors that influence the prong test. Research Paper FPL-RP-537. USDA Forest Service.

Gauquelin X, Courbaud B, Ancelin P, Barthelon C, Berger F, Cardew M, Chauvin C, Descroix L, Dorren LKA, Fay J, Gaudry P, Genin J-R, Joud D, Loho P, Mermin E, Plancheron F, Prochasson A, Rey F, Rubeaud D, Wlérick L. 2006. Guide des sylvicultures de montagne. Cemagref, CRPF Rhône-Alpes, ONF: France

Gerber, C. and Elsener, O., 1998. Geeignet oder nicht geeignet. Niederwaldbetrieb im Steinschlaggebiet. *Wald und Holz* **14**: 8-11.

Gsteiger P. 1993. Steinschlagschutzwald. Ein Beitrag zur Abgrenzung, Beurteilung und Bewirtschaftung. *Schweizerische Zeitschrift für Forstwesen* **144**: 115-132.

GVZ. 2011. Geschäftsbericht 2011. Gebäudeversicherung Kanton Zürich.
<http://www.gvz.ch/Gesch%C3%A4ftsbericht2011/tabid/783/language/de-CH/Default.aspx>. Accessed. 02.05. 2012.

Heim A. 1932. Bergsturz und Menschenleben. Beiblatt zur Vierteljahresschrift der Naturforschenden Gesellschaft in Zürich, Vol. 77.

Hudiburg TW, Law BE, Wirth C, Luysaert S. 2011. Regional carbon dioxide implications of forest bioenergy production. *Nature Climate Change* **1**: 419-423. DOI:10.1038/nclimate1264

Hungr O. 2011. Characterization of rock fall and rock slide hazards for the design of protective measures. Rocexs Interdisciplinary Rockfall Workshop.
<http://www.rocexs2011.at/Vortr%C3%A4ge/Oldrich%20Hungr.pdf>. Accessed: 05.05.12.

Jaboyedoff M, Derron M-H. 2005. Integrated risk assessment process for landslides, in: Landslide risk management, edited by Hungr O, Fell R, Couture RR, Eberhardt E. Taylor and Francis: London

Jahn J. 1988. Entwaldung und Steinschlag. *Interpraevent* 1988 **1**: 185-198.

Jancke O. 2007. Alpine coppice stands - implications of stand age on the rockfall protection function. MSc Thesis. University of Hamburg: Hamburg

Jancke O, Dorren LKA, Berger F, Fuhr M, Köhl M. 2009. Implications of coppice stand characteristics on the rockfall protection function. *Forest Ecology and Management* **259 (1)**: 124-131. DOI: 10.1016/j.foreco.2009.10.003

Jonsson MJ. 2007. Energy absorption of trees in a rockfall protection forest. PhD Thesis Eidgenössische Technische Hochschule Zürich No. 17214: Zurich

Jourez B, Riboux A, Leclercq A. 2001. Anatomical characteristics of tension wood and opposite wood in young inclined stems of poplar (*Populus euramericana* CV "Ghoy"). *IAWA Journal* **22**: 133-157.

Kalberer M, Ammann M, Jonsson M. 2007. Mechanical properties of Norway spruce: Experiments for the analysis of natural hazards. *Schweizerische Zeitschrift für Forstwesen* **158**: 166-175. DOI: 10.3188/szf.2007.0166

Kanton Uri. 2012. Informationen Felssturz Gurtzellen.
<http://www.ur.ch/de/bd/ds/felssturz-gurtzellen-2006-m1293/>. Accessed: 15.04.2012.

Kienholz H, Mani P. 1994. Assessment of geomorphic hazards and priorities for forest management on the Rigi north face, Switzerland. *Mountain Research and Development* **14 (4)**: 321-328.

Köhl M, Frühwald A, Kenter B, Olschofsky K, Köhler R, Köthke M, Rüter S, Pretzsch H, Rötzer T, Makeschin F, Abiy M, Dieter M. 2009. Potenzial und Dynamik der Kohlenstoffspeicherung in Wald und Holz: Beitrag des deutschen Forst und Holzsektors zum Klimaschutz. *Landbauforschung - vTI Agriculture and Forestry Research Sonderheft* **327**: 103-109.

Kollmann F. 1951. *Technologie des Holzes und der Holzwerkstoffe*. Springer Verlag: Berlin

Krautblatter M, Moser, M. 2009. A nonlinear model coupling rockfall and rainfall intensity based on a four year measurement in a high Alpine rock wall (Reintal, German Alps). *Natural Hazards and Earth Systems Sciences* **9**: 1425-1432.

Krech H. 1960. Größe und zeitlicher Ablauf von Kraft und Durchbiegung beim Schlagbiegeversuch an Holz und ihr Zusammenhang mit der Bruchschlagarbeit. *Holz als Roh- und Werkstoff* **3**: 95-105.

Labieuse V, Heidenreich B. 2009. Half-scale experimental study of rockfall impacts on sandy slopes. *Natural Hazards and Earth Systems Sciences* **9**: 1981-1993. doi:10.5194/nhess-9-1981-2009

Lundström T, Jonsson MJ, Volkwein A, Stoffel M. 2008. Reactions and energy absorption of trees subject to rockfall: a detailed assessment using a new experimental method. *Tree Physiology* **29**: 345-359. DOI:10.1093/treephys/tpn030

- Mattheck C. 1997. Wood – The Internal Optimization of Trees. Springer Verlag: Berlin Heidelberg
- Mayer, H. 1992. Waldbau auf soziologisch-ökologischer Grundlage. 4. Auflage. Gustav Fischer Verlag: Jena, Stuttgart, New York
- Meißl G. 1998. Modellierung der Reichweite von Felsstürzen. Fallbeispiele zur GIS-gestützten Gefahrenbeurteilung aus dem Bayrischen und Tiroler Alpenraum. PhD Thesis. Institut für Geographie der Universität Innsbruck: Innsbruck
- Millennium Ecosystem Assessment. 2005. Ecosystems and Human Well-being: Synthesis. Island Press: Washington DC
- Mizuyama T, Narita H. 1988. Debris flow control by woods and their impact energy absorptivity. *Interpraevent* 1988 **1**: 173-181.
- Motta R, Haudemand J-C. 2000. Protective forests and silvicultural stability. An example of planning in the Aosta valley. *Mountain Research and Development* **20 (2)**: 74-81.
- Nemcök A, Pašek J, Rybář J. 1972. Classification of landslides and other mass movements. *Rock Mechanics* **4**: 71-78.
- Nitsch J. 2009. Potenziale erneuerbarer Energien und die Rolle des Energieträgers Holz. *Landbauforschung - vTI Agriculture and Forestry Research Sonderheft* **327**: 91-102.
- O'Hara KL. 2006. Multiaged forest stands for protection forests: concepts and applications. *Forest Snow and Landscape Research* **80 (1)**: 45-56.

Pechmann H. 1953. Untersuchungen über die Bruchschlagarbeit von Rotbuchenholz. Holz als Roh- und Werkstoff **9**: 361-367.

Perlik M. 2011. Alpine gentrification: The mountain village as a metropolitan neighbourhood. Revue de géographie alpine **99** : 1. DOI : 10.4000/rga.1370

Perret S, Dolf F, Kienholz H. 2004. Rockfalls into forests: Analysis and simulation of rockfall trajectories - considerations with respect to mountainous forests in Switzerland. Landslides **1**: 123-130. DOI 10.1007/s10346-004-0014-4

Radtke A, Ambraß S, Zerbe S, Tonon G, Ammer C. 2012. Which environmental factors favor the invasion of *Ailanthus altissima* (Mill.) Swingle and *Robinia pseudoacacia* L. in a coppice forest of the Southern Alps? Forest Ecology and Management: submitted.

Rammer W, Brauner M, Dorren LKA, Berger F, Lexer MJ. 2010. Evaluation of a 3-D rockfall module within a forest patch model. Natural Hazards and Earth Systems Sciences 10: 699-711. doi:10.5194/nhess-10-699-2010

Raetzo H, Lateltin O, Tripet JP, Bollinger D. 2002. Hazard assessment in Switzerland—Codes of Practice for mass movements. Bulletin of Engineering Geology and the Environment **61**: 263-268. DOI: 10.1007/s10064-002-0163-4

Richter HG, Dallwitz, MJ. 2000. Commercial timbers: descriptions, illustrations, identification, and information retrieval. In English, French, German, Portuguese, and Spanish. Version: 25th June 2009. <http://delta-intkey.com>. Accessed 12.05.2012.

Rickli C, Graf F, Gerber W, Frei M, Böll A. 2004. Der Wald und seine Bedeutung bei Naturgefahren geologischen Ursprungs. *Forum für Wissen*: 27-34.

Schneider J, Schlatter HP. 1996. Sicherheit und Zuverlässigkeit im Bauwesen – Grundwissen für Ingenieure, 2. Edition. B.G. Teubner: Stuttgart

Schwitler R. 2001. Zusammenfassung und Schlussfolgerungen. In: Dokumentation der 14. Arbeitstagung der Schweizerischen Gebirgswaldpflegegruppe mit der FAN 1998, Schwitler R. (Ed). Grafenort / Engelberg: 1-5.

Sell J. 1987. Eigenschaften und Kenngrößen von Holzarten. Bau-fachverlag AG: Zürich.

Stokes A, Salin F, Kokutse AD, Berthier S, Jeannin H, Mochan S, Dorren L, Kokutse N, Ghani MA, Fourcaud T. 2005. Mechanical resistance of different tree species to rockfall in the French Alps. *Plant and Soil* **278**: 107-117. DOI: 10.1007/s11104-005-3899-3

Stoffel M. 2005. Assessing the vertical distribution and visibility of rockfall scars in trees. *Schweizerische Zeitschrift für Forstwesen* **156 (6)**: 195-199.

Stoffel M, Schneuwly D, Bollschweiler M, Lièvre I, Delaloyea R, Myint M, Monbarona M. 2005. Analyzing rockfall activity (1600–2002) in a protection forest—a case study using dendrogeomorphology. *Geomorphology* **68**: 224-241. DOI:10.1016/j.geomorph.2004.11.017

- Stoffel M, Wehrli A, Kühne R, Dorren LKA, Perret S, Kienholz H. 2006. Assessing the protective effect of mountain forests against rockfall using a 3D simulation model. *Forest Ecology and Management* **225**: 113-122. DOI: 10.1016/j.foreco.2005.12.030
- Stoffel M, Bollschweiler M, Butler DR, Luckman BH. 2010 *Tree rings and natural hazards: A state-of-the-art*. Springer: Berlin, Heidelberg, New York
- Straub D, Schubert M. 2008. Modelling and managing uncertainty in rock-fall hazards. *Georisk* **2 (1)**: 1-15. DOI: 10.1080/17499510701835696
- Unterrichter M. 1996. Sicherstellung landeskultureller Leistungen durch Niederwälder. Das Projekt „S. Leonardo“ bei Borghetto-Trento. *Forstwissenschaftliches Centralblatt* **115**: 287-293. DOI: 10.1007/BF02738609
- Volkwein A, Schellenberg K, Labiouse V, Agliardi F, Berger F, Bourrier F, Dorren LKA, Gerber W, Jaboyedoff M. 2011. Rockfall characterisation and structural protection – a review. *Natural Hazards and Earth Systems Sciences* **11**: 2617-2011. DOI: 10.5194/nhess-11-2617-2011
- Vorreiter L. 1949. *Holztechnologisches Handbuch*. Fromme & Co: Wien
- Wagenführ R, Scheiber C. 1985. *Holzatlas*. VEB Fachbuchverlag: Leipzig

Woltjer M, Rammer W, Brauner M, Seidl R, Mohren GMJ, Lexer MJ. 2008. Coupling a 3D patch model and a rockfall module to assess rockfall protection in mountain forests. *Journal of Environmental Management* **87**: 373-388. DOI:10.1016/j.jenvman.2007.01.031

8. Annex

8.1 High-speed camera image sequences of selected impacts conducted with the pendulum test device (chapters 3 and 5)

The following image sequences show selected impacts and are aimed to give a better idea of the multitude of breakage behaviors of the stems during impact. Therefore, only every second image is shown (corresponding to a frequency of 100 images per second or one image every 10 ms).

8.1.1 Impacts against beech specimens

Figure 8.1: Image sequence of beech specimen S1 chapter 3, Figure 3.10, Table 3.2). Transverse breakage at ground height.

DBH [m]	Length [m]	Δp [kg ms ⁻²]	ΔE_{kin} [kJ]	Contact time [ms]	Impact height [m]
0.039	3.0	126.9	1.33	105	0.97

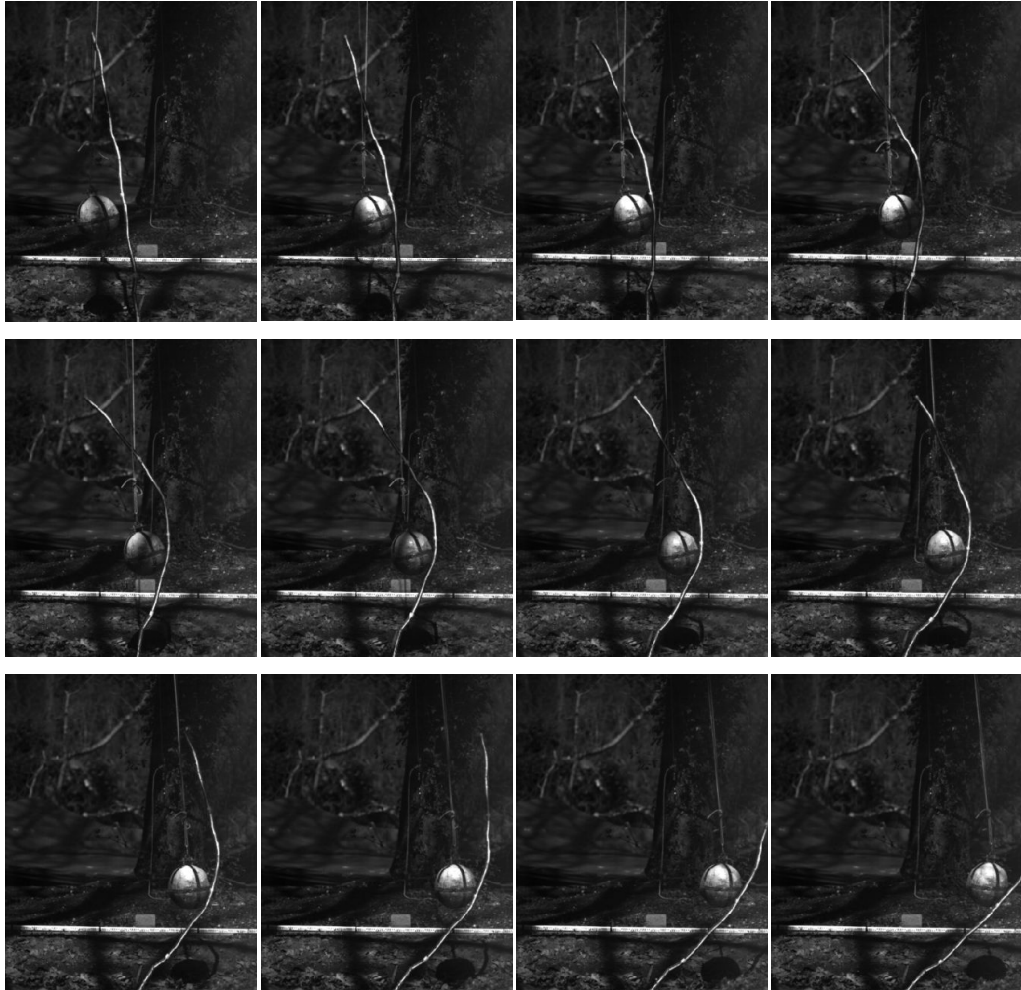


Figure 8.2: Image sequence of beech specimen S2 (chapter 3, Figure 3.10, Table 3.2). Transverse breakage at ground and impact height.

DBH [m]	Length [m]	Δp [kg ms ⁻²]	ΔE_{kin} [kJ]	Contact time [ms]	Impact height [m]
0.043	3.0	183.2	2.14	35	0.35

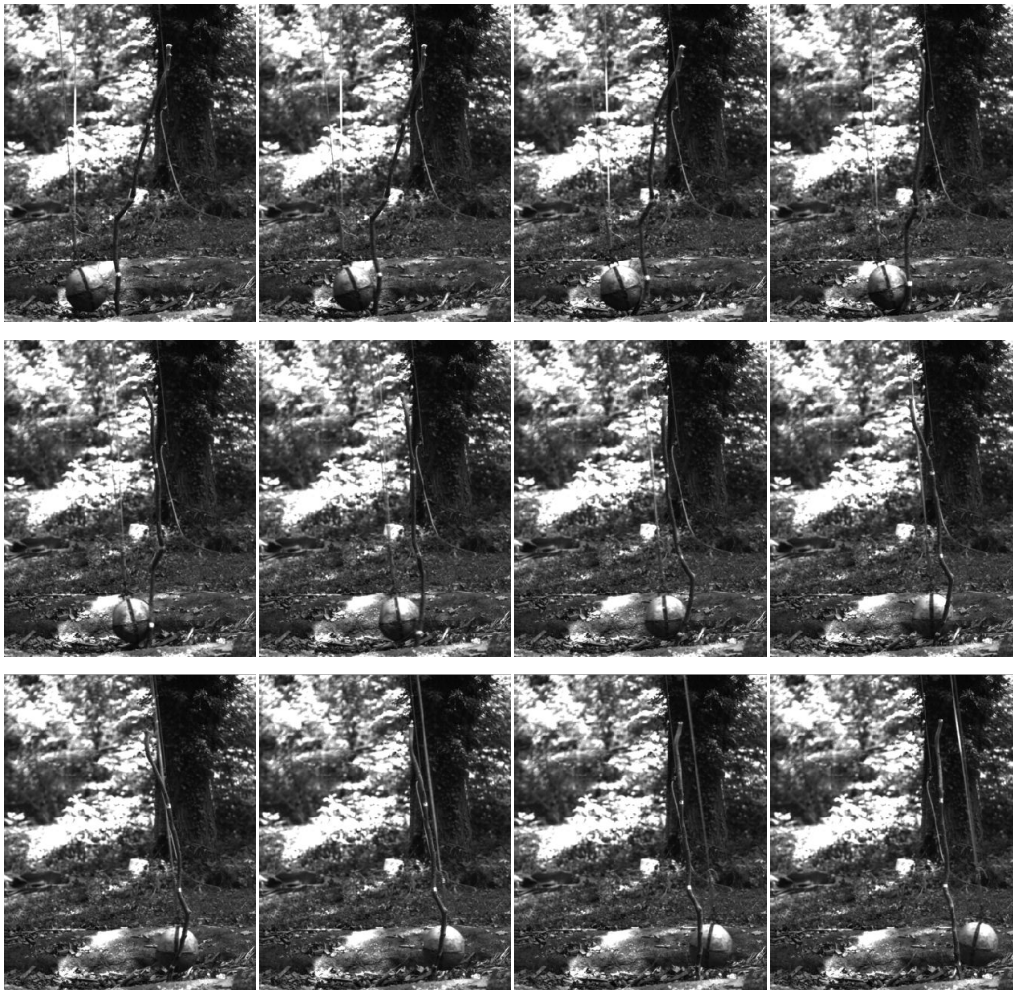


Figure 8.3: Image sequence of beech specimen S3 (chapter 3, Figure 3.10, Table 3.2). Transverse breakage at ground height.

DBH [m]	Length [m]	Δp [kg ms ⁻²]	ΔE_{kin} [kJ]	Contact time [ms]	Impact height [m]
0.095	3.0	640.5	4.36	45	0.95

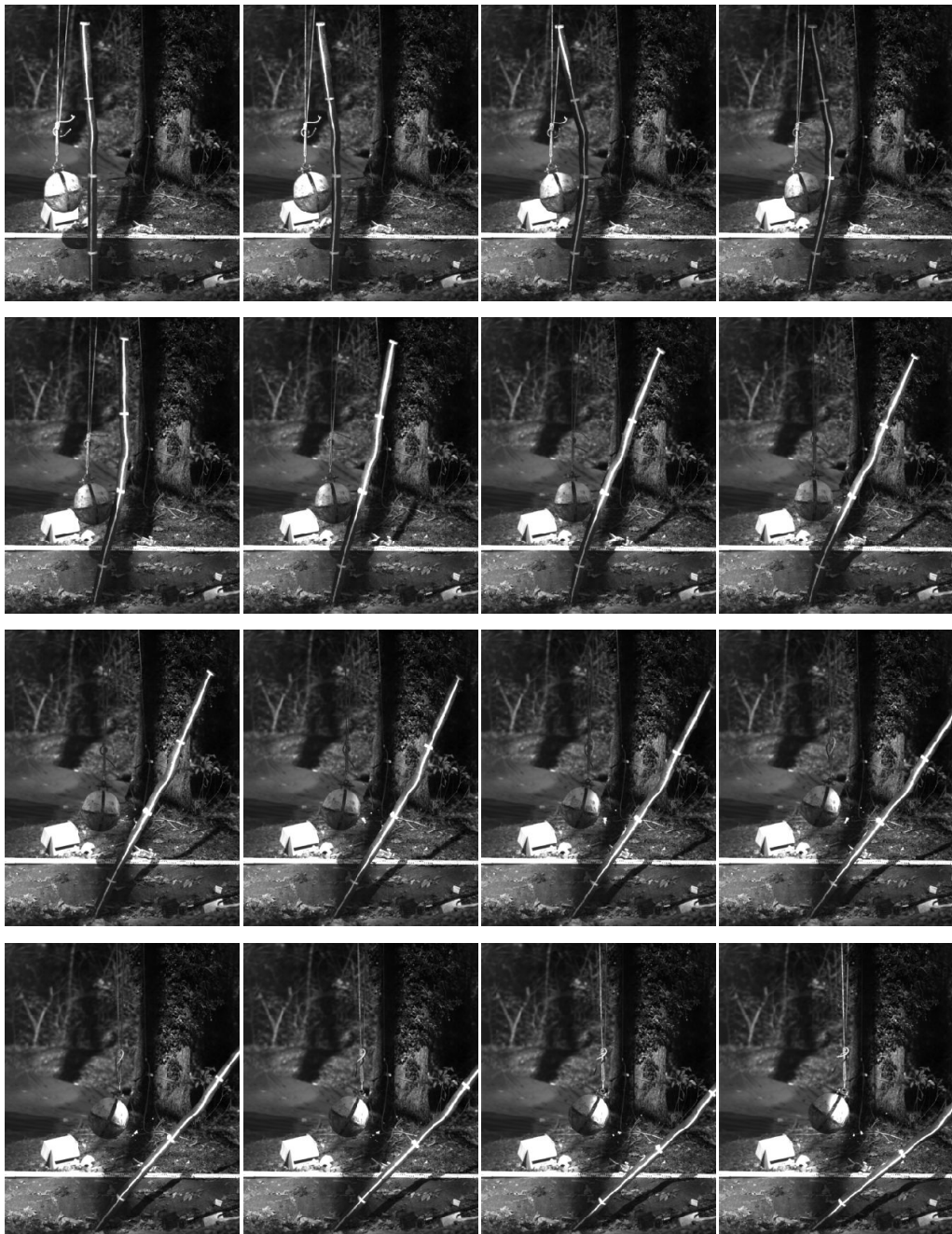


Figure 8.4: Image sequence of beech specimen S4 (chapter 3, Figure 3.10, Table 3.2). Longitudinal crack propagation in two planes starting close to impact height, followed by transverse breakage at ground height.

DBH [m]	Length [m]	Δp [kg ms ⁻²]	ΔE_{kin} [kJ]	Contact time [ms]	Impact height [m]
0.092	3.0	669.2	4.81	105	0.46

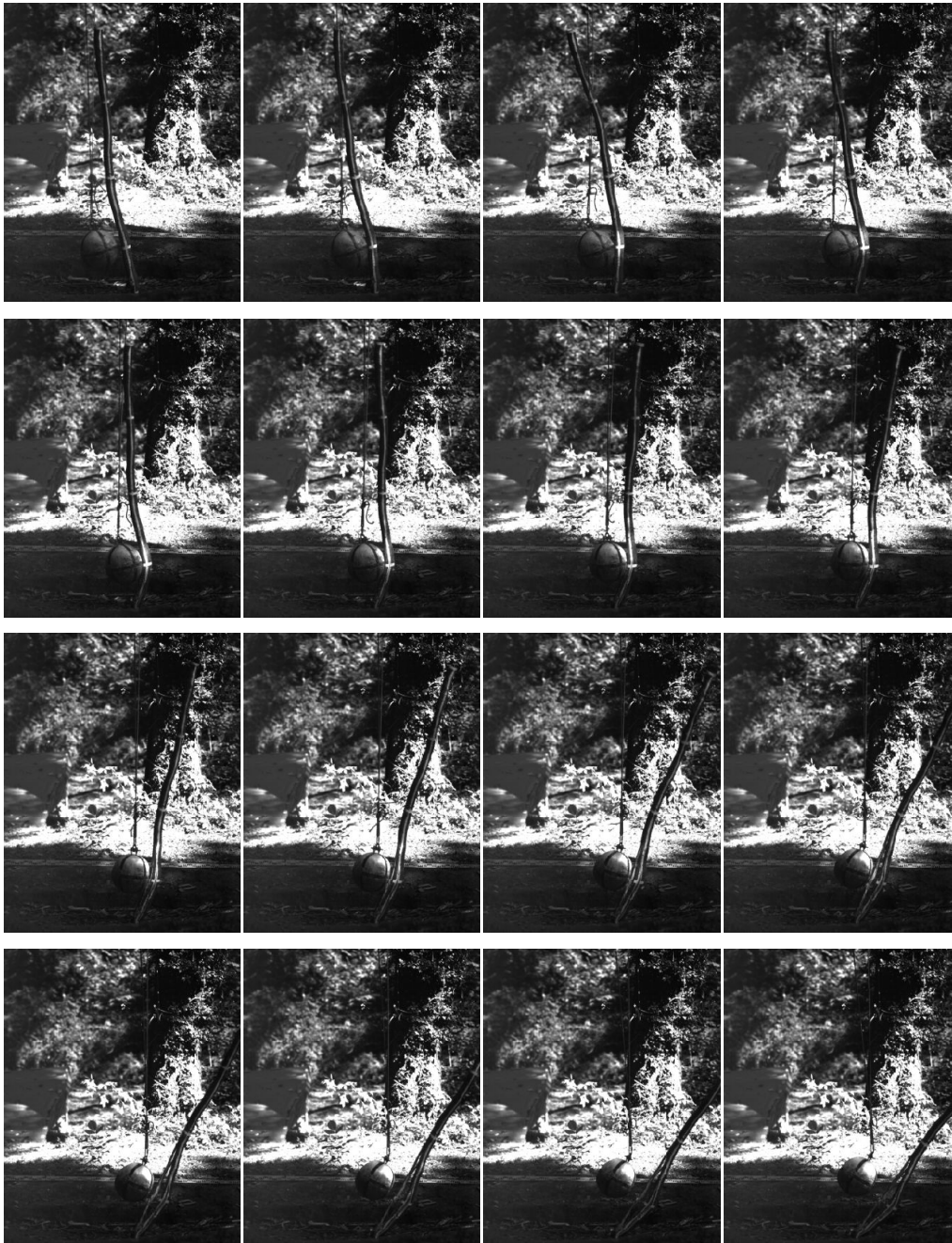


Figure 8.5: Image sequence of beech specimen 73. Longitudinal crack propagation starting on the tension side at impact height leading to breaking off of a stem part. In addition transverse breakage at ground height.

DBH [m]	Length [m]	Δp [kg ms ⁻²]	ΔE_{kin} [kJ]	Contact time [ms]	Impact height [m]
0.071	3.0	446.9	3.58	55	0.40

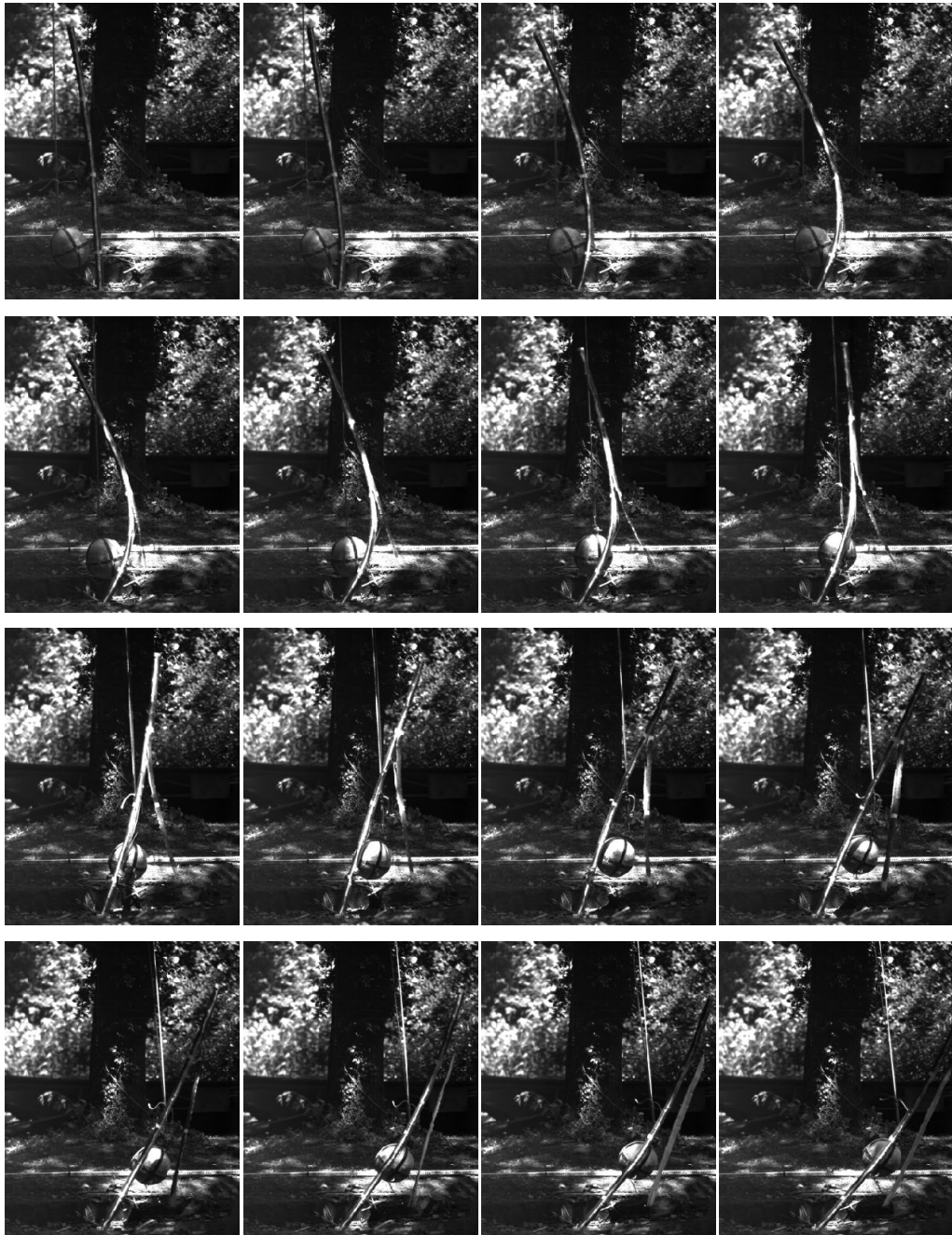


Figure 8.6: Image sequence of beech specimen 75. Longitudinal crack propagation in two planes starting at impact height and leading to breakage at impact height. In addition transverse breakage at ground height.

DBH [m]	Length [m]	Δp [kg ms ⁻²]	ΔE_{kin} [kJ]	Contact time [ms]	Impact height [m]
0.059	3.0	212.2	2.18	75	0.51

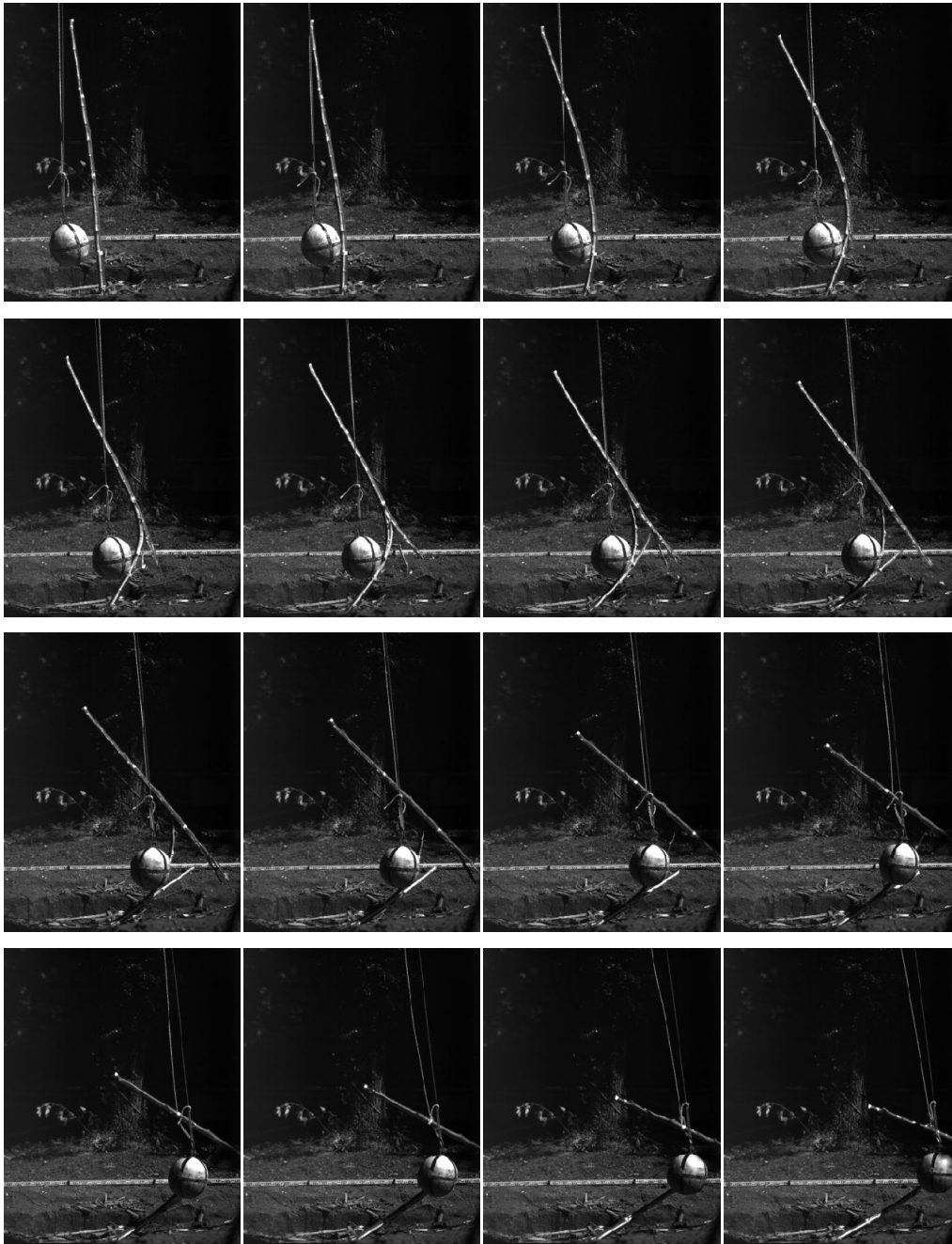


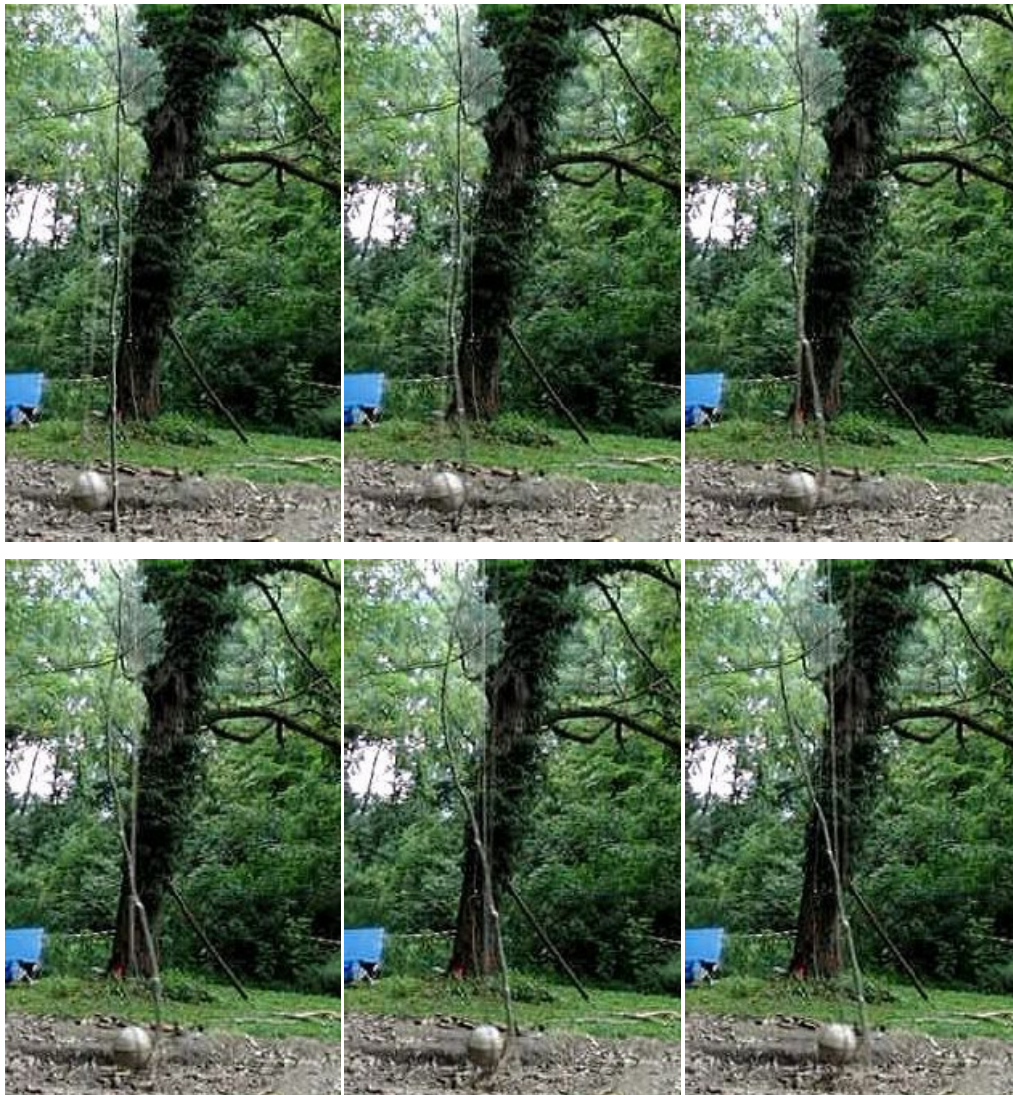
Figure 8.7: Image sequence of beech specimen 166. Longitudinal splintering on the tension side above impact height. In addition transverse breakage at ground height.

DBH [m]	Length [m]	Δp [kg ms ⁻²]	ΔE_{kin} [kJ]	Contact time [ms]	Impact height [m]
0.085	3.0	622.5	5.33	90	0.30



Figure 8.8: Image sequence of beech specimen E8 (entire stem). Longitudinal crack propagation starting at impact height and leading to breakage at impact height. In addition transverse breakage at ground height. After failure the bob entrains the entire specimen.

DBH [m]	Length [m]	Δp [kg ms ⁻²]	ΔE_{kin} [kJ]	Contact time [ms]	Impact height [m]
0.05	6.6	271.7	2.62	80	0.35



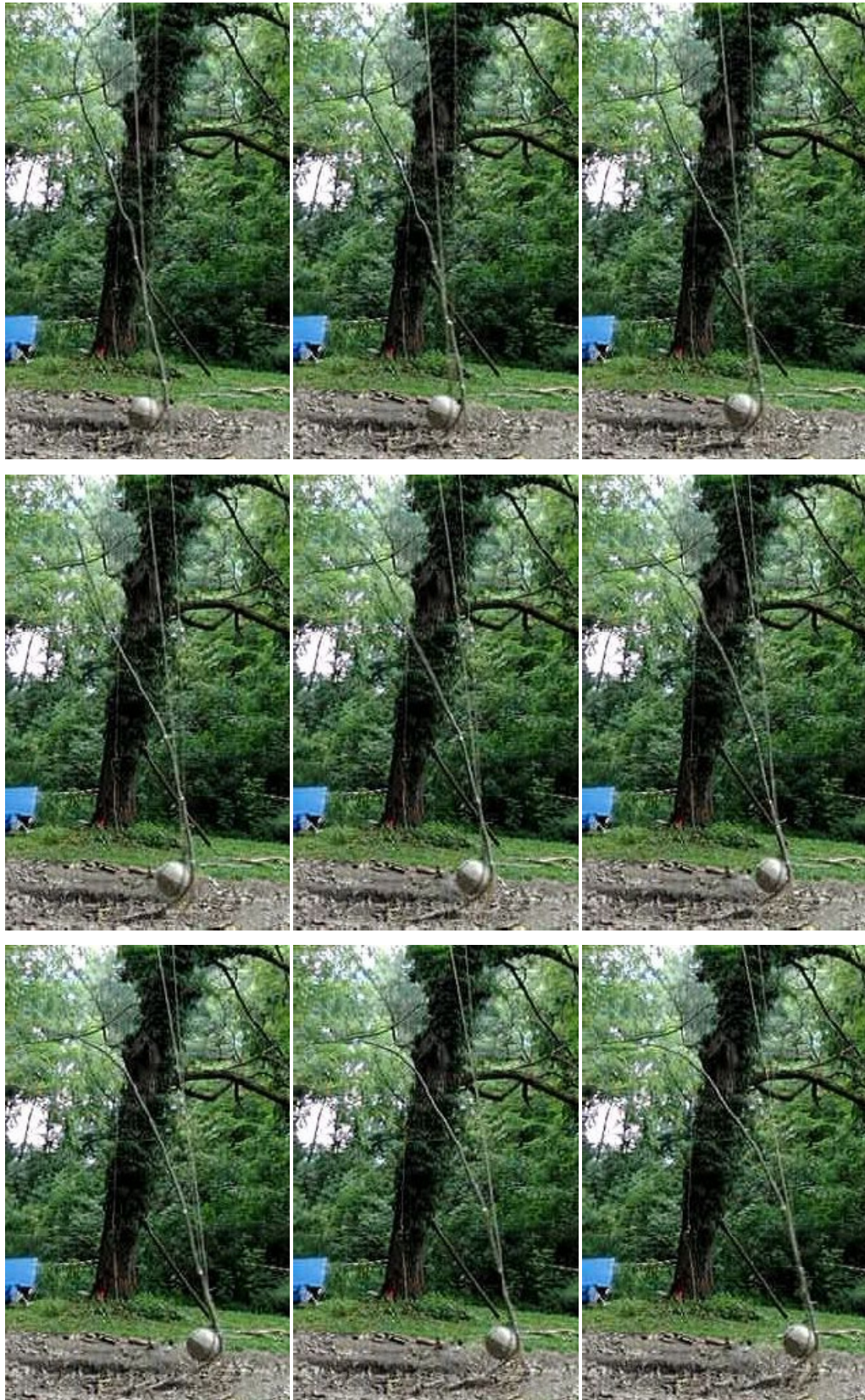
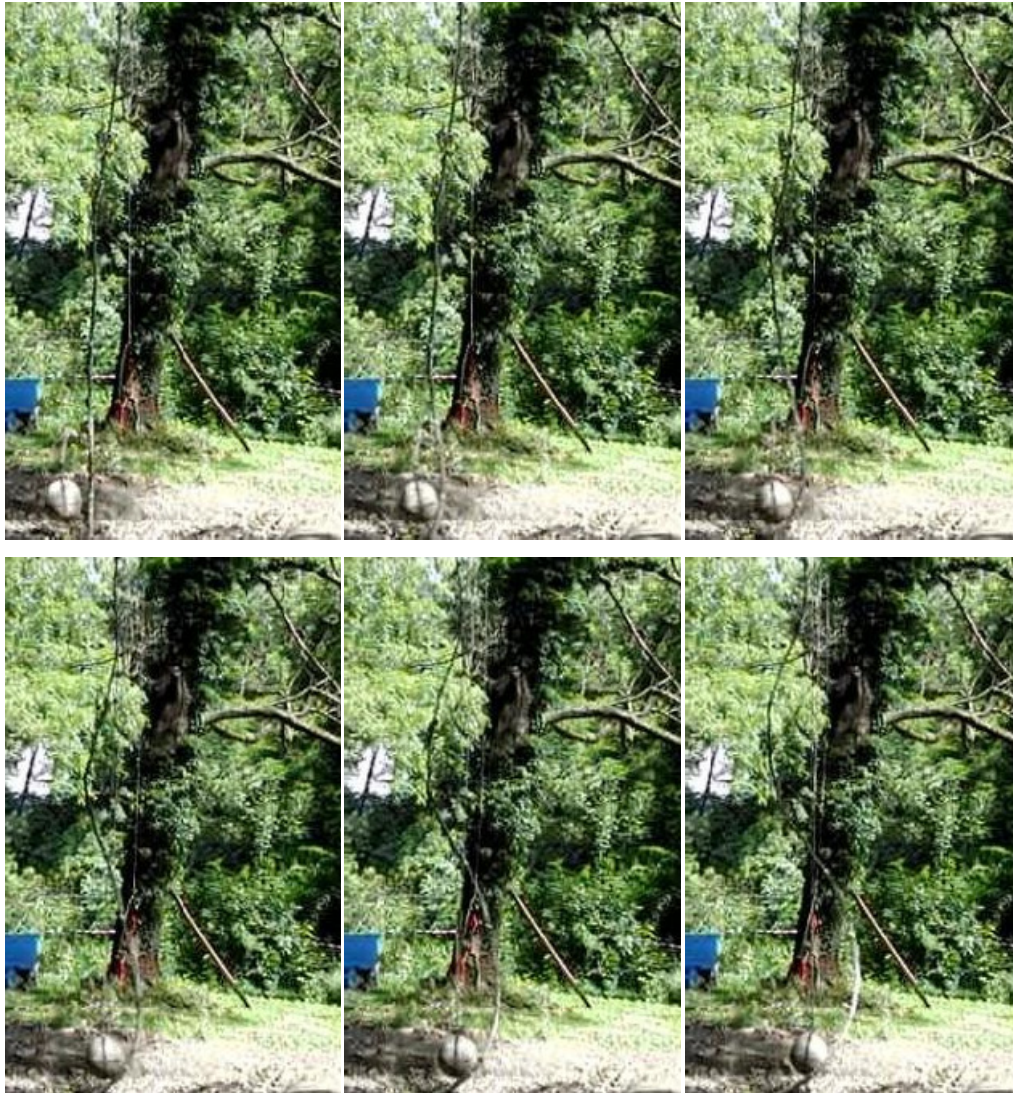
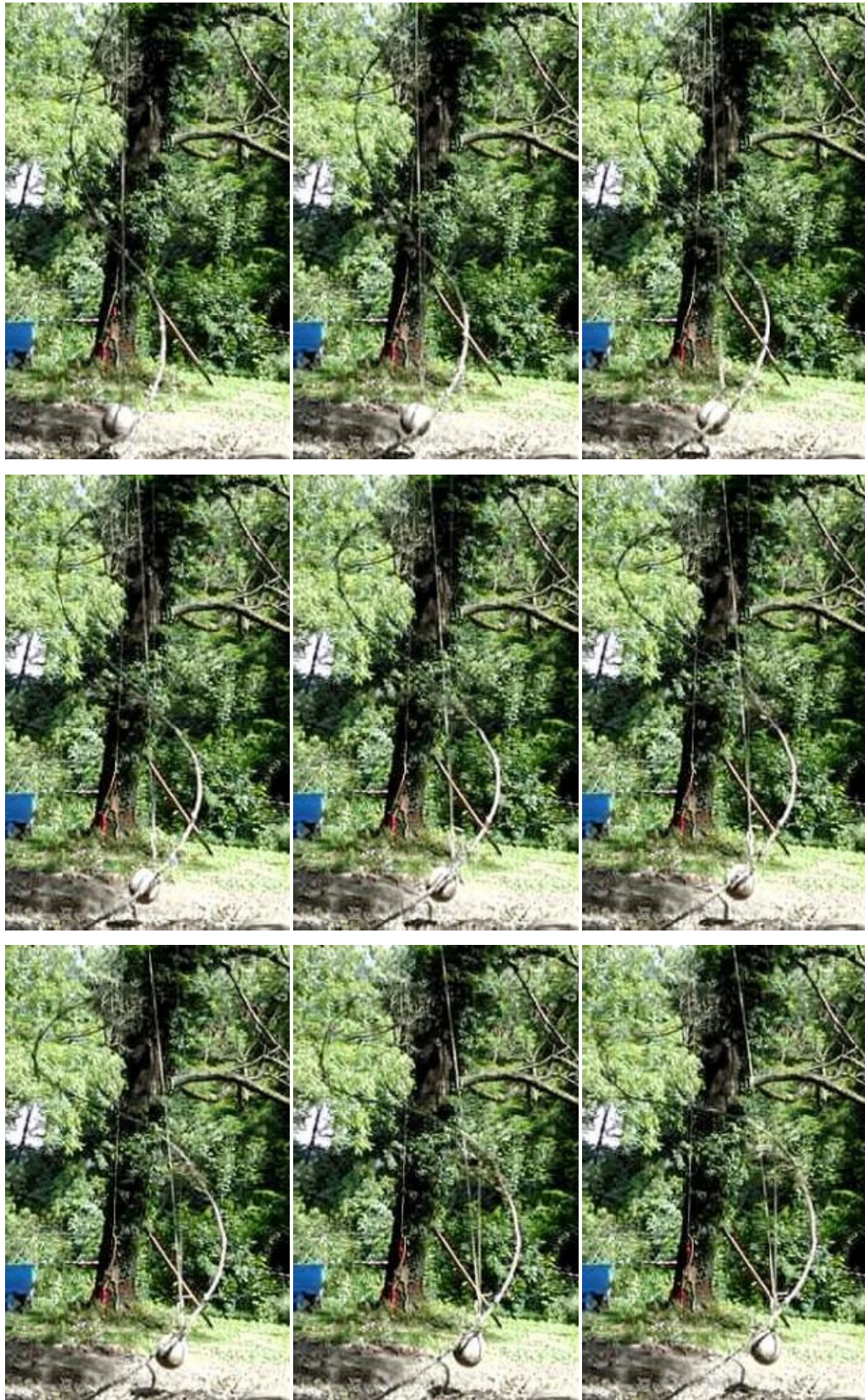
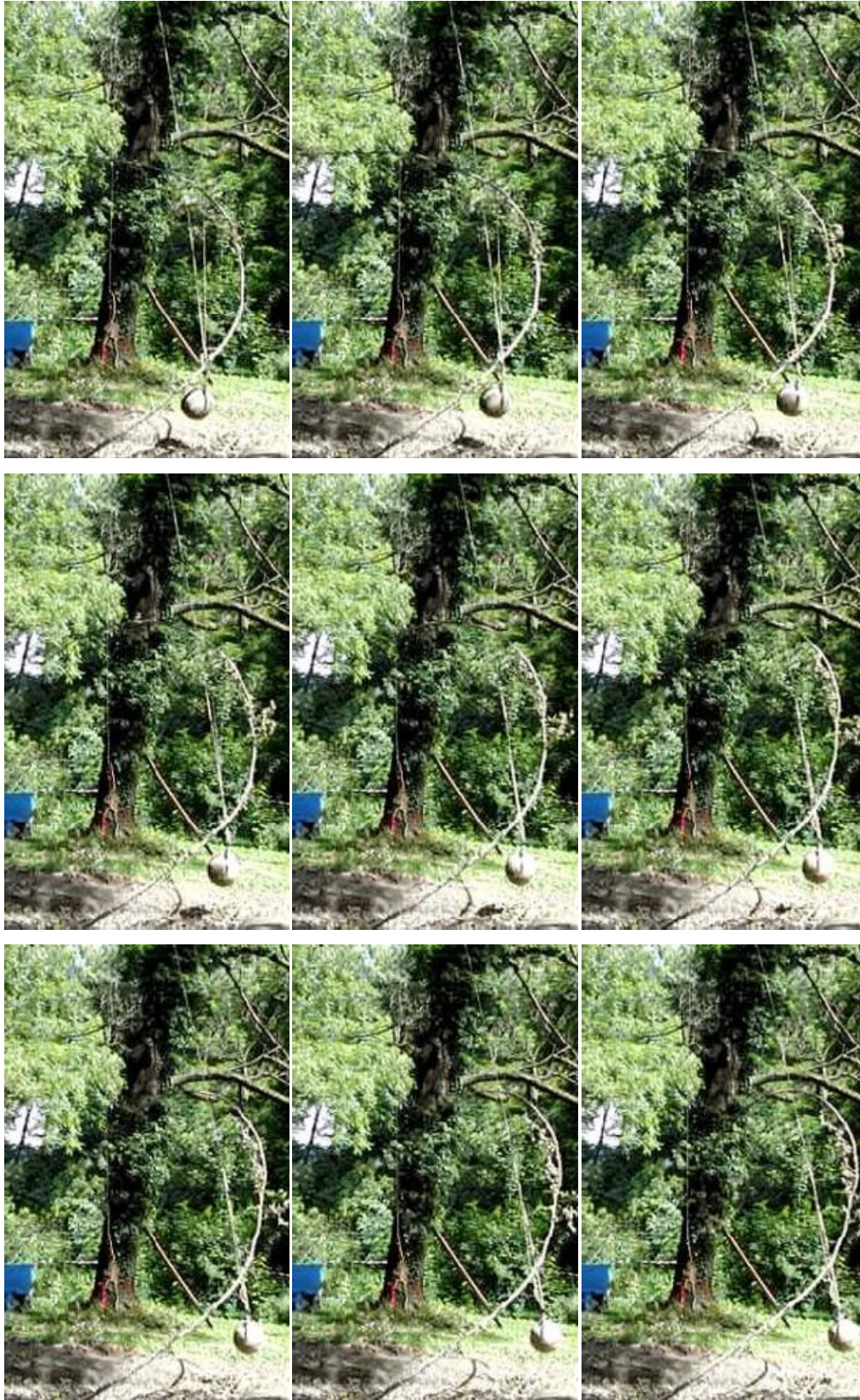


Figure 8.9: Image sequence of beech specimen E9 (entire stem; corresponds to the specimen depicted in Figure 3.5). Transverse breakage at ground height. Propagation of a mechanical wave along the stem leading to a whiplash-like movement of the whole specimen.

DBH [m]	Length [m]	Δp [kg ms ⁻²]	ΔE_{kin} [kJ]	Contact time [ms]	Impact height [m]
0.05	8.3	329.3	3.21	90	0.34







8.1.2 Impacts against chestnut specimens

Figure 8.10: Image sequence of chestnut specimen 822. Transverse breakage at ground height. Very flexible. Hardly any deceleration effect on impactor.

DBH [m]	Length [m]	Δp [kg ms ⁻²]	ΔE_{kin} [kJ]	Contact time [ms]	Impact height [m]
0.026	3.0	33.6	0.39	65	0.57



Figure 8.11: Image sequence of chestnut specimen 832. Transverse breakage at ground height. Very flexible.

DBH [m]	Length [m]	Δp [kg ms ⁻²]	ΔE_{kin} [kJ]	Contact time [ms]	Impact height [m]
0.04	3.0	245.3	2.51	140	0.41

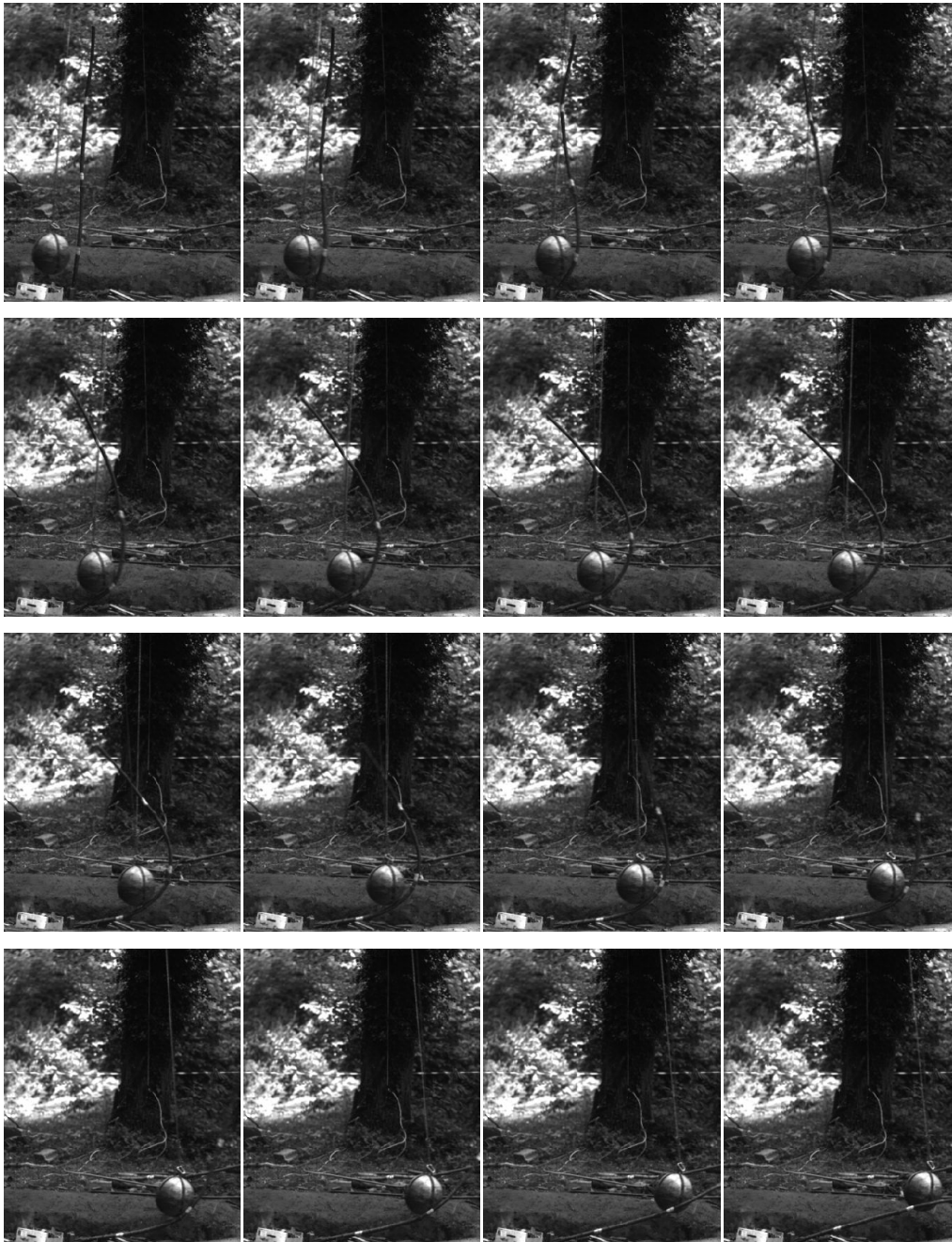
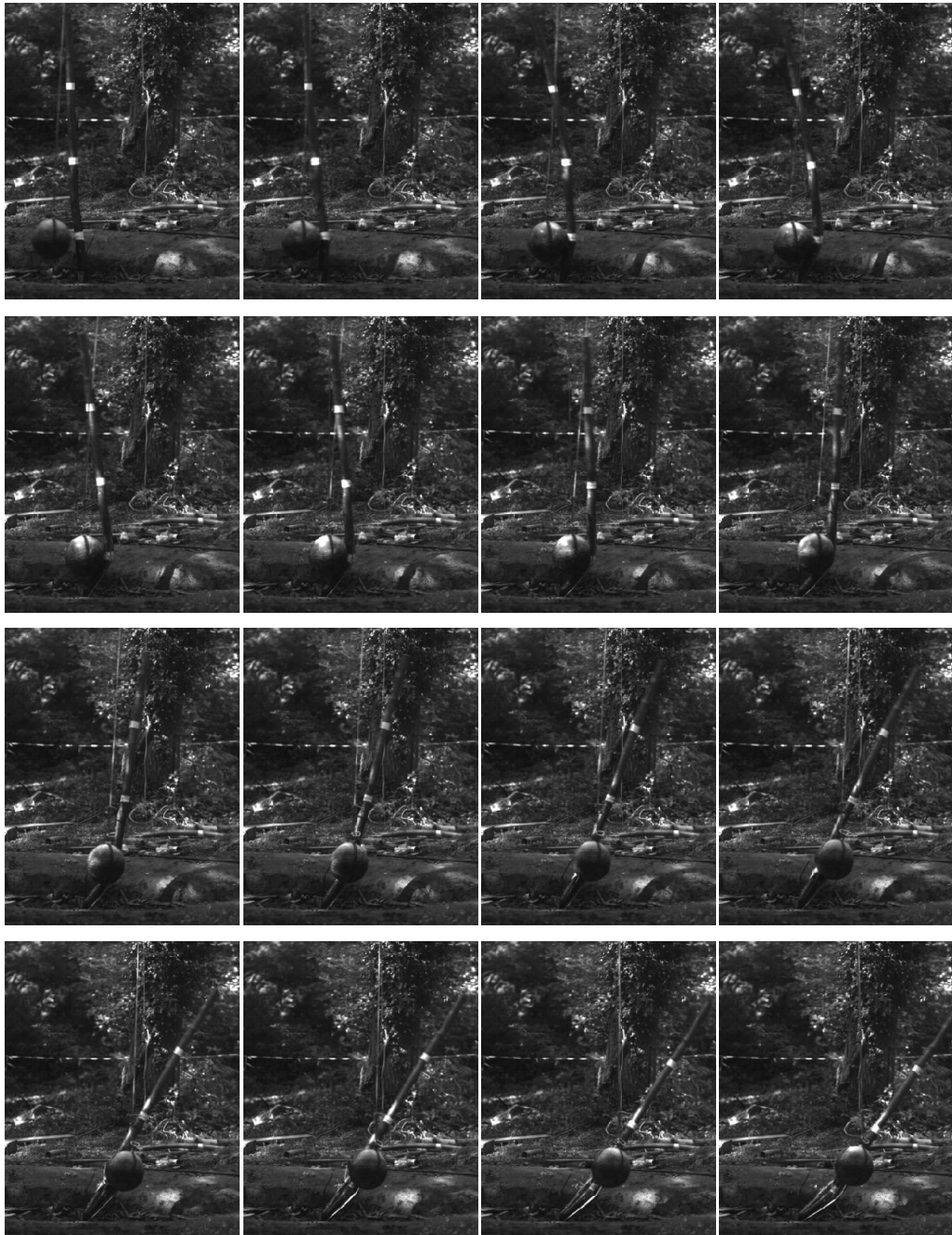
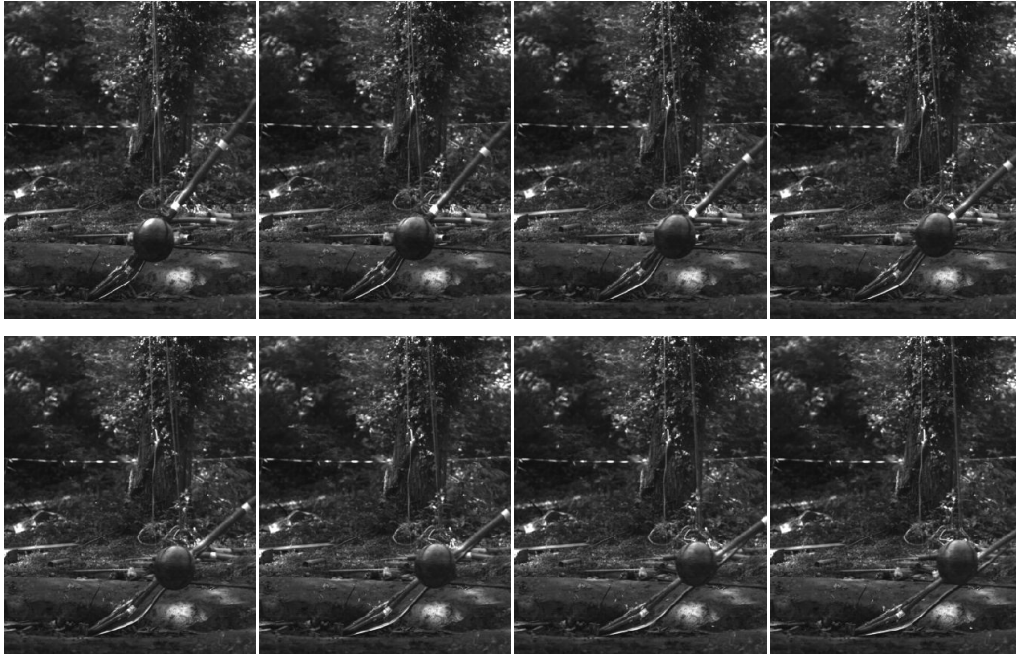


Figure 8.12: Image sequence of chestnut specimen 836. Longitudinal crack propagation in two planes starting close to impact height, leading to cleaving of almost the entire specimen. In addition transverse breakage at ground height.

DBH [m]	Length [m]	Δp [kg ms ⁻²]	ΔE_{kin} [kJ]	Contact time [ms]	Impact height [m]
0.084	3.0	584.6	4.92	85	0.45





8.1.3 Impacts against fir specimens

Figure 8.13: Image sequence of fir specimen 514. In comparison to beech and chestnut few flexural deformations of the stem.

Simultaneous transverse breakage at ground and impact height shortly after start of impact.

DBH [m]	Length [m]	Δp [kg ms ⁻²]	ΔE_{kin} [kJ]	Contact time [ms]	Impact height [m]
0.076	3.0	290.6	3.02	30	0.32



Figure 8.14: Image sequence of fir specimen 532. Longitudinal crack propagation starting from impact height. In addition transverse breakage at ground height and above impact height.

DBH [m]	Length [m]	Δp [kg ms ⁻²]	ΔE_{kin} [kJ]	Contact time [ms]	Impact height [m]
0.064	3.0	331.0	3.21	75	0.41

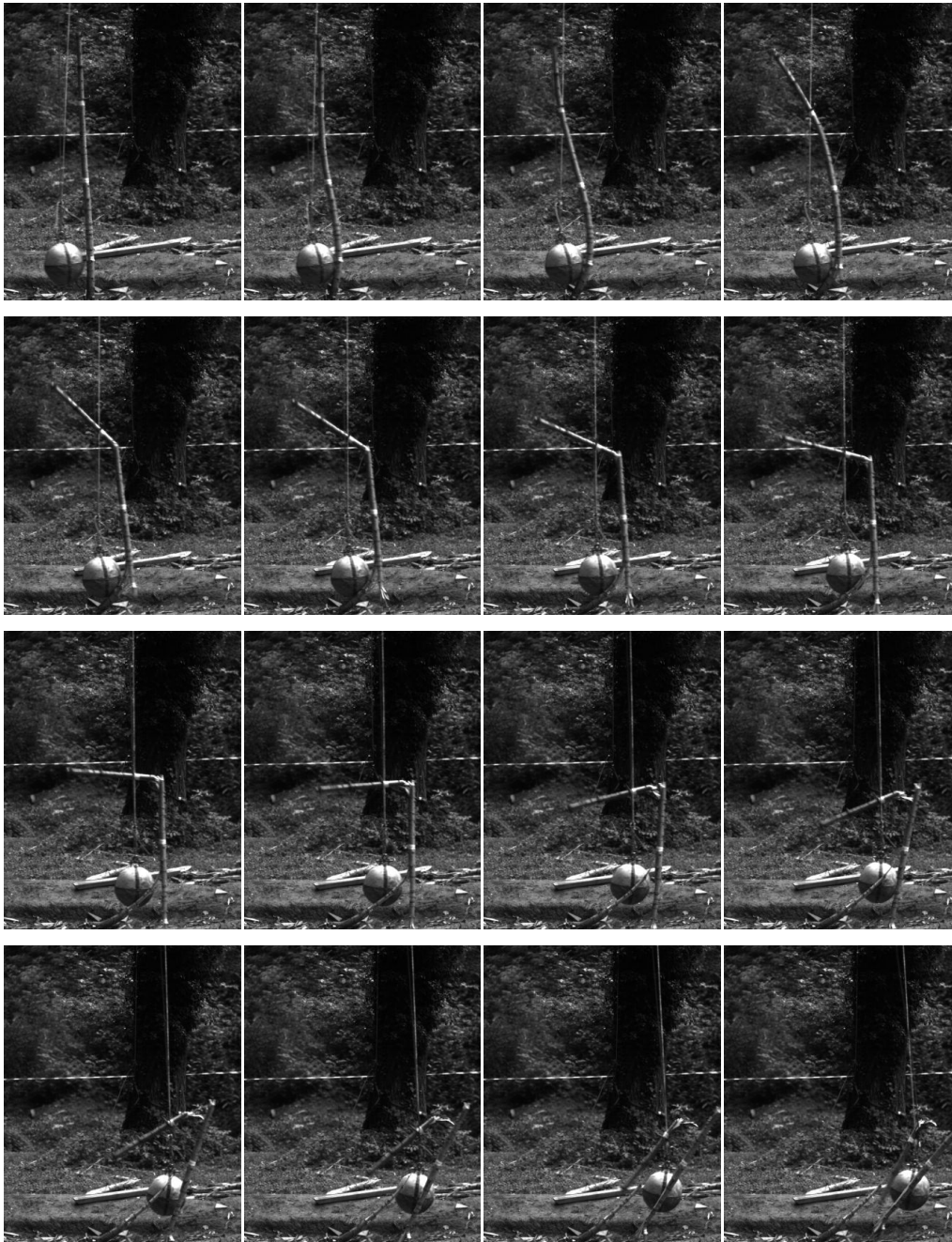
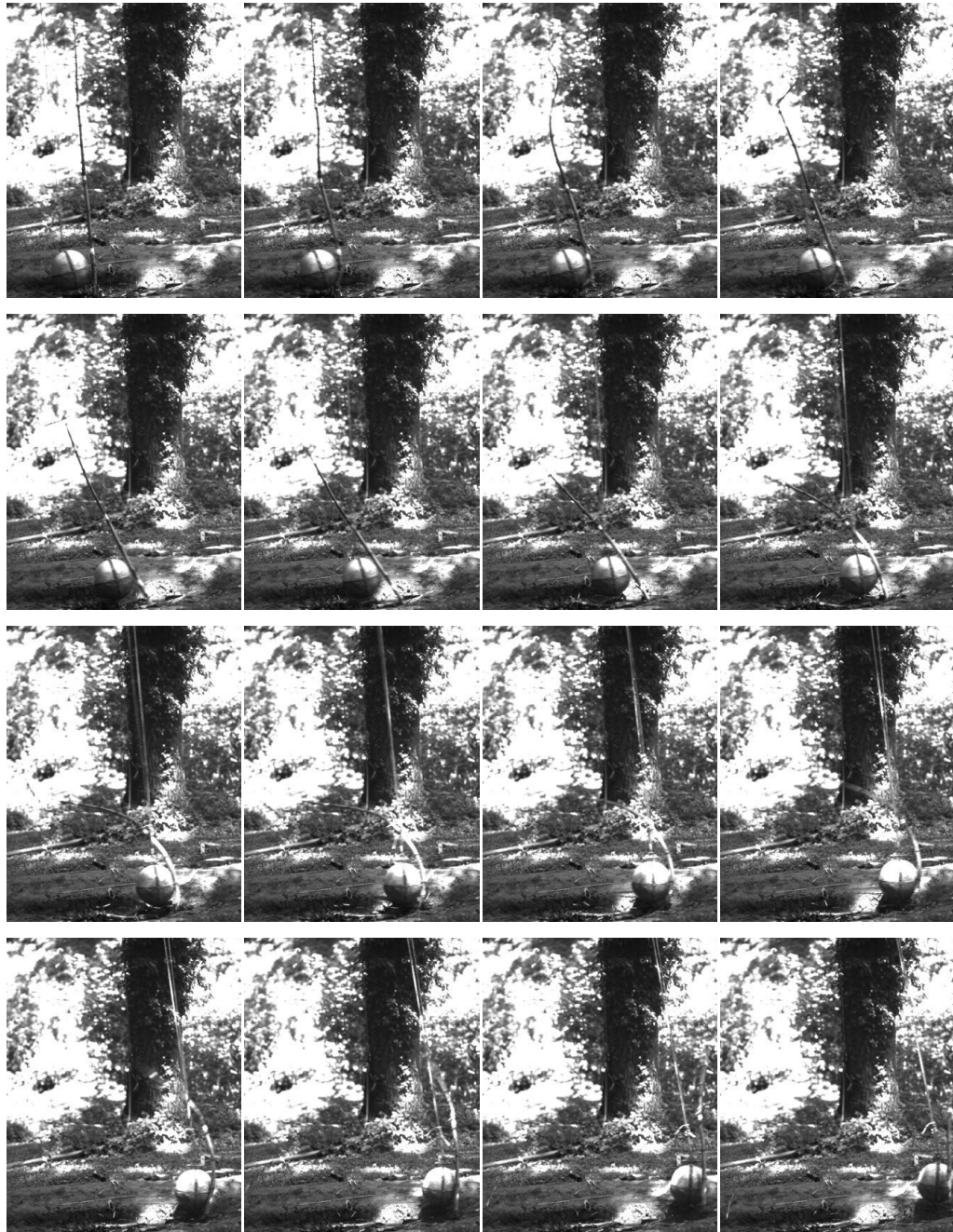


Figure 8.15: Image sequence of fir specimen 537. Propagation of mechanical wave to specimen top leads to loss of a small segment of the upper end. In addition transverse breakage at ground height.

DBH [m]	Length [m]	Δp [kg ms ⁻²]	ΔE_{kin} [kJ]	Contact time [ms]	Impact height [m]
0.037	3.0	163.0	1.79	40	0.26



8.2 High-speed camera image sequences of selected impact tests against beech coppice trees conducted with the forest test device (chapter 4)

The following image sequences show two selected impact tests and are aimed to give a better idea of the interactions of the impactor with both the target tree and unintended subsequent trees that were part of the same clump. Where necessary, image frequency of the chosen images was varied in order to focus on the most insightful scenes. The time steps between the images are indicated below each image.

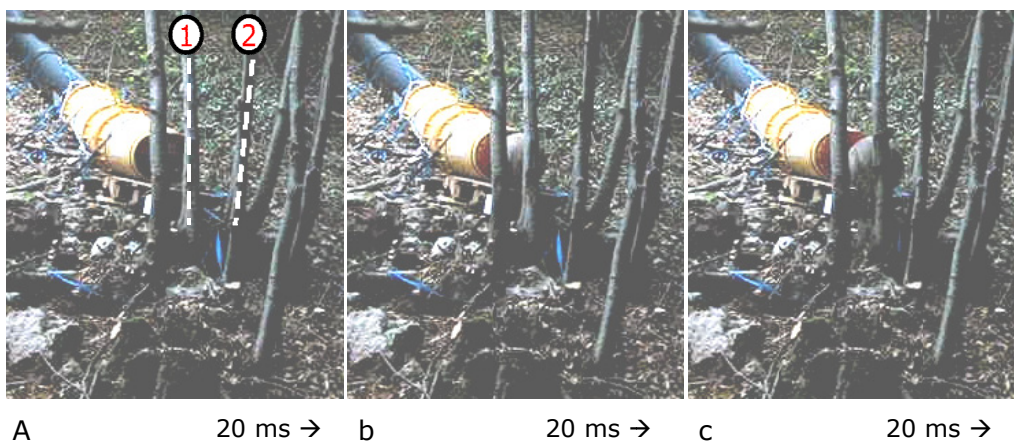
Figure 8.16: Image sequence of two impactor-tree interactions in a coppice clump.

Image b: impact against tree 1 (breakage at ground height; 80% of kinetic energy lost).

Image f: loss of contact with tree 1 and impact against tree 2.

Image i: loss of contact with tree 2.

Image l: impactor nearly stopped on forest ground.





D 20 ms → e 20 ms → f 20 ms →



G 20 ms → h 20 ms → i 20 ms →



j 200 ms → k 200 ms → l

Figure 8.17: Image sequence of four impactor-tree interactions in a coppice clump.

Image b: impact against tree 1 (breakage at ground height; 70% of kinetic energy lost).

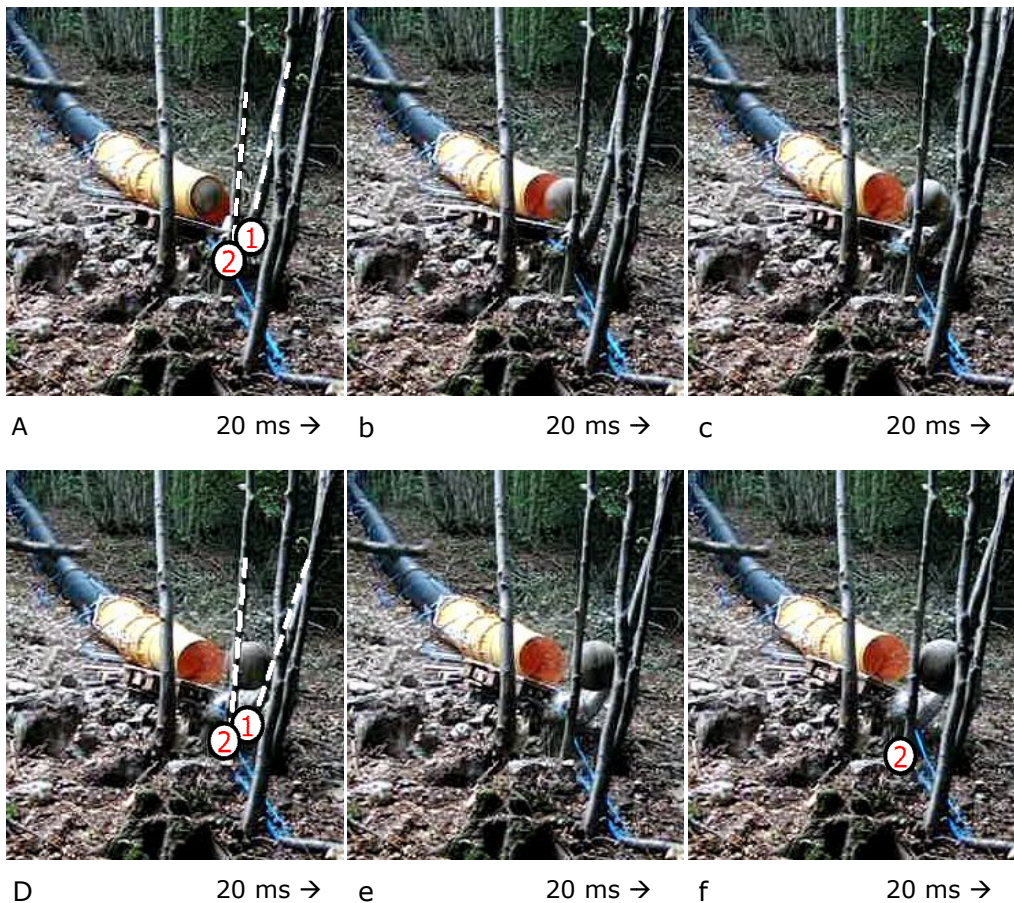
Image f: scratch on tree 2.

Image g: eccentric impact against tree 3.

Image h: impact against tree 4 while staying in contact with tree 3.

Impactor remains rotating against trees 3 and 4 during approximately 300 ms.

Image i: impactor nearly stopped on forest ground.





g 20 ms → h 20 ms → i 200 ms →



j 200 ms → k 200 ms → l 200 ms →

